

IMPROVED LEAF AREA INDEX ESTIMATION BY CONSIDERING BOTH TEMPORAL AND SPATIAL VARIATIONS

A Thesis Submitted to the College of
Graduate Studies and Research
in Partial Fulfillment of the Requirements
for the Degree of Master Science
in the Department of Geography and Planning
University of Saskatchewan
Saskatoon

By

ZHAOQIN LI

PERMISSION TO USE

In presenting this thesis in partial fulfillment of the requirements for a Postgraduate degree from the University of Saskatchewan, I agree that the Libraries of the University may make it freely available for inspection. I further agree that permission for copying of this thesis in any manner, in whole or in part, for scholarly purposes may be granted by the professors who supervised my thesis work or, in their absence, by the Head of the Department or the Dean of the College in which my thesis work was completed. It is understood that any copying or publication of use of this thesis or parts thereof for financial gain shall not be allowed without my written permission. It is also understood that due recognition shall be given to me and to the University of Saskatchewan in any scholarly use which may be made of any material in my thesis.

Requests for permission to copy or to make any other use of the material in this thesis in whole or in part should be addressed to:

Head of the Department of Geography and Planning
University of Saskatchewan
Saskatoon, Saskatchewan, S7N 5C8, Canada

ABSTRACT

Variations in Leaf Area Index (LAI) can greatly alter output values and patterns of various models that deal with energy flux exchange between the land surface and the atmosphere. Customarily, such models are initiated by LAI estimated from satellite-level Vegetation Indices (VIs) including routinely produced Normalized Difference Vegetation Index (NDVI) products. However, the accuracy from LAI-VI relationships greatly varies due to many factors, including temporal and spatial variations in LAI and a selected VI. In addition, NDVI products derived from various sensors have demonstrated variations in a certain degree on describing temporal and spatial variations in LAI, especially in semi-arid areas. This thesis therefore has three objectives: 1) determine a suitable VI for quantifying LAI temporal variation; 2) improve LAI estimation by considering both temporal and spatial variations in LAI; and 3) evaluate routinely produced NDVI products on monitoring temporal and spatial variations in LAI.

The study site was set up in conserved semi-arid mixed grassland in St. Denis, Saskatchewan, Canada. One 600 m - long sampling transect was set up across the rolling topography, and six plots with a size of 40 × 40 m each were randomly designed and each was in a relatively homogenous area. Plant Area Index (PAI, which was validated to obtain LAI), ground hyperspectral reflectance, ground covers (grasses, forbs, standing dead, litter, and bare soil), and soil moisture data were collected over the sampling transect and plots from May through September, 2008. Satellite data used are SPOT 4/5 images and 16-day Moderate Resolution Imaging Spectroradiometer (MODIS) 250m, 1km as well as 10-day SPOT-vegetation (SPOT-VGT) NDVI products from May to October, 2007 and 2008. The results show that NDVI is the most suitable VI for quantifying temporal variation of LAI. LAI estimation is much improved by considering both temporal and spatial variations. Based on the ground reflectance data, the r^2 value is increased by 0.05, 0.31, and 0.23 and an averaged relative error is decreased by 1.57, 1.62, and 0.67 in the early, maximum, and late growing season, respectively. MODIS 250m NDVI products are the most useful datasets and MODIS 1km NDVI products are superior to SPOT-VGT 1km composites for monitoring intra-annual spatiotemporal variations in LAI. The proposed LAI estimation

approach can be used in other studies to obtain more accurate LAI, and thus this research will be beneficial for grassland modeling.

ACKNOWLEDGEMENTS

First of all, I would like to thank my supervisor, Dr. Xulin Guo, for her invaluable mentoring and encouragement. Without her constant guidance and encouragement, I would never have completed my thesis. I would like to express my appreciation to my advisory committee members, Dr. Cherie Westbrook and Dr. Abraham Akkerman, for their valuable assistance and guidance and for their precious time on my MSc program.

I would like to acknowledge Natural Sciences and Engineering Research Council of Canada for the funding awarded to Dr. Xulin Guo to make this research happen. I would also like to thank the Department of Geography and Planning and College of Graduate Studies and Research for providing funding to support my study and life.

My gratitude and acknowledgement go to Dr. Steve Shirtliffe, Dr. Cherie Westbrook, and Dr. Xue Li for providing instruments and facilities for my laboratory data collection. Many thanks are given to Xiaohui Yang, Ginette Felske, Yunpei Lu, and Zimu Yu for their essential assistance in collecting field data. I would like to thank the NASA LP DAAC and SPOT VITA data centers for creating and providing NDVI data, and thank Dr. Chris Spence and St. Denis Automatic Weather Station Team for providing the climate data. Thanks also go to the board of St. Denis Wildlife Reserve Area for allowing an access to that area for field data collection. I would also like to acknowledge Aslak Grinsted for developing and providing the wavelet analysis codes.

Finally, I would like to thank my family and friends for their support. Special thanks are given to Zimu Yu, my husband, for his encouragement and unconditional support.

TABLE OF CONTENTS

PERMISSION TO USE.....	i
ABSTRACT.....	ii
ACKNOWLEDGEMENTS.....	iv
TABLE OF CONTENTS.....	v
LIST OF TABLES.....	vii
LIST OF FIGURES.....	viii
LIST OF ACRONYMS OR ABBREVIATIONS USED.....	ix
CHAPTER 1 – INTRODUCTION.....	1
1.1 Research Background.....	1
1.1.1 LAI Estimation Approaches.....	2
1.1.2 Feasibility of LAI Estimation at Different Temporal and Spatial Scales.....	3
1.1.3 Major Factors Affecting the Accuracy of LAI Estimation.....	5
1.1.4 Evaluation of Routinely Produced NDVI Products.....	6
1.1.5 Research Gaps.....	8
1.2 Research Objectives.....	9
1.3 Study Site and Field Data.....	9
1.3.1 Study Site and Sampling Design.....	9
1.3.2 Field Data Sampling and Post-processing.....	11
1.4 Thesis Structure.....	12
1.5 References.....	13
CHAPTER 2 - A SUITABLE VEGETATION INDEX FOR QUANTIFYING TEMPORAL VARIATIONS OF LAI IN SEMI-ARID MIXED GRASSLAND.....	21
2.1 Introduction.....	21
2.2 Materials and Methods.....	23
2.2.1 Data.....	23
2.2.2 VIs Selected for the Study.....	23
2.2.3 Methods for Determining a Suitable VI at Each Growing Stage.....	25
2.2.4 Methods for Determining a Suitable VI for Quantifying LAI Temporal Variation	26
2.3 Results and Discussion.....	26
2.3.1 Temporal Variation of LAI and Effects of Ground Covers.....	26
2.3.2 A Suitable VI for LAI Estimation at Each Growing Stage.....	28
2.3.3 A Suitable VI for LAI Temporal Variation Quantification.....	35
2.4 Conclusions.....	37
2.5 References.....	38

CHAPTER 3 - LAI ESTIMATION IN SEMI-ARID MIXED GRASSLAND BY CONSIDERING BOTH TEMPORAL AND SPATIAL VARIATIONS	42
3.1 Introduction.....	42
3.2 Materials and Methods.....	43
3.2.1 Field Data.....	43
3.2.2 Satellite Data and Preprocessing	43
3.2.3 Methods to Identify the Optimum Spatial Scale for LAI Estimation.....	44
3.2.4 Methods for LAI Estimation from Ground NDVI.....	46
3.2.5 Methods for LAI Estimation from Satellite-Level NDVI	46
3.3 Results and Discussion	47
3.3.1 The Optimum Spatial Scales for LAI Estimation.....	47
3.3.2 LAI Estimation Based on Ground NDVI	50
3.3.3 LAI Estimation from Satellite-Level NDVI.....	53
3.4 Conclusions.....	54
3.5 References.....	55
 CHAPTER 4 - EVALUATION OF NDVI PRODUCTS FOR MONITORING SPATIOTEMPORAL VARIATIONS OF LAI IN SEMI-ARID MIXED GRASSLAND	 59
4.1 Introduction.....	59
4.2 Materials and Methods.....	60
4.2.1 Ground-level Data	60
4.2.3 Satellite-level Data.....	60
4.2.4 Methods	62
4.3 Results and Discussion	64
4.3.1 Comparisons between Satellite-Level and Ground Hyperspectral NDVI.....	64
4.3.2 Differentiating Spatiotemporal Variations of LAI	67
4.4 Conclusions.....	75
4.5 References.....	76
 CHAPTER 5 - SUMMARY	 80
5.1 Conclusions.....	80
5.1.1 A Suitable Vegetation Index for Quantifying Temporal Variations of LAI in Semi-Arid Mixed Grassland.....	80
5.1.2 Improved LAI Estimation While Considering Temporal and Spatial Variations	81
5.1.3 The Most Suitable NDVI Products on Monitoring Variations in LAI.....	82
5.2 Potential Applications.....	83
5.3 Limitations	83
5.4 References.....	84
 APPENDIX A - THE VALIDATION OF PLANT AREA INDEX.....	 87
 APPENDIX B - VALIDATION OF SOIL MOISTURE METER.....	 90
 APPENDIX C - THE SOIL LINE IN St. DENIS.....	 92

LIST OF TABLES

Table 2.1 Vegetation Indices (VIs) selected.....	24
Table 2.2 Correlation of coefficient (r) and coefficient of determination (r^2) between canopy covers and LAI.....	27
Table 2.3 Correlation coefficients (r) between spectral vegetation indices (VIs) and LAI, and percentage of variations in VIs with bare ground reflectance (B), green vegetation (GV), dead vegetation (DV), and their interactions.....	32
Table 2.4 Performances of VIs on quantifying temporal variation of LAI measured by the mean Pearson's r, standard deviation (SD), coefficient of variation (CV), and their ranges.....	36
Table 3.1 The r^2 , root mean squared error (RMSE), averaged relative error (ARE), and bivariate regression equations between NDVI and LAI.....	51
Table 4.1 Characteristics for ground hyperspectral and satellite-level NDVI datasets	61
Table 4.2 Change rates (Slopes) at each two adjacent observation dates of MODIS 250m, 1km, and SPOT-VGT 1km NDVI products in 2007 and 2008.....	71
Table A.1 Differences between plant area index (PAI) and green leaf area index (LAI)	89

LIST OF FIGURES

Figure 1.1 (a) A topography map of the study area with the sampling transect and plots, (b) plot design, and (c) topography profile of the transect derived from LiDAR DEM data.	10
Figure 2.1 Temporal variations in LAI and ground covers from May to September	27
Figure 2.2 The spectral response curves of dead vegetation (Dead veg), green vegetation (green veg), and their mixture (40% green veg) as well as bare soil.....	29
Figure 3.1 Profiles of LAI and soil moisture on 4 June 2008 in St. Denis, SK, Canada..	47
Figure 3.2 Spatial variations of (a) LAI and (b) soil moisture derived from Morlet wavelet analysis on 4 June 2008 in St. Denis, SK, Canada	48
Figure 3.3 The spectra of (a) cross-wavelet and (b) wavelet coherence analysis between LAI and soil moisture on 4 June 2008 in St. Denis, SK, Canada.....	49
Figure 3.4 The relationship between LAI and satellite-level NDVI derived from SPOT 4/5 images at the 95% significance interval during the entire growing season	53
Figure 3.5 Relationships between LAI (y) and NDVI (x) derived from SPOT 4/5 images at the 95% significance interval in different vegetation growing seasons.....	54
Figure 4.1 The NDVI sampling transect on the SPOT imagery with geographic coordinates of the four corners.....	64
Figure 4.2 The scatter plot of satellite-level NDVI against ground NDVI, with Pearson's r values	65
Figure 4.3 Ground hyperspectral and SPOT 4/5 NDVI on monitoring spatiotemporal variations of LAI in semi-arid mixed grassland in 2008	68
Figure 4.4 MODIS 250m NDVI products on monitoring spatiotemporal variations of LAI in the semi-arid mixed grassland in 2007 and 2008.	69
Figure 4.5 MODIS and SPOT-VGT 1km NDVI products on monitoring temporal variations of LAI in the semi-arid mixed grassland in 2007 and 2008.....	70
Figure 4.6 Modeled and experimental variograms of NDVI from (a) SPOT 4 image on May 2 and (b) SPOT 5 image on August 30, 2008.....	74
Figure A.1 The relationship between green leaf area index and plant area index	88
Figure C.1 The soil line developed in St. Denis, Saskatchewan, Canada.....	93

LIST OF ACRONYMS OR ABBREVIATIONS USED

ARE	Averaged Relative Error
ASTER	Advanced Spaceborne Thermal Emission and Reflection Radiometer
ATSAVI	Adjusted Transformed Soil-adjusted Vegetation Index
AVHRR	Advanced Very High Resolution Radiometer
AVNIR-2	Advanced Visible and Near Infrared Radiometer Type 2
CBERS-2	China-Brazil Earth Resources Satellite-2
COI	Cone of Influence
CV	Coefficient of Variation
CV-MVC	Constrained-View MVC
DEM	Digital Elevation Model
DMC	Satellite Disaster Monitoring Constellation
EO-1	Earth Observing-1
GCOS	Global Climate Observation System
GNP	Grasslands National Park
GPS	Global Positioning System
GTOS	Global Terrestrial Observation System
IRS	Indian Resourcesat-1
IRTM	Inversion of Radiative Transfer Model
LAI	leaf Area Index
L-ATSAVI	Litter-Corrected ATSAVI
LiDAR	Light Detection and Ranging
LP DAAC	Land Processes Distributed Active Archive Center
MCARI	Modified Chlorophyll Absorption Ratio Index
MCARI 2	Modified Chlorophyll Absorption Ratio Index 2
MCARI1	Modified Chlorophyll Absorption Ratio Index 1
MODIS	Moderate Resolution Imaging Spectroradiometer
MSAVI	Modified Soil-Adjusted Vegetation Index
MSR	Modified Simple Ratio

MTVI1	Modified Triangular Vegetation Index 1
MTVI2	Modified Triangular Vegetation Index 2
MVC	Maximum Value Compositing
MVI	Multiband Vegetation Imager
NASA	National Aeronautics and Space Administration
NDVI	Normalized Difference Vegetation Index
NIR	Near-Infrared
NOAA	National Oceanic and Atmospheric Administration
PAI	Plant Area Index
PSF	Point Spread Function
PVI	Perpendicular Vegetation Index
RDVI	Renormalized Difference Vegetation
RMSE	Root Mean Squared Error
SARVI	Soil and Atmospheric Resistant Vegetation Index
SAVI	Soil-adjusted Vegetation Index
SD	Standard Deviation
SeaWiFS	Sea-viewing Wide Field-of-view Sensor
SIN	Sinusoidal Projection
SLAID	Standardized LAI Determining Index
SLAIDI*	Modified Standardized LAI Determining Index
SPOT-VGT	SPOT-Vegetation
TRAC	Tracing Radiation and Architecture of Canopies
TSAVI	Transformed Soil-Adjusted Vegetation Index
TVI	Triangular Vegetation Index
USA	The United States of America
UTM	Universal Transverse Mercator
VI	Vegetation Index
VI _s	Vegetation Indices
WCT	Wavelet Coherence Transform
XWT	Cross-Wavelet Transform

CHAPTER 1 – INTRODUCTION

1.1 Research Background

Vegetation plays an important role in the energy, mass and momentum exchange between the land surface and the atmosphere. Leaf Area Index (LAI), defined as one-half the total green leaf area per unit of ground surface area (Chen and Black, 1992), is an indicator of the vertical structure of vegetation. It can reflect vegetation condition, and also can determine canopy water interception, radiation extinction, and water and carbon gas exchange between the land surface and the atmosphere. Therefore, LAI is a key parameter of the land surface-atmosphere interaction modeling (Knyazikhin et al., 1998). Currently, the models are initiated by either field validation of simulated LAI, remotely sensed LAI estimation (Running et al., 1999), or Normalized Difference Vegetation Index (NDVI, the ratio of difference and sum of reflectance of Near-infrared and red bands) data routinely derived from satellite imagery (Lu and Shuttleworth, 2002). However, the accuracy of LAI estimation greatly varies as methods, locations, and time vary, and differences in NDVI data from various remote sensors are observable. Practically, many models are very sensitive to LAI and its temporal and spatial variations (Bonan, 1993; Chase et al., 1996). Therefore, accurate LAI estimation and the most appropriate NDVI product, which can successfully monitor temporal and spatial variations in LAI, are needed for successful modeling.

Thus, this research aims to improve LAI estimation and to determine the optimum NDVI product on monitoring LAI temporal and spatial variations. The purposes of this literature review therefore are to review: 1) LAI estimation approaches and their advantages and disadvantages; 2) the feasibility of LAI estimation at different temporal and spatial scales; 3) the effect of different factors on LAI estimation; and 4) evaluation of routinely produced NDVI products on monitoring spatiotemporal variations of LAI.

1.1.1 LAI Estimation Approaches

Direct and indirect methods are the two main categories for determining LAI. The former is a ground-based approach which involves destructive sampling, litterfall collection, and point contact sampling (Norman and Campbell, 1989; Daughtry et al., 1990; Andrieu and Sinoquet, 1993). It is the most accurate on a per plant or site basis (Jonckheere et al., 2004), but with the disadvantages of being extremely time consuming, tedious (Lang, 1985), and destructive to plants. As a consequence, a large-scale implementation is only marginally feasible (Jonckheere et al., 2004). The other drawback of direct methods is that the definition of LAI, the up-scaling method, or the error accumulation due to frequently repeating measurements can result in large errors (Jonckheere et al., 2004). Overall, direct LAI determination is not really compatible with the long-term monitoring of spatial and temporal dynamics of leaf area development (Chason et al., 1991).

In contrast, indirect optical methods, consisting of the LAI instrument measurement and LAI estimation from remotely sensed data, hold the greatest potential to carry out quick and low-cost measurements. However, commercial optical instruments, such as LAI-2000 plant canopy analyzer (LI-COR, Lincoln, Nebraska) and Sunfleck Ceptometer (Decagon Devices, Pullman, Washington), are sometimes constrained because of the complexity of natural canopy architecture. Several studies have drawn the conclusion that, compared to the direct measurements, indirect instrument measurements underestimate LAI (e.g., Chason et al., 1991; Lang et al., 1991; Smith et al., 1993; Fassnacht et al., 1994; Vertessy et al., 1995; Comeau et al., 1998; Kùßner and Mosandl, 2000). About 25% - 50% underestimation is explored in different stands (Gower and Norman, 1991; Cutini et al., 1998; Gardingen et al., 1999; Gower et al., 1999). The degree of error in the LAI measurement is mainly determined by ‘clumping’, a term used to describe the canopy’s deviation from the assumption of random dispersion (Nilson, 1971; Lang, 1986, 1987; Chen et al., 1997; Kucharik et al., 1997). The error is also influenced by the boundary and illumination conditions, data aggregation techniques, and sampling schemes. Many solutions have been introduced to lessen the clumping bias. For example, two new

instruments have been developed to measure the between-shoot clumping factor: the Tracing Radiation and Architecture of Canopies (TRAC) developed by Chen et al. (1997) and the Multiband Vegetation Imager (MVI) developed by Kucharik et al. (1997). Besides the underestimation problem of LAI instruments, it is also time consuming and impossible to acquire highly accurate and frequent LAI values across a large area. As a site-based measurement, it can impede the ability to input information into a grid-based model, such satellite images can do.

The other indirect method is implemented by deriving LAI from remotely sensed data, which makes it possible to estimate LAI at local, regional, and global scales. The main approaches of retrieving LAI from remotely sensed reflectance data include a spectral mixture analysis (Peddle and Johnson, 2000; Pacheco et al., 2001; Hu et al., 2004), an inversion of Radiative Transfer Models (RTM) (Goel and Thompson, 1984; Running et al., 1996), and empirical models of spectral vegetation indices (VIs, calculated from the combined information of two or more bands of remote sensing)-LAI relationships. The spectral mixture analysis has not been widely used due to the difficulty and uncertainty in obtaining end-members. The RTM approach is constrained by a long-time computation and complex inputs (Goel and Thompson, 1984; Running et al., 1996). To shorten the computation time, Look Up Table (LUT) (Knyazikhin et al., 1998; Weiss et al., 2000) and Neural Network (NN) (Danson et al., 2003) approaches have been developed. To reduce the complexity of inputs, the concept of canopy invariants (Huang et al., 2007) recently has been proposed. Although the LUT and NN approaches as well as the concept of canopy invariants make it more applicable, the RTM approach is more suitable for LAI estimation in a homogeneous area (Fang et al., 2003). Thus, establishing an empirical model from a LAI-VI relationship becomes the most commonly and widely used approach for LAI estimation (Chen and Cihlar, 1996; Fassnacht et al., 1997; Wulder et al., 1998).

1.1.2 Feasibility of LAI Estimation at Different Temporal and Spatial Scales

With the advent of the Earth Observation System (EOS) and other satellite systems, planet Earth can be closely watched by multiple sensors with various observing geometries and

spatial and temporal resolutions. The characteristics of hypertemporal images, which usually refer to daily acquired imagery, such as MODIS (the Moderate Resolution Imaging Spectroradiometer) and NOAA/AVHRR (the National Oceanic and Atmospheric Administration/Advanced Very High Resolution Radiometer), make it possible to estimate LAI over different time scales. However, it might be difficult to obtain daily LAI estimates with a good quality because the images are easily contaminated by clouds. Fortunately, vegetation does not change too much in a short time period, so the daily LAI estimates can be obtained by an interpolation or extrapolation from LAI collected on adjacent dates. At the same time, the multiple-spatial resolution satellite imagery (e.g., MODIS 250m, AVHRR 1km, SPOT 4 20m, SPOT 5 10m, and Landsat TM 30m), together with the LAI-VI relationships or radiative transfer models, make it theoretically feasible to estimate LAI over different spatial scales.

In practice, however, it is difficult to obtain accurate LAI values over different scales especially on a heterogeneous land surface. The difficulty is caused by the scale-dependence of the factors affecting LAI estimation (Wu et al., 2002; He et al., 2006), the surface heterogeneity in terms of mixed cover types (Fernandes et al., 2004), and the development of downscaling or upscaling techniques. Pixels with mixed cover types are considered to be the main cause of random errors because radiative signals from different vegetation types are quite different at the same LAI. Accurate information about a subpixel mixture of various cover types is identified as the key to improving the accuracy of LAI estimates based on the satellite imagery (Chen, 1999; Tian et al., 2002; Fernandes et al., 2004). Rahman et al. (2003) and He et al. (2006) suggested that an appropriate spatial scale for studying different variables can avoid the potential errors arising from heterogeneity and the patchiness from upscaling or downscaling physiological processes. Chen (1999) declared that the relation between LAI and NDVI was scale-dependent, although conflicting information was observed in the literature as to whether it was spatial resolution dependent or invariant (Hall et al., 1992; Friedl, 1996; Hu and Islam, 1997). Hence, it is necessary to determine the most suitable spatial resolution for LAI estimation to minimize the effects of a subpixel mixture of various cover types.

1.1.3 Major Factors Affecting the Accuracy of LAI Estimation

LAI is determined by vegetation structures. Vegetation is highly related to its phenology, which is driven by either temperature in mid-latitude and high latitude zones (Zhang et al., 2004) or the soil water budget in arid and semiarid areas (Loik et al., 2004). The soil water budget is influenced by precipitation and it determines soil moisture. At the same time, soil moisture is highly controlled by topography (Western et al., 1998). Thus, LAI is a function of vegetation condition, which further is a function of species composition, soil moisture, topography, temperature, and precipitation.

Research has been carried out to investigate the relationships between LAI and ecological parameters (e.g. soil moisture and topography) as well as environmental variables. The LAI values of both maritime pine (*Pinus pinaster*, *Hort.Kew.3:367*) and the understory of dwarf moor grass (*Molinia caerulea*, *Methodus 183*) depend on the moisture deficit in the soil (Loustau et al., 1992, 1996). A further study in the area shows that a linear LAI will decrease with the soil moisture deficit above a threshold and within the relevant period (Kramer et al., 2000). He et al. (2006) asserted that LAI within a 30m scale is controlled by soil moisture in semi-arid grasslands and it is determined by topography at a 110m scale. LAI as an important indicator of biomass, is also highly related to the climate variables, and is further strengthened by the close relationship between biomass and climate variables (e.g. Elliott et al., 2006). The accuracy of LAI estimation can be increased by considering the effects of factors, such as soil moisture and climate variables.

The Vegetation Index (VI), a single value estimated from multispectral scanning measurements to assess and predict vegetative characteristics including LAI, is another factor to determine the accuracy of LAI estimation from remotely sensed data. A VI is usually associated with vegetation densities, species composition, background soil, atmospheric effects, as well as bandwidth and radiometric resolutions of the sensors. Normally Vegetation Indices (VIs) increase along with the vegetation density, which can be characterized by a LAI increase, until the density reaches a maximum threshold. Beyond the peak point, VIs remain relatively unchanged as the vegetation density

increases (e.g., Chen and Cihlar, 1996; Carlson and Rizley, 1997). This situation is called saturation, which limits the application of VIs for LAI estimation. Since the first well-known VI—the simple ratio, the ratio of reflectance of red band and near-infrared band (Jordan, 1969), was proposed, hundreds of VIs have been developed. These VIs establish the connections between LAI and remotely sensed data. However, various VIs perform differently for LAI estimation, and the performance of a certain VI varies with different ground cover and species composition. Furthermore, each VI has its own drawbacks and merits according to its own theoretical base. Therefore, evaluating VIs and selecting an appropriate VI are essential for improving LAI estimation.

1.1.4 Evaluation of Routinely Produced NDVI Products

Frequently and internally consistent remotely sensed information on spatial complexity and temporal dynamic is essential for successfully monitoring or quantifying spatial and temporal variability in LAI at a local, regional or global scale. Such information is now regularly processed into VIs (DeFries and Belward, 2000; Cracknell, 2001; Tarnavsky et al., 2008). NDVI, one of the most widely used VIs, has been routinely derived from NOAA/AVHRR satellite imagery since 1981 (Tarnavsky et al., 2008). The routinely produced NDVI products have since become one of the important data sources for monitoring LAI spatiotemporal variation (Huete et al., 1994; Leprieur et al., 2000). Recently, NDVI products have also been generated from MODIS and the SPOT-Vegetation (SPOT-VGT) imaging sensors that are improved upon the spectral, spatial, and radiometric properties of AVHRR (Myneni et al., 1995). MODIS and SPOT-VGT NDVI products therefore are considered to be the improved measurements of surface vegetation dynamic (Justice et al., 2000; Huete et al., 2002; Maisongrande et al., 2004; Tarnavsky et al., 2008). Although their data records are about 20 years shorter than AVHRR NDVI products, which will hamper their use in climate change studies, both MODIS and SPOT-VGT NDVI products have a relatively long data record starting from 2000 and 1998, respectively. Consequently, these NDVI products have been widely used as intermediaries in the assessment of various biophysical parameters, such as LAI, in

various models at different spatial scales (Van den Hurk et al., 2003). However, differences in diverse NDVI products are observable due to the differences in sensor characteristics, such as spectral response function (Trishchenko et al., 2002) and point spread function (Wolfe et al., 1998; Tan et al., 2006; Tarnavsky et al., 2008). Besides, the differences are also attributed to the compositing period (Fensholt et al., 2007) and methodology (Wolfe et al., 1998), and other factors including atmospheric correction (van Leeuwen et al., 2006) and geolocation accuracy (Wolfe et al., 2002). The difference in NDVI products from different sensors could result in 1.5% variations in averaged annual evapotranspiration in the Semi-distributed Land Use-based Runoff Processes (SLURP) model (Ha et al., 2008). Thus, close attention to the consistency of various NDVI products has been paid since they were routinely produced. Substantial efforts have been exerted to investigate the inter-annual consistency of NDVI products related to spectral differences (Goetz, 1997; Thomlinson et al., 1999; Justice et al., 2000; Steven et al., 2003; Tucker et al., 2005; Brown et al., 2006). Some studies have also been carried out on the assessment of the spatial consistency (Goodin and Henebry, 2002; Tarnavsky et al., 2008). These studies have made a significant contribution to combining various NDVI products from different sensors into a long data record.

In conclusion, the directly measured LAI from destructive methods is important for validating LAI estimation from remotely sensed data, although it is practically impossible to be used in a large scale. The ground-based indirect approach, referring to LAI instrument measurements, is another important data source for validating LAI estimation. However, similar as direct measurements, it is also impractical in the use of large-scale. The other indirect methods related to remote sensing, mainly involving LAI-VI relationships, spectral mixture analysis, and RTM, are promising to estimate LAI over different scales as the advent of imagery with multiple temporal and spatial resolutions. Among the three methods, the LAI-VI relationship is the most commonly used and applicable approach. However, its accuracy is limited by the spatial and temporal variations in LAI controlled by ground cover, soil moisture and other factors, such as temperature and precipitation. It therefore is necessary to improve LAI estimation by

considering the most appropriate temporal and spatial scales. Besides, determining the optimum VI is also important to improve LAI estimation.

Routinely produced NDVI products have become one of the most important spectral information resources for estimating biophysical parameters for the land surface-atmosphere interaction modeling. Nonetheless, performances of NDVI composites derived from different imaging sensors are different in a certain degree due to dissimilar intrinsic properties of sensors and post-processing methods. These differences in NDVI will ultimately alter model outputs. Hence, it is essential to determine the suitable NDVI products for modeling in which NDVI is used to estimate LAI or other biophysical parameters.

1.1.5 Research Gaps

A LAI-VI relationship is the most effective and practical approach to timely and efficiently obtain LAI data over multiple scales. The accuracy of LAI estimation from a VI derived from satellite imagery, however, varies a lot due to the spatial and temporal variations of LAI affected by ground cover, topography, soil moisture, temperature, and precipitation. Many studies have pinpointed that LAI estimation can be improved by selecting the optimum time, spatial resolution imagery, or a VI. Relatively few studies, however, have been accomplished to estimate LAI while taking all the three factors into account.

NDVI products have been more and more widely used to be intermediaries of biophysical parameters, such as LAI, in various models. However, the difference in NDVI values from various sensors is observable, which thus results in different model outputs. Considerable efforts therefore have been exerted on investigating inter-annual and spatial agreements of NDVI products. However, relative little research has been done to evaluate NDVI products on monitoring or quantifying intra-annual temporal and spatial variations of LAI. In addition, performances of one specific NDVI product are changeable under different land

covers. Therefore, it is necessary to determine the optimum NDVI products for monitoring spatiotemporal variations in LAI in semi-arid mixed grassland.

1.2 Research Objectives

To fill up the research gaps and thus provide more accurate LAI data for the land surface-atmosphere interaction modeling, this thesis aims to

- Determine a suitable VI for quantifying LAI temporal variation
- Improve LAI estimation by considering both temporal and spatial variations in LAI
- Evaluate routinely produced NDVI products on monitoring temporal and spatial variations in LAI

1.3 Study Site and Field Data

1.3.1 Study Site and Sampling Design

To share the biophysical data and climatic data with other research groups in the university of Saskatchewan, the study site was selected in tamed and native grassland in St. Denis National Wildlife Reserve Area (NWA) (52° 12' 29" N, 106° 5'30" W), Saskatchewan, Canada. Tamed grassland was transformed from the previously cultivated land by seeding smooth brome grass (*Bromus inermis*, *Fl. Halens.* 16) and alfalfa (*Medicago sativa*, *Sp. Pl.* 2: 778-779) for the nesting cover of birds. Native grassland is a typical mixed grass prairie with dominant vegetation of June grass (*Koeleria spp.*, *Ess. Agrostogr.* 84, 166, 175), and forbs. Wheat grass (*Agropyron spp.*, *Novi Comment. Acad. Sci. Imp. Petrop.* 14:540) was also observed in native grassland. Since neither grazing nor fire conservation has been applied since 1960's (Environment Canada, 2009), non-photosynthesis vegetation, including standing dead and litter, is predominant in the early and late growing season. The annual mean air temperature at the Saskatoon Airport is 2°C, with monthly means of -19°C in January and 18°C in July, and the mean annual precipitation in Saskatoon is 360mm.

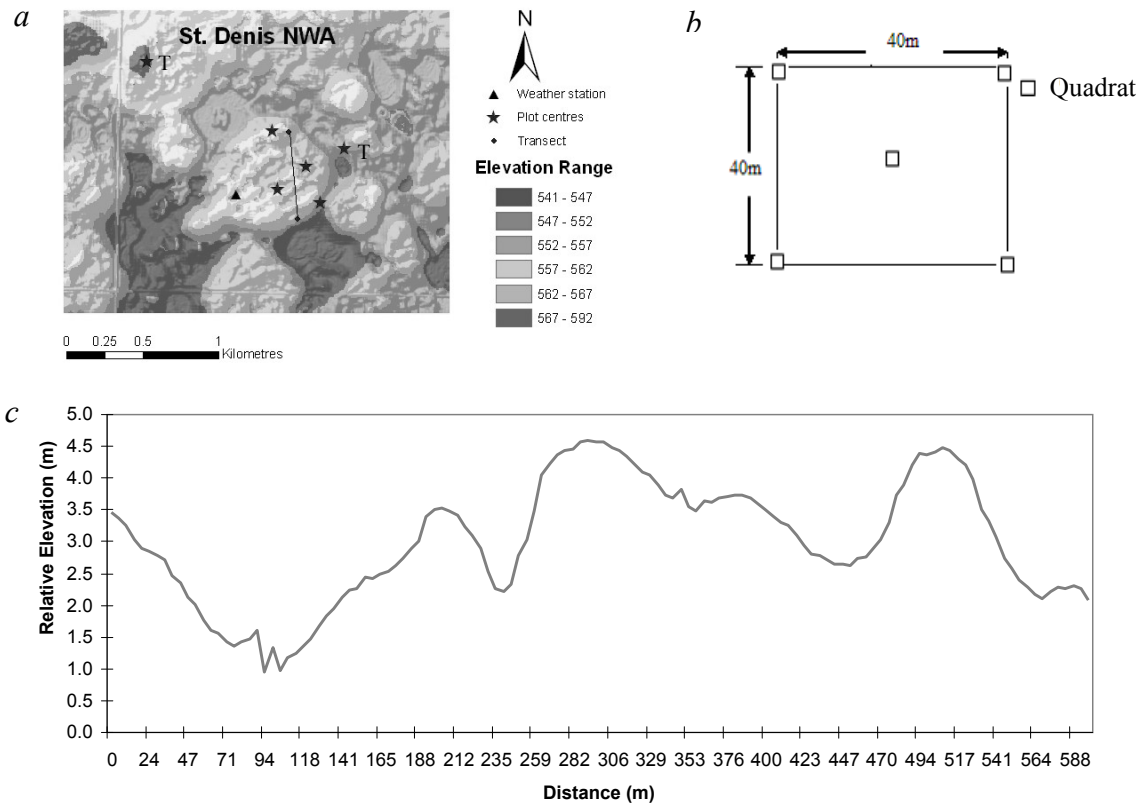


Figure 1.1 (a) A topography map of the study area with the sampling transect and plots, (b) plot design, and (c) topography profile of the transect derived from LiDAR DEM data.

One sampling transect and six plots were set up for data collection. The approximate 600 m-long transect was set up with 128 sampling points at a 4.7 m interval (**Figure 1.1a**) across the rolling topography (**Figure 1.1c**). It is paralleled to the transect used by Si and Farrell (2004), which was specifically designed for utilizing a wavelet approach to investigate spatial variation scales of soil moisture. The transect used in this study is 20 m away from Si's transect to avoid the trampled vegetation. Thus the two transects are across a similar topography with three rolling cycles.

The six plots were randomly set up in different vegetation communities, and each plot covers a relatively homogenous area with a size of 40×40 m, which was specifically designed for the application of SPOT 4 and 5 images (McCoy, 2005). Five measurements were taken within each plot (**Figure 1.1b**), and each measurement was completed within a

50×50 cm quadrat. The five quadrat measurements were arithmetically averaged to represent the mean value of a measured variable within one plot for data analyses.

1.3.2 Field Data Sampling and Post-processing

Field data collected were Plant Area Index (PAI, the projected area of all vegetation parts normalized by subtending ground area, Zhang and Guo, 2008), soil moisture, ground covers and canopy reflectance. They were collected over the sampling transect and plots on 19 May, 4 June, 17 June, 2 July, 21 July, 15 August, 29 August, and 15 September in 2008. The accuracy of the plot sampling design on LAI measurements was estimated by computing the relative error between the simulated NIR (790-870nm) reflectance from quadrats and NIR reflectance retrieved from SPOT 4/5 images from the entire plot. The accuracy can be estimated in this approach because LAI is highly associated with NIR reflectance. The estimated accuracy of the sampling design is 91.8% to 98.2%.

PAI was measured by a LAI-2000 Plant Canopy Analyzer (LI-COR Inc., Lincoln, Nebraska, USA) through the inversion of a radiative transfer model based on the canopy light interception. The canopy light interception within each quadrat is the result of one above-canopy reading and six below-canopy readings. The term “PAI” was used instead of LAI due to the big contribution of dead vegetation and other parts of green vegetation except green leaves on the light interception. To obtain LAI, PAI was validated by a destructive sampling method (**Appendix A**). In this thesis, LAI refers to the validated PAI.

Soil moisture was measured over a 6–cm depth using the ThetaProbe ML2X soil moisture meter (Delta–T Devices Ltd, Burwell, Cambridge, UK). The meter was validated following the procedures recorded in **Appendix B**. Ground cover was visually estimated on the basis of 100%.

Canopy reflectance was measured via an ASD Spectroradiometer (Boulder, Colorado, USA) within two hours of solar noon on sunny days. The wavelength ranges from 350 to 2500 nm with a spectral resolution of 3 nm at 700 nm and 10 nm at 1400 nm and 2100 nm.

The field of view of the probe was 25° and the sensor was pointing down to the canopy at 1m above ground.

1. 4 Thesis Structure

This thesis was organized in five chapters. Chapter 1 consists of a general review of pertinent literature, research gaps, the research objectives, the study area and field data collection, and the thesis structure. The literature reviewed LAI estimation approaches and their advantages and disadvantages, LAI estimation at different spatial and temporal scales, major factors affecting the accuracy of LAI estimation, and evaluations of routinely produced NDVI products in a broad way.

Chapter 2 focuses on determining a suitable VI for quantifying LAI temporal variation, which is the basis to achieve the objective 2 (to improve LAI estimation by considering both temporal and spatial variations). This chapter mainly consists of three sections. The first section is to investigate temporal variation of LAI and effects of ground cover. The second places an emphasis on determining a suitable VI for LAI estimation at each growing stage. Finally, a suitable VI for LAI estimation and quantifying LAI temporal variation is determined.

Chapter 3 comprised of three sections is to achieve the objective 2. Section 1 is to find out the optimum spatial scale for LAI estimation. Section 2 is to estimate LAI by considering temporal and spatial variations using the ground hyperspectral NDVI. Section 3 validates the LAI estimation approach by determining LAI from SPOT 4 and SPOT 5 satellite imagery.

Chapter 4 investigates performances of 16-day MODIS 250m and 1km, and 10-day SPOT-VGT 1km NDVI products on monitoring temporal and spatial variations in LAI in the study area.

In chapter 5, the conclusions of chapter 2, 3, and 4 are summarized and linked back to the literature review. In addition, potential applications and limitations of the present research are discussed, and recommendations for future work relating to this thesis are made.

1.5 References

- Andrieu, B., and Sinoquet, H. 1993. Evaluation of structure description requirements for predicting gap fraction of vegetation canopies. *Agricultural and Forest Meteorology*, Vol. 65, pp. 207-227.
- Bonan, G.B. 1993. Importance of leaf area index and forest type when estimating photosynthesis in boreal forests. *Remote Sensing of Environment*, Vol. 43, pp. 303- 313.
- Brown, M.E., Pinzón, J.E., Didan, K., Morisette, J.T., and Tucker, C.J. 2006. Evaluation of the Consistency of Long-Term NDVI Time Series Derived From AVHRR, SPOT-Vegetation, SeaWiFS, MODIS, and Landsat ETM+ Sensors. *IEEE Transactions on Geoscience and Remote Sensing*, Vol. 44, no. 7, pp.1787-1793.
- Carlson, T.N., and Riziley, D.A. 1997. On the Relation between NDVI, Fractional Vegetation Cover, and Leaf Area Index. *Remote Sensing of Environment*, Vol. 62, pp. 241-252.
- Chase, T.N., Pielke, R.A., Kittel, T.G.F., Nemani, R., and Running, S.W. 1996. The sensitivity of a general circulation model to global changes in leaf area index. *Journal of Geophysical Research*, Vol. 101, pp. 7393-7408.
- Chason, J.W., Baldocchi, D.D., and Huston, M.A. 1991. A comparison of direct and indirect methods for estimating forest canopy leaf area. *Agricultural and Forest Meteorology*, Vol. 57, pp. 107-28.
- Chen, J.M., and Black, T.A. 1992. Defining leaf area index for non-flat leaves. *Plant, Cell and Environment*, Vol. 15, pp. 421-429.
- Chen, J.M., and Cihlar, J. 1996. Retrieving leaf area index of boreal conifer forests using Landsat TM images. *Remote Sensing of Environment*, Vol. 55, pp. 153-162.
- Chen, J.M., Rich, P.M., Gower, T.S., Norman, J.M., and Plummer, S. 1997. Leaf area index of boreal forests: theory, techniques and measurements. *Journal of Geophysical Research*, Vol. 102, pp. 429-444.

- Chen, J.M. 1999. Spatial scaling of a remotely sensed surface parameter by contexture. *Remote Sensing of Environment*, Vol. 69, pp. 30-42.
- Comeau, P.G., Gendron, F., and Letchford, T. 1998. A comparison of several methods for estimating light under a paper birch mixed wood stand. *Canadian Journal of Forest Research*, Vol. 28, pp. 1843-1850.
- Cracknell, A.P. 2001. The exciting and totally unanticipated success of the AVHRR in applications for which it was never intended. *Advances in Spatial Research*, Vol. 28, No. 1, pp. 233-240.
- Cutini, A., Matteucci, G., and Mugnozza, G.S. 1998. Estimation of leaf area index with the LI-COR LAI 2000 in deciduous forests. *Forest Ecology and Management*, Vol.15, pp.55-65.
- Danson, F.M., Rowland, C. S., and Baret, F. 2003. Training a neural network with a canopy reflectance model to estimate crop leaf area index. *International Journal of Remote Sensing*, Vol. 24, No. 23, pp. 4891-4905.
- Daughtry, C.S.T., Kustas, W.P., Moran, M.S., Pinter, P.J., Jackson, R.D., Brown, P.W., Nichols, W.D., and Gay, L.W. 1990. Spectral estimates of net-radiation and soil heat-flux. *Remote Sensing of Environment*, Vol. 32, No.2-3, pp. 111-124.
- DeFries, R.S., and Belward, A.S. 2000. Global and regional lands cover characterization from satellite data: An introduction to the special issue. *International Journal of Remote Sensing*, Vol. 21, No. 6&7, pp.1083-1092.
- Elliott, J.A., Jones, I.D., and Thackeray, S.J. 2006. Testing the sensitivity of phytoplankton communities to changes in water temperature and nutrient load, in a temperate lake. *Hydrobiologia*, Vol. 559, pp. 401-411.
- Environment Canada, 2009, available online at: www.mb.ec.gc.ca/whp/nwa/df06s09.en.html (accessed 24 March 2009)
- Fang, H., Liang, S., and Kuusk, A. 2003. Retrieving leaf area index using a genetic algorithm with a canopy radiative transfer model. *Remote Sensing of Environment*, Vol. 85, No. 3, pp. 257-270.
- Fassnacht, K.S., Gower, S.T., Norman, J. M., and Mcmurtrie, R. E. 1994. A comparison of optical and direct methods for estimating foliage surface area index in forests. *Agricultural and Forest Meteorology*, Vol. 94, No. 71, pp. 183-207.
- Fassnacht, K.S., Gower, S.T., Mackenzie, M.D., Nordheim, E.V., and Lillesand, T.M. 1997. Estimating the leaf area index of north central Wisconsin forest using Landsat Thematic Mapper. *Remote Sensing of Environment*, Vol. 61, pp. 229-245.

- Fensholt, R., Anyamba, A., Stisen, S., Sandholt, I., Pak, E., and Small, J. 2007. Comparison of compositing period length for vegetation index data from polar-orbiting and geostationary satellites for the cloud-prone region of West Africa. *Photogrammetric Engineering and Remote Sensing*, Vol. 73, No. 3, pp. 297-309.
- Fernandes, R., Fraser, R., Latifovic, R., Cihlar, J., Beaubien, J., and Du, Y. 2004. Approaches to fractional land cover and continuous field mapping: A comparative assessment over the BOREAS study region. *Remote Sensing of Environment*, Vol. 89, pp. 234-251.
- Friedl, M. A. 1996. Examining the effects of sensor resolution and subpixel heterogeneity on spectral vegetation indices: implications for biophysical modeling. *Scaling of Remote Sensing Data for GIS*, D.A. Quattrochi, and M. F. Goodchild Eds., Lewis, New York. pp. 113-139.
- Gardingen, P.R.van, Jackson, G.E., Hernandez-Daumas, S., Russell, G., and Sharp, L. 1999. Leaf area index estimates obtained for clumped canopies using hemispherical photography. *Agricultural and Forest Meteorology*, Vol. 94, No. 3-4, 243-257.
- Goel, N.S., and Thompson, R.L. 1984. Inversion of Agricultural and Forest Meteorology vegetation canopy reflectance models. IV. Total inversion of the SAIL model. *Remote Sensing of Environment*, Vol. 15, pp. 237-253.
- Goetz, S.J. 1997. Multi-sensor analysis of NDVI, surface temperature, and biophysical variables at a mixed grassland site. *International Journal of Remote Sensing*, Vol. 18, No. 1, pp. 71-94.
- Goodin, D.G., and Henebry, G.M. 2002. The effect of rescaling on fine spatial resolution NDVI data: A test using multi-resolution aircraft sensor data. *International Journal of Remote Sensing*, Vol. 23, No. 18, pp. 3865-3871.
- Gower, S.T., and Norman, J.M. 1991. Rapid Estimation of Leaf Area Index in Conifer and Broad-Leaf Plantations. *Ecology*, Vol. 72, No. 5, pp.1896-1900.
- Gower, S.T., Kucharik, C.J., and Norman, J.M. 1999. Direct and indirect estimation of leaf area index, f (APAR), and net primary production of terrestrial ecosystems. *Remote Sensing of Environment*, Vol. 70, No. 1, pp. 29-51.
- Ha, R., Shin, H.J., Park, G.A., and Kim, S.J. 2008. The Influence of Remotely Sensed Leaf Area Index (LAI) on the Estimation of Evapotranspiration from SLURP Model. The 2008 ASABE Annual International Meeting, June 29-July 2, Providence, Rhode Island.

- Hall, F.G., Huemmrich, K.F., Goetz, S.J., Sellers, P.J., and Nickeson, J. E. 1992. Satellite remote sensing of surface energy balance: success, failures, unresolved issues in FIFE. *Journal of Geophysical Research*, Vol. 97, No. D17, pp. 19061-19089.
- He, Y., Guo, X., Wilmshurst, J., and Si, B. 2006. Studying mixed grassland ecosystems II: optimum pixel size. *Canadian Journal of Remote Sensing*, Vol. 32, No. 2, pp. 108-115.
- Hu, Z., and Islam, S. 1997. A framework for analyzing and designing scale invariant remote sensing algorithms. *IEEE Transactions on Geoscience Remote Sensing*, Vol. 35, No. 3, pp. 747-755.
- Huang, D., Knyazikhin, Y., Dickinson, R.E., Rautiainen, M., Stenberg, P., Disney, M., Lewis, P., Cescatti, A., Tian, Y., Verhoef, W., Martonchik J.V., and Myneni, R.B. 2007. Canopy spectral invariants for remote sensing and model applications. *Remote Sensing of Environment*, Vol. 106, No. 1, pp. 106-122.
- Huete, A., Justice, C., and Liu, H. 1994. Development of vegetation and soil indices for MODIS-EOS. *Remote Sensing of Environment*, Vol. 49, pp. 224-234.
- Huete, A., Didan, K., Miura, T., and Rodriguez, E. 2002. Overview of the radiometric and biophysical performance of the MODIS vegetation indices. *Remote Sensing of Environment*, Vol. 83, No. 1 & 2, pp.195-213.
- Jonckheere, I., Fleck, S., Nackaerts, K., Muys, B., Coppin, P., Weiss, M., and Baret, F. 2004. Review of methods for in situ leaf area index determination Part I. Theories, sensors and hemispherical photography. *Agricultural and Forest Meteorology*, Vol. 121, No. 1-2, pp.19-35.
- Jordan, C.F. 1969. Derivation of leaf-area index from quality of light on the forest floor. *Ecology*, Vol. 50, pp. 440-151.
- Justice, C., Belward, A.S., Morisette, J., Lewis, P., Privette, J., and Baret, F. 2000. Developments in the 'validation' of satellite sensor products for the study of the land surface. *International Journal of Remote Sensing*, Vol. 21, No. 17, pp. 3383-3390.
- Knyazikhin, Y., Martonchik, J.V., Myneni, R.B., Diner, D.J., and Running, S.W. 1998. Synergistic algorithm for estimating vegetation canopy leaf area index and fraction of absorbed photosynthetically active radiation from MODIS and MISR data. *Journal of Geophysical Research*, Vol. 103, No. D24, pp. 32257-32276.
- Kramer, K., Leinonen, I., and Loustau, D. 2000. The importance of phenology for the evaluation of impact of climate change on growth of boreal, temperate and Mediterranean forests ecosystems: an overview. *International Journal of Biometeorology*, Vol. 44, pp. 67-75.

- Kucharik, C.J., Norman, J.M., Murdock, L.M., and Gower, S.T. 1997. Characterizing canopy nonrandomness with a multiband vegetation imager (MVI). *Journal of Geophysical Research*, Vol. 102, No. D24, pp. 29455-29473.
- Küßner, R., and Mosandl, R. 2000. Comparison of direct and indirect estimation of leaf area index in mature Norway spruce stands of eastern Germany. *Canadian Journal of Forest Research*, Vol. 30, pp. 440-447.
- Lang, R.H. 1985. Microwave inversion of leaf area index and inclination angle distributions from backscattered data. *IEEE transactions on Geosciences and Remote Sensing*, Vol. 23, pp. 685-694.
- Lang, A.R.G. 1986. Leaf area and average leaf angle from transmission of direct sunlight. *Australian Journal of Botany*, Vol. 34, pp. 349-355.
- Lang, A.R.G. 1987. Simplified estimate of leaf area index from transmittance of the sun's beam. *Agricultural and Forest Meteorology*, Vol. 41, pp. 179-186.
- Lang, A.R.G., McMurtrie, R.E., and Benson, M.L. 1991. Validity of surface area indices of *Pinus radiata* estimated from transmittance of the sun's beam. *Agricultural and Forest Meteorology*, Vol. 57, pp. 157-170.
- Loik, M.E., Breshears, D.D., Lauenroth, W.K., and Belnap, J. 2004. A multi-scale perspective of water pulses in dryland ecosystems: climatology and ecohydrology of the western USA. *Oecologia*, Vol. 141, pp. 269-281.
- Leprieur, C., Kerr, Y.H., Mastorchio, S., and Meunier, J.C. 2000. Monitoring vegetation cover across semi-arid regions: Comparison of remote observations from various scales. *International Journal of Remote Sensing*, Vol. 21, No. 2, pp. 281-300.
- Loustau, D., Berbigier, P., Granier, A., and El Hadj Moussa, F. 1992. Interception loss, through fall and stemflow in a maritime pine stand. I. Variability of throughfall and stemflow beneath the pine canopy. *Journal of Hydrology*, Vol.138, pp. 449-467.
- Loustau, D., Berbigier, P., Roumagnac, P., Arruda-Pacheco, C., David, S.A., Ferreira, M.I., Perreira, J.S., and Tavares, R. 1996. Transpiration of a 64-year-old maritime pine stand in Portugal. I. Seasonal course of water flux through maritime pine. *Oecologia*, Vol. 107, pp. 33-42.
- Lu, L.X., and Shuttleworth, W.J. 2002. Incorporating NDVI-derived LAI into the climate version of RAMS and its impact on regional climate. *Journal of Hydrometeorology*, Vol. 3, pp. 347-362.

- Maisongrande, P., Duchemin, B., and Dedieu, G. 2004. Vegetation/SPOT: An operational mission for the Earth monitoring: Presentation of new standard products. *International Journal of Remote Sensing*, Vol. 25, No. 1, pp. 9-14.
- Mccooy, R. M. (Ed.) 2005. *Field Methods in Remote Sensing*, pp. 23 (New York: The Guildford Press).
- Myneni, R.B., Hall, F.G., Sellers, P.J., and Marshak, A.L. 1995. The interpretation of spectral vegetation indexes. *IEEE Transactions Geosciences and Remote Sensing*, Vol. 33, No. 2, pp. 481-486.
- Nilson, T. 1971. A theoretical analysis of the frequency of gaps in plant stands. *Agricultural and Forest Meteorology*, Vol. 8, pp. 25-38.
- Norman, J.M., and Campbell, G.S. 1989. Canopy structure. In: Pearcy RW, Ehleringer JR, Mooney HA, Rundel PW, eds. *Plant physiological ecology: field methods and instrumentation*. London: Chapman and Hall, pp. 301-325.
- Pacheco, A., Bannari, A., Deguise, J-C., Mcnaim, H., and Staenz, K. 2001. Application of hyperspectral remote sensing for LAI estimation in precision farming. In *proceedings of the 23rd Canadian Symposium on Remote Sensing, 20-24 August 2001, Ste. Foy, Quebec, Canada*, pp. 281-287.
- Peddle, D., and Johnson, R. 2000. Spectral mixture analysis of airborne remote sensing imagery for improved prediction of LAI in mountainous terrain, Kananaskis Alberta. *Canadian Journal of Remote Sensing*, Vol. 26, pp. 177-188.
- Rahman, A.F., Gamon, J.A., Sims, D.A., and Schmidts, M. 2003. Optimum pixel size for hyperspectral studies of ecosystem function in southern California chaparral and grassland. *Remote Sensing of Environment*, Vol. 84, pp. 192-207.
- Running, S.W., Nemani, R., and Glassy, J.M. 1996. MOD17 PSN/NPP Algorithm Theoretical Basis Document, MODIS PSN (Net Photosynthesis) and MODIS NPP (Net Primary Productivity), Version 3.0.
- Running, S.W., Nemani, R., Glassy, J.M, and Thornton, P.E. 1999. Modis Daily Photosynthesis (PSN) and Annual Net Primary Production (NPP) Product (Mod17), Version 3.0.
- Si, B.C., and Farrell, R.E. 2004. Scale-dependent relationships between wheat yield and topographic indices: A wavelet approach. *Soil Science Society of America Journal*, Vol. 68, pp. 577-588.
- Smith, N.J., Chen, J.M., and Black, T.A. 1993. Effects of clumping on estimates of stand leaf area index using the LI-COR LAI-2000. *Canadian Journal of Forest Research*, Vol. 23, No. 9, pp.1940-1943.

- Steven, M.D., Malthus, T.J., Baret, F., Xu, H., and Chopping, M.J. 2003. Intercalibration of vegetation indices from different sensor systems. *Remote Sensing of Environment*, Vol. 88, No. 4, pp. 412-422.
- Tan, B., Woodcock, C.E., Hu, J., Zhang, P., Ozdogan, M., Huang, D., Yang, W., Knyazikhin, Y., and Myneni, R.B. 2006. The impact of geolocation offsets on the local spatial properties of MODIS data: Implications for validation, compositing, and band-to- band registration. *Remote Sensing of Environment*, Vol. 105, pp. 98-114.
- Tarnavsky, E., Garrigues, S., and Brown, M.E. 2008. Multiscale geostatistical analysis of AVHRR, SPOT-VGT, and MODIS global NDVI products. *Remote Sensing of Environment*, Vol. 112, pp. 535-549.
- Thomlinson, J.R., Bolstad, P.V., and Cohen, W.B. 1999. Coordinating methodologies for scaling landcover classifications from site-specific to global: Steps toward validating global map products. *Remote Sensing of Environment*, Vol. 70, No. 1, pp. 16-28.
- Tian, Y., Wang, Y., Zhang, Y., Knyazikhin, Y., Bogaert, J., and Myneni, R.B. 2002. Raidative transfer based scaling of LAI retrievals from reflectance data of different resolutions. *Remote Sensing of Environment*, Vol. 84, pp.143-159.
- Trishchenko, A.P., Cihlar, J., and Li, Z. 2002. Effects of spectral response function on surface reflectance and NDVI measured with moderate resolution satellite sensors. *Remote Sensing of Environment*, Vol. 81, pp. 1-18.
- Tucker, C.J., Pinzon, J.E., Brown, M.E., Slayback, D., Pak, E.W., Mahoney, R., Vermote R., and El Saleous, N. 2005. An extended AVHRR 8-km NDVI data set compatible with MODIS and SPOT-vegetation NDVI data. *International Journal of Remote Sensing*, Vol. 26, No. 20, pp. 4485-4498.
- van den Hurk, B.J.J.M., Viterbo, P., and Los, S.O. 2003. Impact of leaf area index seasonality on the annual land surface evaporation in a global circulation model. *Journal of Geophysical Research (Atmospheres)*, Vol. 108, No. D6, pp. 4191-4203.
- van Leeuwen, W.J.D., Orr, B.J., Marsh, S.E., and Herrmann, S.M. 2006. Multi-sensor NDVI data continuity: Uncertainties and implications for vegetation monitoring applications. *Remote Sensing of Environment*, Vol.100, pp. 67-81.
- Vertessy, R.A., Benyon, R.G., O'Sullivan, S.K.,and Gribben, P.R. 1995. Relationships between stem diameter, sapwood area, leaf area and transpiration in a young mountain ash forest. *Tree Physiology*, Vol. 15, No. 9, pp. 559-567.

- Weiss, M., Baret, F., Myneni, R., Pragne`re, A., and Knyazikhin, Y. 2000. Investigation of a model inversion technique to estimate canopy biophysical variables from spectral and directional reflectance data. *Agronomie*, Vol. 20, pp. 3-22.
- Western, A.W., Blöschl, G., and Grayson, R.B. 1998. Geostatistical characterisation of soil moisture patterns in the Tarrawarra catchment. *Journal of Hydrology*, Vol. 205, No. 1-2, pp. 20-37.
- Wolfe, R.E., Roy, D.P., and Vermote, E.F. 1998. MODIS land data storage, gridding, and compositing methodology: Level 2 grid. *IEEE Transactions Geosciences and Remote Sensing*, Vol. 36, No. 4, pp.1324-1338.
- Wolfe, R.E., Masahiro, N., Fleig, A.J., Kuyper, J.A., Roy, D.P., Storey, J.C., and Patt, F.S. 2002. Achieving sub-pixel geolocation accuracy in support of MODIS land science. *Remote Sensing of Environment*, Vol. 83, pp. 31-49.
- Wu, J., Shen, W., Sun, W., and Tueller, P.T. 2002. Empirical patterns of the effects of changing scale on landscape metrics. *Landscape Ecology*, Vol. 17, No. 8, pp. 761-782.
- Wulder, M.A., Drew Le, E.F., Franklin, S.E., and Lavigne, M.B. 1998. Aerial image texture information in the estimation of the northern deciduous and mixed wood forest leaf area index (LAI). *Remote Sensing of Environment*, Vol. 64, pp. 64-76.
- Zhang, X., Friedl, M.A., Schaaf, C.B., and Starhler, A.H. 2004. Climate controls on vegetation phenological patterns in northern mid- and high latitudes inferred from MODIS data. *Global Change Biology*, Vol. 10, pp. 1133-1145.
- Zhang, C., and Guo, X. 2008. Monitoring northern mixed prairie health using broadband satellite imagery. *International Journal of Remote Sensing*, Vol. 29, No. 8, pp. 2257-2271.

CHAPTER 2 - A SUITABLE VEGETATION INDEX FOR QUANTIFYING TEMPORAL VARIATIONS OF LAI IN SEMI-ARID MIXED GRASSLAND

2.1 Introduction

Accurate LAI values and temporal variation are important for the land surface-atmosphere interaction processes (Sellers et al., 1986; Chen, 1996; Running et al., 1999; van den Hurk, 2003) associated with evapotranspiration and photosynthesis (Gutman and Ignatov, 1998). Uncertainties on LAI estimates could result in 10-15% evaporation variations in the global circulation model (van den Hurk et al., 2003), and seasonal variations in LAI highly influence the temporal change of evaporation (Wever et al., 2002; van den Hurk et al., 2003). Besides, seasonal variations in Gross Primary Production (GPP) are also closely and positively related to changes in LAI in grasslands (Xu et al., 2004; Risch and Frank, 2006). Thus, it is important to accurately determine LAI and quantify temporal variations of LAI.

Temporal variations in LAI can be timely and effectively quantified by remote sensing due to its ability to provide often-repeated observations and large coverage. VIs are commonly used to accomplish the task of monitoring or quantifying LAI (Huete et al., 2002). However, quantifying LAI variations through VIs in semi-arid mixed grasslands is challenging (Fava et al., 2009) due to the complex canopy architecture (Cho et al., 2007; Darvishzadeh et al., 2008; Numata et al., 2008) and the presence of a high fraction of dead vegetation (Guo, 2002; He et al., 2006; Beerli et al., 2007) and exposed soil (Boschetti et al., 2007). At the same time, semi-arid grasslands, which cover about 11 percents of the earth's surface excluding Greenland and Antarctica (White et al., 2000), play an important role in modifying global climate through effects on carbon budget (Owensby, 1998) which is highly related to LAI (Xu et al., 2004; Risch and Frank, 2006). It therefore is essential to determine the most suitable VI for accurately quantifying LAI temporal variation.

Theoretically, the better VIs for LAI estimation should be more sensitive to canopy structure partially determined by species composition, and less sensitive to chlorophyll, dead materials, bare soil, and atmosphere. Numerous VIs have been developed in past decades, aiming to minimize the effects of litter (He et al., 2006), chlorophyll (Haboundane et al., 2004), bare soil (Huete, 1988; Baret et al., 1989; Baret and Guyot, 1991; Qi et al., 1994; Chen, 1996), and the atmosphere (Kaufman and Tanré, 1992) on estimating vegetation biophysical parameters. However, most VIs, defined from both red and near Infrared (NIR) reflectance bands, are affected not only by LAI, but also by chlorophyll (Haboundane et al., 2004; Delalieux et al., 2008). LAI and chlorophyll have similar effects on canopy reflectance from the green (~ 550 nm) to the red-edge (~ 750 nm) region of the electromagnetic spectrum. Thus, Delalieux et al. (2008) specifically developed a new VI (Standardized LAI Determining Index, SLAID) based on the two NIR bands for LAI determination to eliminate the chlorophyll effect. Nonetheless, SLAID is specifically designed for green leaves in an experimental orchard. Its performance in semi-arid mixed grasslands needs to be investigated.

Comprehensive comparisons of hyperspectral VIs on LAI estimation have been made through the simulated reflectance from the RTM (Goel, 1994; Chen, 1996; Broge and Leblanc, 2000; Haboudane et al., 2004). They have made a big contribution to select a suitable VI for LAI estimation. However, their comparisons only focused on the sensitivity of VIs to canopy architecture, soil background, and atmospheric conditions. The prediction power of VIs could be very different in semi-arid mixed grasslands characterized by a large amount of dead materials which have a significant contribution to the variation (Galvao et al., 2000). He et al. (2006) has evaluated the performances of some selected VIs based on canopy hyperspectral data in mid and late June in Grasslands National Park (GNP (49° 10' 37" N, 107° 25'33" W)), a semi-arid grassland in southern Saskatchewan, Canada. However, the performance of each VI changes with time (Haboundane et al., 2004), and the temporal dynamics of VIs are different (Broge and Leblanc, 2000). So the main

purpose of this chapter is to determine a suitable VI for estimating LAI and quantifying LAI temporal variation in semi-arid mixed grassland.

2.2 Materials and Methods

2.2.1 Data

Data used in this chapter are LAI, canopy reflectance, and ground covers of grass, forbs, standing dead, litter, and bare soil collected over the sampling transect from May to September in 2008.

2.2.2 VIs Selected for the Study

The selected VIs were classified into six categories and shown in **Table 2.1**. The advantages and disadvantages of the VIs were summarized by Haboudane et al. (2004), He et al. (2006), and Delalieux et al. (2008). The widely used Modified Triangular Vegetation Indices (MTVI1 and MTVI2) were not included, because I found that they share the same algorithm with the Modified Chlorophyll Absorption Ratio Indices (MCARI1 and MCARI2), respectively. Both MTVI1 and MCARI1 were defined to reduce the sensitivity to variations of pigment content, while increase the sensitivity to change of LAI. They were expressed as equation (2.1) and (2.2), respectively (Haboudane et al., 2004):

$$\text{MTVI1} = 1.2[1.2(\rho_{800} - \rho_{550}) - 2.5(\rho_{670} - \rho_{550})] \quad (2.1)$$

$$\text{MCARI1} = 1.2[2.5(\rho_{800} - \rho_{670}) - 1.3(\rho_{800} - \rho_{550})] \quad (2.2)$$

Both the equation (2.1) and (2.2) can be transformed into:

$$\text{MTVI1 or MCARI1} = 1.2 (1.2\rho_{800} - 2.5\rho_{670} + 1.3\rho_{550}) \quad (2.3)$$

At the same time, the expression of MTVI2 (equation (2.4)) shares the same numerator and denominator with MCARI2 (equation (2.5)) to decrease the effects of bare soil, while

preserving the high sensitivity to LAI and low sensitivity to chlorophyll influence (Haboudane et al., 2004).

$$MTVI2 = \frac{1.5[1.2(\rho_{800}-\rho_{550})-2.5(\rho_{670}-\rho_{550})]}{\sqrt{(2\rho_{800}+1)^2-(6\rho_{800}-5\sqrt{\rho_{670}})-0.5}} \quad (2.4)$$

$$MCARI2 = \frac{1.5[2.5(\rho_{800}-\rho_{670})-1.3(\rho_{800}-\rho_{550})]}{\sqrt{(2\rho_{800}+1)^2-(6\rho_{800}-5\sqrt{\rho_{670}})-0.5}} \quad (2.5)$$

Table 2.1 Vegetation Indices (VIs) selected

Categories	VI Names	VI Expressions	Citations
Ratio-based	NDVI, Normalized difference vegetation index	$(\rho_{800} - \rho_{670})/(\rho_{800} + \rho_{670})$	Rouse et al., 1974
	PVI, Perpendicular vegetation index	$(\rho_{800} - \rho_{670})/\sqrt{(\rho_{800} + \rho_{670})}$	Reujean and Breon, 1995
	RDVI, Renormalized difference vegetation index	$\left(\frac{\rho_{800}}{\rho_{670}} - 1\right) / \sqrt{\left(\frac{\rho_{800}}{\rho_{670}} + 1\right)}$	Chen, 1996
Soil-line-related	SAVI, Soil-adjusted vegetation index	$\frac{(1+L)(\rho_{800} - \rho_{670})}{(\rho_{800} + \rho_{670} + L)}$ where L =0.5	Huete, 1988
	MSAVI, Modified soil-adjusted vegetation index	$\frac{[2(\rho_{800} + 1) - \sqrt{(2\rho_{800} + 1)^2 - 8(\rho_{800} - \rho_{670})}]}{2}$	Qi et al., 1994
	TSAVI, Transformed soil-adjusted vegetation index	$\frac{a(\rho_{800} - a\rho_{670} - b)}{(a\rho_{800} + \rho_{670} - ab)}$	Baret et al., 1989
	ATSAVI, Adjusted transformed soil-adjusted vegetation index	$\frac{a(\rho_{800} - a\rho_{670} - b)}{(a\rho_{800} + \rho_{670} - ab + X(1 + a^2))}$ where X = 0.08	Baret and Guyot, 1991

Soil and atmospheric resistant	SARVI, Soil and atmospheric resistant vegetation index	$\frac{(1+L)(\rho_{800}-\rho_{rb})}{(\rho_{800}+\rho_{rb}+L)}$ where $\rho_{rb} = 2\rho_{red} - \rho_{blue}$, $L = 0.5$	Kaufman and Tanre, 1992
Soil-line-litter-corrected	L-ATSAVI, Litter-corrected ATSAVI	$\frac{a(\rho_{800} - a\rho_{670} - b)}{(a\rho_{800} + \rho_{670} - ab + X(1 + a^2) + L \times CAI)}$ Where $X = 0.08$, $L = 1, 100$ $CAI = 0.5(\rho_{2000} + \rho_{2200}) - \rho_{2100}$	He et al., 2006
	TVI, Triangular vegetation index	$0.5[120(\rho_{750} - \rho_{550}) - 200(\rho_{670} - \rho_{550})]$	Broge and Leblanc, 2000
	MCARI, Modified chlorophyll absorption ratio index	$[(\rho_{700} - \rho_{670}) - 0.2(\rho_{700} - \rho_{550})] \left(\frac{\rho_{700}}{\rho_{670}} \right)$	Daughtry et al., 2000
Chlorophyll-corrected	MCARI1, Modified chlorophyll absorption ratio index 1	$1.2[2.5(\rho_{800} - \rho_{670}) - 1.3(\rho_{800} - \rho_{550})]$	Haboudane et al., 2004
	MCARI2, Modified chlorophyll absorption ratio index 2	$\frac{1.5[2.5(\rho_{800}-\rho_{670})-1.3(\rho_{800}-\rho_{550})]}{\sqrt{(2\rho_{800}+1)^2-(6\rho_{800}-5\sqrt{\rho_{670}})-0.5}}$	Haboudane et al., 2004
Chlorophyll-independent	SLAID, Standardized LAI Determining Index	$S(\rho_{1050} - \rho_{1250}) / (\rho_{1050} + \rho_{1250})$	Delalieux et al., 2008
	SLAIDI*, Modified standardized LAI Determining Index	$\frac{S(\rho_{1050}-\rho_{1250})}{(\rho_{1050}+\rho_{1250})} \cdot \rho_{1555}$ where $S = 5$	Delalieux et al., 2008

Note: a and b used in some VIs are the slope (1.95) and the intercept (-0.01) of the soil line (**Appendix C**) in the study area.

2.2.3 Methods for Determining a Suitable VI at Each Growing Stage

First, the spectral properties of green vegetation, dead vegetation, and bare soil and their effects on the selected VIs were investigated. Second, both VIs and LAI were scaled up by arithmetically averaging the values in the area within a 30 m-size window, which is the

spatial variation scale of LAI in the study area (Li and Guo, 2010), to minimize the effects of spatial autocorrelation. The correlation coefficient between LAI and each VI was then calculated to measure VIs' performances in the early, maximum, and late growing season, respectively. In addition, the analysis of variance (ANOVA) was implemented to account for the performances of VIs at each growing stage. It is a useful statistical approach for the sensitivity analysis of VIs to their effect factors (Rondeaux et al., 1996; Daughtry et al., 2000), such as green vegetation, dead vegetation, and bare soil.

2.2.4 Methods for Determining a Suitable VI for Quantifying LAI Temporal Variation

A suitable VI for quantifying LAI temporal variation must have a good and stable performance throughout the growing season. Thus, the correlation coefficient of each VI and LAI at each growing stage was arithmetically averaged to measure the overall performance during the entire growing season. Also, standard deviation (SD) and coefficient of variation (CV) of the correlation coefficient between LAI and each VI were calculated to measure the stability of the performance of each VI.

2.3 Results and Discussion

2.3.1 Temporal Variation of LAI and Effects of Ground Covers

As shown in **Figure 2.1**, LAI demonstrated a distinct temporal variation, varying from 0.14 to 0.92 over the course of a season. Throughout the growing season, LAI rapidly increased and reached the maximum in late July. After that, LAI started decreasing and reached the minimum in the senescence season from late August to mid September.

Both covers of grasses and forbs increased as LAI increased in the early growing season, and then reached the maximum. Subsequently, both decreased as LAI decreased, however, the cover of forbs changed more dramatically than did the cover of grasses. In contrast,

standing dead cover dramatically decreased as LAI increased, and then rapidly increased during the senescence season. Litter cover was relatively steady, as was bare ground.

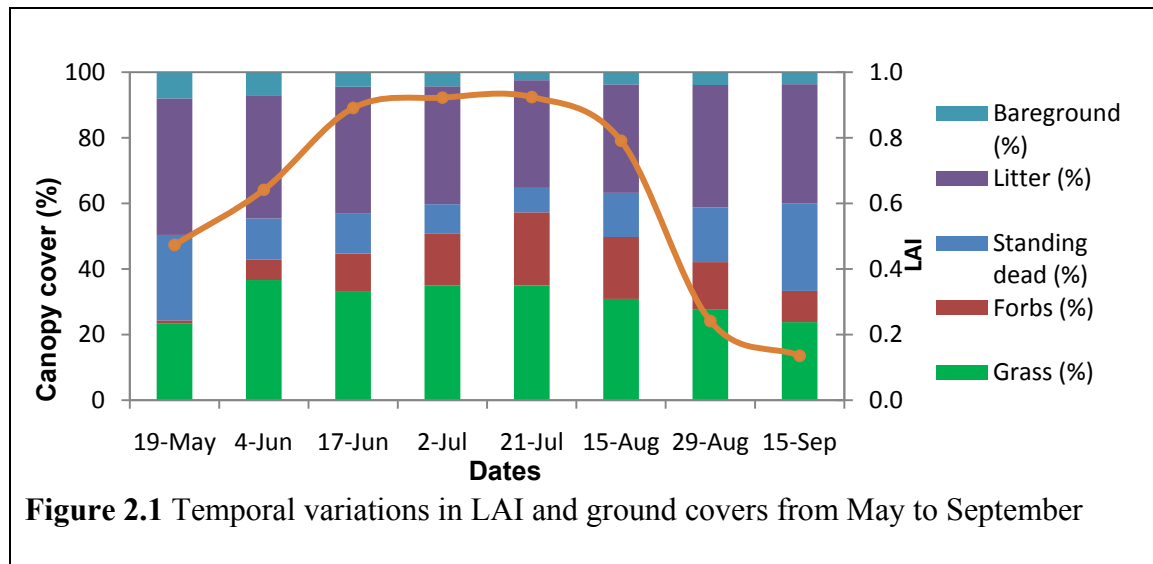


Table 2.2 shows the correlation coefficient (r) and coefficient of determination (r^2) between ground covers and LAI for the entire growing season. Temporal variations in covers of grasses, forbs, standing dead, and litter can significantly account for a total of 91.2% of the variations in LAI. Variations in grass cover can only account for 11.9% of the temporal variations in LAI, while temporal variations in forbs can significantly ($P < 0.001$) account for approximately 31.9% of the variations. In contrast, variations in standing dead cover and litter cover can explain 32.1% and 15.3% of the total variances of LAI, respectively, although the relationships with LAI are negative. Totally, dead vegetation covers (standing dead and litter) can account for 47.4% of the variances of LAI, while green covers can only explain 43.8%.

Table 2.2 Correlation of coefficient (r) and coefficient of determination (r^2) between canopy covers and LAI

Canopy composition	r	r^2	P
Grass	0.345	0.119	0.000
Forbs	0.565	0.319	0.000
Standing dead	-0.567	0.321	0.000
Litter	-0.391	0.153	0.000

Note: P is the significant value at the 99% interval.

The fact that variations in forbs' cover can explain more variances of LAI than grasses' cover indicates that species composition has a significant effect on LAI in semi-arid mixed grassland, similar to temperate mixed grasslands (Spehn et al., 2000). Thus, species composition would influence the performance of a VI. At the same time, litter and standing dead are often dominant in the above ground biomass in semi-arid grasslands (Asner et al., 1998; Guo, 2002), and dead vegetation accounts for about 4% more variations in LAI than green vegetation in the study area. A large amount of dead materials would present a serious problem to the interpretation of VIs (Duncan et al., 1993; Galvao et al., 2000). Therefore, selecting a VI with less sensitivity to dead vegetation and bare soil but more sensitivity to green vegetation is a key to accurately quantify LAI temporal variations in semi-arid mixed grasslands.

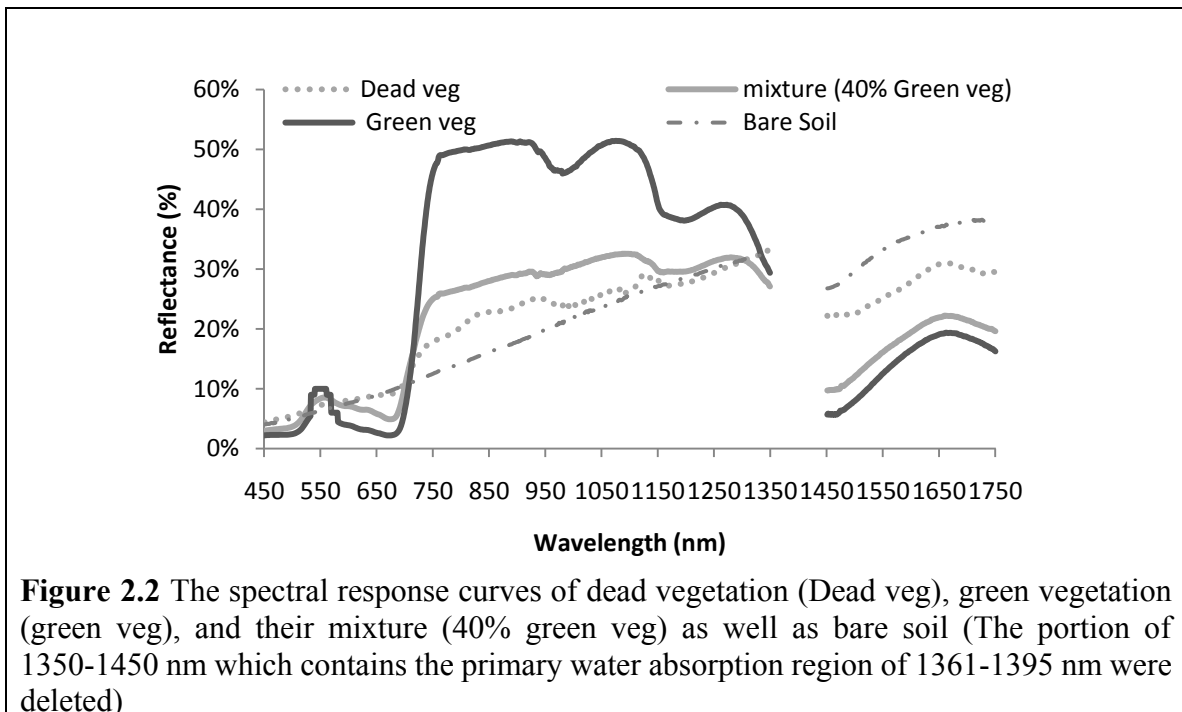
2.3.2 A Suitable VI for LAI Estimation at Each Growing Stage

2.3.2.1 The spectral response curves of ground covers

Reflectance spectra of dead vegetation, green vegetation, and their mixture with 40% green vegetation, as well as natural bare soil are shown in **Figure 2.2**. The other intermediate mixture rates of dead and green vegetation were not illustrated for clarity. Large differences are observed in spectral response curves of dead vegetation, green vegetation, and their mixture in the visible, NIR, and shortwave wavelength regions. Reflectivity of vegetation in a visible wavelength region is pigment dependent. Light absorption by chlorophyll in the blue (450 nm) and red (670 nm) wavelength regions is minimized in a dead vegetation reflectance response curve due to the lack of chlorophyll. Thus, higher reflectance of dead vegetation in blue and red wavelength than green vegetation is observed, whereas reflectivity of dead vegetation in the green (550 nm) wavelength region is lower. In the NIR (750-1400 nm) wavelength region, where vegetation reflectivity is structure dependent, reflectance of dead vegetation is much reduced compared to that of green vegetation. Also, water absorption zones at around 950 nm and 1150 nm wavelength regions, clearly shown in the spectral response curve of green vegetation, are smoothed in

the spectral response curve of dead vegetation due to the less water content. In the shortwave (1450-1750 nm in the chart) wavelength region, which is mainly used for the studies on vegetation water content, dead vegetation shows much more reflectivity than green vegetation due to less light absorption attributed to reduced water content within the vegetation. A mixture of dead and green vegetation demonstrates intermediate reflectivity in the wavelength regions (**Figure 2.2**).

Reflectivity of bare soil demonstrates a similarity with dead vegetation in visible wavelength (450 nm-750 nm) regions. Thus, the spectral response curve of bare soil, with lower reflectance in green wavelength region and higher reflectivity in blue and red wavelength regions, is different from green vegetation. However, bare soil has much lower reflectivity in one portion of NIR wavelength (750 nm-1150 nm) region than green, dead vegetation, and their mixture. In the shortwave wavelength region, bare soil demonstrates the highest reflectivity among the demonstrated ground covers. Nonetheless, reflectivity of bare soil is subjected to change depending on its water content.



The similar reflectivity between dead vegetation and bare soil in the visible wavelength range indicates that they have similar influences on VIs which integrates peak green reflectance (550 nm) and chlorophyll absorption at 450nm and 670 nm. The dissimilarity in the spectral response curve of green vegetation from those of dead vegetation and bare soil indicates: 1) VIs combined all ρ_{550} , ρ_{670} , and ρ_{800} or either two of them are able to differentiate LAI from green vegetation, dead vegetation, and bare soil; and 2) VIs comprised of two NIR bands or together with shortwave bands also have the capability to identify variations in LAI. The differences in the reflectivity of ground covers further confirm that the composition of ground covers would influence the performances of VIs, and the influence is different for each VI due to the diverse bands and band combination approaches.

2.3.2.2 Performances of each VI

The correlation coefficient between LAI and each selected VI, and the percentages of variations in spectral variables explained by the ground covers in different growing seasons are shown in **Table 2.3**. The r values indicate the performances of VIs, which can be accounted for by their sensitivity to variations of green vegetation and the resistance to the influence of dead vegetation and bare soil. The more variations of VIs explained by green vegetation, the greater sensitivity of VIs have. Contrarily, the fewer variations accounted by dead vegetation or bare soil, the greater resistance of VIs to their influence.

In the early growing season (Jun 4-Jul 2), the r values in chlorophyll-independent VIs (0.51-0.53) and ratio-based VIs (0.46-0.54) are greater than those in soil-line-related VIs (0.41-0.51) and chlorophyll-corrected VIs (0.38-0.51). Within each category, the r values of SLAIDI* (0.53), NDVI (0.54), TSAVI (0.51), and MCARI (0.51) are slightly larger, whereas of SLAIDI (0.51), RDVI (0.46), MSAVI (0.41), and MCARI1 (0.38) are slightly smaller than those of the other VIs in their group. L-ATSAVI has a moderate r value of 0.49. SARVI has the smallest r value (0.23), and the difference of the r value in the worst VI (SARVI) from the best VI (NDVI) is as large as 0.31.

The better performances of ratio-based VIs and chlorophyll-independent VIs are attributed to their comprehensive response to variations in the ground covers. The percentages of variations accounted for by green vegetation/dead vegetation in ratio-based VIs (39.0-40.5%/35-42.6%) and chlorophyll-independent VIs (35.8-43.6%/34.2-38.9%) are generally greater than the other selected VI categories. In addition, the percentages of variations contributed by bare soil in ratio-based VIs (8.7-11.4%) and chlorophyll-independent VIs (4.0-5.5%) are generally smaller than the other VIs. Specifically, NDVI, with high sensitivity to green vegetation variation, and medium and high resistance to dead vegetation and bare ground influence, outperforms all the other selected VIs. Although SLAIDI is more sensitive to variations of green vegetation than NDVI, the lower resistance to dead vegetation influence limits its performance. SARVI, with the least sensitivity to green vegetation and the smallest resistance to bare soil, demonstrates the worst performance for LAI estimation.

During the maximum growing season (Jul 21-Aug 15), the r values of chlorophyll-independent VIs (0.74-0.80) are slightly better than those of soil-line-related VIs (0.74-0.79), ratio-based VIs (0.71-0.78), L-ATSAVI (0.75), SARVI (0.66), and chlorophyll-corrected VIs (0.45-0.78). Within each category, the r values of SLAIDI (0.80), PVI (0.79), MSR (0.78), and MCARI2 (0.78) are larger, while of SLAIDI* (0.74), ATSAVI (0.74), NDVI (0.71), and TVI (0.46) are smaller than those of the other VIs in their groups. The r difference of TVI from SLAIDI is as large as 0.35. NDVI, ranked the 9th among the selected VIs, however, the difference in performances of NDVI and SLAIDI is subtle with an r value of 0.04. The best performance of SLAIDI is supported by the second greatest sensitivity to green vegetation variation (75.9%) and medium resistance to the influence of dead vegetation (70.4%) and bare soil (15.9%). TVI demonstrates the worst performance for LAI estimation due to its low sensitivity to variations of green vegetation (18.4%), despite high resistance to the effects of dead vegetation (17.4%) and bare soil (6.0%). The performances of the other VIs can also be well explained by the variations in the ground covers.

In the late growing season (Aug 29-Sep 15), the r values of ratio-based VIs (0.74-0.76), L-ATSAVI (0.76), soil-line-related (0.73-0.77), and chlorophyll-independent (0.68-0.73) are greater than those of SARVI (0.48) and chlorophyll-corrected (0.36-0.73). Within each category, the r values of MSR (0.76), TSAVI (0.77), SLAIDI (0.73), and MCARI 2 (0.73) are larger, whilst of RDVI (0.74), PVI (0.73), SLAIDI* (0.68), and TVI (0.36) are smaller than those of the others within their group. The r difference between TVI and TSAVI is 0.41. NDVI is in the 5th place among the selected VIs, however, the difference in the r values of NDVI and TSAVI is subtle (0.02). TSAVI becomes the optimal representative of LAI with a moderate sensitivity to green vegetation (69.2%) and medium to high resistance to dead vegetation (56.9%) and bare soil influence (3.0%), respectively. At the same time, TVI demonstrates the worst performance with the least sensitivity to green vegetation (22.9%), despite the high resistance to the influence of dead vegetation (18.1%) and bare soil (3.3%).

Table 2.3 Correlation coefficients (r) between spectral vegetation indices (VIs) and LAI, and percentage of variations in VIs with bare ground reflectance (B), green vegetation (GV), dead vegetation (DV), and their interactions (* indicates that the r values are significant at the 0.05 level with 66, 44, 44 samples at each growing stage, respectively)

Spectral Variable	r^*	Source of Variable				
		B	GV	B*GV	DV	B*DVI
Jun 4 - Jul 2						
NDVI	0.54	8.7	39.0	8.0	36.2	8.7
MSR	0.51	11.4	40.5	5.0	42.6	11.5
RDVI	0.46	9.7	39.7	5.6	35.0	11.6
SLAIDI*	0.53	4.0	35.8	5.7	34.2	8.0
SLAIDI	0.51	5.5	43.6	5.6	38.9	11.3
TSAVI	0.51	10.1	33.8	6.3	35.5	6.2
ATSAVI	0.5	9.2	37.3	7.2	33.7	8.9
PVI	0.45	11.6	34.4	4.7	36.0	9.5
SAVI	0.42	12.0	34.6	4.7	37.2	12.4
MSAVI	0.41	12.9	35.4	4.8	37.7	15.0
	0.49	1.7	22.6	7.7	12.1	7.9

L-ATSAVI

SARVI	0.23	15.8	16.9	7.6	16.0	14.7
MCARI	0.51	6.8	30.9	7.6	31.4	5.4
TVI	0.44	3.9	38.0	11.6	35.1	8.2
MCARI2	0.41	10.9	41.2	5.6	35.8	13.2
MCARI1	0.38	12.8	33.0	5.3	34.8	14.1

Jul 21 - Aug 15

MSR	0.78	10.9	47.5	7.3	68.6	57.0
NDVI	0.76	13.9	75.1	13.8	73.5	26.2
RDVI	0.71	9.9	70.8	14.5	68.0	11.0
SLAIDI	0.80	15.9	75.9	20.8	70.4	20.7
SLAIDI*	0.74	20.8	71.4	13.7	70.6	11.4
PVI	0.79	12.6	52.6	8.2	61.8	39.0
SAVI	0.79	11.8	53.7	7.2	62.1	37.0
MSAVI	0.79	11.5	51.6	8.5	61.1	38.5
TSAVI	0.78	15.0	56.9	5.4	62.4	38.9
ATSAVI	0.74	13.5	73.7	12.7	70.4	17.2

L-ATSAVI

SARVI	0.66	10.7	34.0	10.9	42.3	28.9
MCARI2	0.78	11.3	70.5	16.1	65.8	13.2
MCARI1	0.77	11.6	51.3	9.0	58.3	35.2
MCARI	0.76	12.1	43.0	19.8	59.4	49.5
TVI	0.45	6.0	18.4	9.2	17.4	3.3

Aug 29- Sep 15

MSR	0.76	13.0	47.9	15.6	35.6	12.7
NDVI	0.75	13.2	79.0	19.3	59.6	15.4
RDVI	0.74	11.4	53.8	20.0	36.6	9.7
SLAIDI	0.73	16.2	81.6	20.8	53.8	10.9

SLAIDI*	0.68	17.3	75.6	10.2	58.5	12.7
TSAVI	0.77	3.0	69.2	5.8	56.9	5.4
SAVI	0.75	9.4	49.4	18.2	38.2	7.5
MSAVI	0.74	9.3	49.4	17.6	37.1	6.9
ATSAVI	0.74	15.0	56.7	19.8	38.6	13.1
PVI	0.73	9.3	48.7	17.1	36.4	8.6
L-ATSAVI	0.76	14.9	55.2	18.9	39.6	12.6
SARVI	0.48	2.4	33.9	11.7	27.4	9.5
MCARI2	0.73	10.9	55.7	19.1	36.0	7.7
MCARI1	0.73	8.5	48.8	17.7	37.6	5.4
MCARI	0.61	11.1	37.2	6.7	25.7	17.2
TVI	0.36	3.3	22.9	9.9	18.1	3.7

The results in the early growing season were compared to the findings of He et al. (2006) in upland area of GNP. The similarity of my study area and their study area is 1) both are semi-arid mixed grasslands characterized by a large amount of dead materials and bare soil in the boreal climate region. Percentage of bare soil is even larger in GNP than that in my study area; 2) LAI and canopy reflectance data used in these two studies were measured by the same instruments and approaches, although, their measurements were done in mid and late June in 2004; and 3) the most VIs compared are the same, with only chlorophyll-independent VIs added and MTVI1 and MTVI2 excluded in my study. The difference in the two study areas is mainly in the different dominant vegetation and ground covers. The dominant vegetation of GNP is blue grama grass (*Bouteloua gracilis*, *Contr. U.S. Natl. Herb. 14: 375*), needlegrass (*Nassella spp.*, *Fl. Chil. 6: 263*), and silver sagebrush (*Artemisia cana*, *Fl. Amer. Sept. 2: 521*), and moss (*Lycopodiaceae*, *Hist. Nat. Vég. 4: 293*) are also observed as ground covers. Both research found that the ratio-based VIs and soil-line-related VIs are better than chlorophyll-corrected VIs, and TSAVI and ATSAVI are superior to the other selected soil-line-related VIs. The inferiority of chlorophyll-corrected VIs may be attributed to the less influence of chlorophyll than dead

vegetation and bare soil. However, the superiority of each individual VI within the ratio-based and chlorophyll-corrected VIs is different. NDVI outperforms MSR and RDVI, and MCARI is the best within chlorophyll-corrected VIs in St. Denis, while RDVI is the best within the ratio-based VIs and MCARI2 is superior to the others within their group in their study. In addition, NDVI is slightly better than L-ATSAVI, and SARVI is the worst VI amongst the selected VIs in St. Denis, while L-ATSAVI is better than NDVI and MCARI is the worst in GNP.

2.3.3 A Suitable VI for LAI Temporal Variation Quantification

Performances of VIs on quantifying temporal variation of LAI were evaluated by the averaged correlation coefficient, SD, and CV (**Table 2.4**). The averaged r values of chlorophyll-independent VIs (0.65-0.68), soil-line-related VIs (0.65-0.68), ratio-based VIs (0.64-0.68), and of L-ATSAVI (0.67) are larger than those of SARVI (0.46) and chlorophyll-corrected VIs (0.42-0.64). Within each group, the r values of SLAIDI (0.68), TSAVI (0.68), NDVI (0.68), and MCARI2 (0.64) are larger, and of SLAIDI* (0.65), MSAVI (0.65), RDVI (0.64), and TVI (0.42) are smaller than those of the other VIs in their group. The r difference of TVI from NDVI is as large as 0.26. The CV values indicate the stability of the performances of VIs. The CV of SARVI (0.99) is much larger than those of chlorophyll-corrected VIs (0.32-0.37), soil-line-related (0.22-0.33), ratio-based (0.18-0.28), chlorophyll-independent (0.18-0.22), and of L-ATSAVI (0.23). Within each category, the CV values of MCARI (0.37), SAVI (0.33), and of RDVI (0.28) are larger, while of TVI (0.32), ATSAVI (0.22), and of NDVI (0.18) are smaller than the others within their group. The CV (0.18) of chlorophyll-independent SLAIDI* is smaller than that of SLAIDI (0.22). The range between CV of SARVI and NDVI is as large as 0.81. The SD values indicate the same stability of the performances of VIs as the CV.

Table 2.4 Performances of VIs on quantifying temporal variation of LAI measured by the mean Pearson's r , standard deviation (SD), coefficient of variation (CV), and their ranges

VIs	r	SD	CV
NDVI	0.68	0.12	0.18
MSR	0.68	0.15	0.22
RDVI	0.64	0.18	0.28
SLAIDI	0.68	0.15	0.22
SLAIDI*	0.65	0.12	0.18
TSAVI	0.68	0.15	0.22
PVI	0.66	0.19	0.29
ATSAVI	0.66	0.14	0.22
SAVI	0.65	0.21	0.33
MSAVI	0.65	0.21	0.33
L-ATSAVI	0.67	0.16	0.23
SARVI	0.46	0.45	0.99
MCARI2	0.64	0.21	0.33
MCARI1	0.63	0.23	0.37
MCARI	0.63	0.20	0.32
TVI	0.42	0.13	0.32
Range	0.26	0.33	0.81

NDVI demonstrates the most stable and best performance on quantifying temporal variations in LAI in the semi-arid mixed grassland. This is confirmed by the assertion of Galvao et al. (2000) that a narrow red band at 670 nm and a narrow NIR band at 800 nm

can maximize the NDVI contrast between green vegetation and dead vegetation, or bare soil. It is consistent with the research of Broge and Leblanc (2000) that NDVI is the best index at low and medium LAIs. However, it is not in agreement with the finding of Chen (1996), which indicates that MSR is the best choice for LAI estimation in a forest area, nor of Haboudane et al. (2004) that MTVI2 and MCARI2 are the most robust indices to estimate LAI in croplands. The incongruence is due to the reasons that my study considered dead materials as an important effect factor while their research did not, and also the saturation issue of NDVI for dense vegetation is not a serious problem in semi-arid mixed grasslands where quadrat LAIs are typically lower than 4.

2.4 Conclusions

Distinct variations in LAI were observed throughout the growing season in the semi-arid mixed grassland. These temporal variations can largely be explained by the changes in covers of grasses, forbs, standing dead, and litter. Dead materials, including standing dead and litter, could account for 4% more of the variation in LAI than green vegetation could. Standing dead has the greatest effect on temporal variations in LAI, although the influence was negative. This information will be beneficial for modeling CO₂ exchange, evapotranspiration, and other energy flux exchanges between the land surface and the atmosphere.

The sensitivity of VIs to green vegetation and resistance to dead vegetation and bare soil influence are different as growing stages change. As a result, performances of VIs on LAI estimation vary as the vegetation growing stage changes. VIs demonstrate the most capability to be a representative of LAI during the time period of Jul 21-Aug 15, followed by Aug 29-Sep 15 and Jun 4-Jul 2. Also, VIs perform differently at each growing stage, and the difference between the best and the worst VI is quite large, ranging from 0.31 to 0.41, although the discrepancy is small or even subtle among some VIs. NDVI, SLAIDI, and TSAVI demonstrate the best performances on LAI estimation in the early, maximum, and late growing season, respectively.

The performances of ratio-based, chlorophyll-independent, L-ATSVI, soil-line-related VIs are better and more stable than chlorophyll-corrected VIs and SARVI. Within each group, performances of NDVI, SLAIDI, TSAVI, and MCARI2 are better, while RDVI, SLAIDI*, MSAVI, and TVI are worse than those of the other VIs within their group. NDVI, SLAIDI*, ATSAVI, and TVI are more stable, while RDVI, SLAIDI, SAVI, and MCARI are less stable than the others within their group. Overall, NDVI is the most suitable VI for quantifying temporal variation in LAI in semi-arid mixed grassland. This makes it possible to parameterize routinely produced NDVI composites into models to be intermediaries of LAI.

2.5 References

- Asner, G.P., Wessman, C.A., Schimel, D.S., and Archer, S. 1998. Variability in leaf and litter optical properties: implications for canopy BRDF model inversions using AVHRR, MODIS, and MISR. *Remote Sensing of Environment*, Vol. 63, pp. 200-215.
- Baret, F., Guyot, G., and Major, D.J. 1989. TSAVI: a vegetation index which minimizes soil brightness effects on LAI and APAR estimation. In the *IEEE International Geoscience and Remote Sensing Symposium and 12th Canadian Symposium on Remote Sensing*, 10-14 July 1989, Vancouver, B.C. pp. 1355-1358.
- Baret, F., and Guyot, G. 1991. Potentials and limits of vegetation indices for LAI and APAR assessment. *Remote Sensing of Environment*, Vol. 35, pp. 161-173.
- Beeri, O., Phillips, R., Hendrickson, J., Frank, A.B., and Kronberg, S. 2007. Estimating forage quantity and quality using aerial hyperspectral imagery for northern mixed-grass prairie. *Remote Sensing of Environment*, Vol. 110, pp. 216-225.
- Boschetti, M., Bocchi, S., and Brivio, P.A. 2007. Assessment of pasture production in the Italian Alps using spectrometric and remote sensing information. *Agriculture, Ecosystem, and Environment*, Vol.118, pp. 267-272.
- Broge, N.H., and Leblanc, E. 2001. Comparing prediction power and stability of broadband and hyperspectral vegetation indices for estimation of green leaf area index and canopy chlorophyll density. *Remote Sensing of Environment*, Vol.76, pp. 156-172.

- Chen, J.M., 1996. Optically-based methods for measuring seasonal variation of leaf area index in boreal conifer stands. *Agriculture and Forest Meteorology*, Vol. 80, pp. 135-163.
- Cho, M.A., Skidmore, A., Corsi, F., van Wieren, S.E., and Sobhan, I. 2007. Estimation of green grass/herb biomass from airborne hyperspectral imagery using spectral indices and partial least squares regression. *International Journal of Applied Earth Observation and Geoinformation*, Vol. 9, pp. 414-424.
- Darvishzadeh, R., Skidmore, A., Atzberger, C., and van Wieren, S. 2008. Estimation of vegetation LAI from hyperspectral reflectance data: Effects of soil type and plant architecture. *International Journal of Applied Earth Observation and Geoinformation*. Vol. 10, pp. 358-373.
- Daughtry, C.S.T., Walthall C.L., Kim, M.S., de Colstoun E.B., and McMurtrey III, J.E. 2000. Estimating corn leaf chlorophyll concentration from leaf and canopy reflectance. *Remote Sensing of Environment*, Vol. 74, No. 2, pp. 229-239.
- Delalieux, S., Somers, B., Hereijgers, S., Verstraeten, W.W., Keulemans, W., and Coppin, P. 2008. A near-infrared narrow-waveband ratio to determine Leaf Area Index in orchards. *Remote Sensing of Environment*, Vol. 112, pp. 3762-3772.
- Duncan, J., Stow, D., Franklin, J., and Hope, A. 1993. Assessing the relationship between spectral vegetation indices and shrub cover in the Jornada Basin, New Mexico. *International Journal of Remote Sensing*, Vol. 14, pp. 3395-3416.
- Fava, F., Colombo, R., Bocchia, S., Meroni, M., Sitzia, M., Fois, N., and Zucca, C. 2009. Identification of hyperspectral vegetation indices for Mediterranean pasture characterization. *International Journal of Applied Earth Observation and Geoinformation*, Vol. 243, pp. 1-11.
- Galvao, L.S., Vitorello, I., and Pizarro, M.A. 2000. An adequate band positioning to enhance NDVI contrasts among green vegetation, senescent biomass, and tropical soils. *International Journal of Remote Sensing*, Vol. 21, No. 9, pp. 1953-1960.
- Goel, N.S. 1994. Influences of canopy architecture on relationships between various vegetation indices and LAI and Fpar: A computer simulation. *Remote Sensing Reviews*, Vol.10, pp.309 -347.
- Guo, X., 2002. Discrimination of Saskatchewan prairie ecoregions using multitemporal 10-day composite NDVI data. *Prairie Perspectives*, Vol. 5, pp. 174-186.
- Gutman, G., and Ignatov, A. 1998. The derivation of the green vegetation fraction from NOAA/AVHRR data for use in numerical weather prediction models. *International Journal Remote Sensing*, Vol. 19, No. 8, pp. 1533-1543.

- Haboudane, D., Miller, J.R., Pattery, E., Zarco-Tejad, P.J., and Strachan, I.B. 2004. Hyperspectral vegetation indices and novel algorithms for predicting green LAI of crop canopies: modeling and validation in the context of precision agriculture. *Remote Sensing of Environment*, Vol. 90, pp. 337-352.
- He, Y., Guo, X., and Wilmshurst, J. 2006. Studying mixed grassland ecosystems I: suitable hyperspectral vegetation indices. *Canadian Journal of Remote Sensing*, Vol. 32, pp. 98-107.
- Huete, A.R. 1988. A soil adjusted vegetation index (SAVI). *International Journal of Remote Sensing*, Vol. 9, pp. 295-309.
- Huete, A., Didan, K., Miura, T., and Rodriguez, E. 2002. Overview of the radiometric and biophysical performance of the MODIS vegetation indices. *Remote Sensing of Environment*, Vol. 83, No. (1-2), pp. 195-213.
- Kaufman, Y.J., and Tanré, D. 1992. Atmospherically Resistant Vegetation Index (ARVI) for EOS-MODIS. *IEEE Transactions on Geoscience and Remote Sensing*, Vol. 30, pp. 261-270.
- Li, Z., and Guo, X. 2000. Improved LAI estimation in mixed grassland by considering both temporal and spatial variations. *International Journal Remote Sensing*, (Submitted).
- Numata, I., Roberts, D.A., Chadwick, O.A., Schimel, J.P., Galvão, L.S., and Soares, J.V. 2008. Evaluation of hyperspectral data for pasture estimate in the Brazilian Amazon using field and imaging spectrometers. *Remote Sensing of Environment*, Vol. 112, No. 4, pp. 1569-1583.
- Qi, J., Chehbouni, A., Huete, A.R., Kerr, Y.H., and Sorooshian, S. 1994. A modified soil adjusted vegetation index. *Remote Sensing of Environment*, Vol. 48, pp. 119-126.
- Reujean, J., and Breon, F. 1995. Estimating PAR absorbed by vegetation from bidirectional reflectance measurements. *Remote Sensing of Environment*, Vol.51, pp. 375-384.
- Risch, A.C., and Frank, D.A. 2006. Carbon dioxide fluxes in a spatially and temporally heterogeneous temperate grassland. *Ecosystem Ecology*, Vol. 147, pp. 291-302.
- Rondeaux, G., Steven, M., and Baret, F. 1996. Optimization of soil-adjusted vegetation indices. *Remote Sensing of Environment*, Vol. 55, No.2, pp.95-107.
- Rouse, J.W., Haas, J.R.H., Schell, J.A., and Deering, D.W. 1974, Monitoring vegetation systems in the Great Plains with ERTS. In: *Proc. ERTS-1 Symp.*, 3rd . Greenbelt, MD. 10–15 Dec. 1973. Vol. 1. NASA SP-351. NASA, Washington, DC. pp. 309-317.

- Running, S.W., Baldocchi, D. D., Turner, D. P., Gower, S. T., Bakwin, P. S., and Hibbard, K.A. 1999. A global terrestrial monitoring network integrating tower fluxes, flask sampling, ecosystem modeling and EOS satellite data. *Remote Sensing of the Environment*, Vol. 70, pp. 108-127.
- Sellers, P.J., Mintz, Y., Sud, Y.C., and Dalcher, A. 1986. A simple biosphere model (SiB) for use within general circulation models. *Journal of the Atmospheric Science*, Vol. 43, pp. 505- 531.
- Spehn, E.M., Joshi, J., Schmid, B., Diemer, M., and Korner, C. 2000. Above-Ground Resource Use Increases with Plant Species Richness in Experimental Grassland Ecosystems. *Functional Ecology*, Vol. 14, No. 3, pp. 326-337.
- van den Hurk, B.J.J.M., Viterbo, P., and Los, S.O. 2003. Impact of leaf area index seasonality on the annual land surface evaporation in a global circulation model. *Journal of Geophysics Research*, Vol. 108, No.D6, pp. 4191-4203.
- Wever, L.A., Flanagan, L.B., and Carlson, P.J. 2002. Seasonal and interannual variation in evapotranspiration, energy balance and surface conductance in a northern temperate grassland. *Agricultural and Forest Meteorology*, Vol. 112, No. 1, pp. 31-49.
- White, R., Murray, S., and Rohweder, M. 2000. Pilot analysis of global ecosystems-Grassland ecosystems. World Resources Institute Washington, DC. Available at <http://www.wri.org/wr2000>.
- Xu, L., and Baldocchi, D.D. 2004. Seasonal variation in carbon dioxide exchange over a Mediterranean annual grassland in California. *Agricultural and Forest Meteorology*, Vol. 1232, pp. 79-96.

CHAPTER 3 - LAI ESTIMATION IN SEMI-ARID MIXED GRASSLAND BY CONSIDERING BOTH TEMPORAL AND SPATIAL VARIATIONS

3.1 Introduction

As discussed in Chapter 1&2, accurate LAI estimates are urgently required for the land surface-atmosphere interaction modeling (Running et al., 1999) and a LAI-VI relationship is the most commonly used approach to determine LAI from remotely sensed data. However, the coefficient of determination (r^2) of LAI estimation from VIs derived from satellite imagery (satellite-level VIs) has demonstrated a wide range from 0.05 to 0.66 (Haboudane et al., 2002). The wide r^2 range is partially attributed to the influence of the effect factors, namely LAI spatial (horizontal and vertical) and temporal variations controlled by land surface heterogeneity and ecological parameters, such as soil moisture and topography. Considerable research has concluded that the accuracy of LAI estimation can be improved by taking the effect factors into account. Wulder et al. (1998) integrated texture into the LAI-VI relationships to increase the accuracy of LAI estimation in forest area. Rahman et al. (2003) and He et al. (2006a) found that an appropriate spatial scale or a suitable spatial resolution image for estimating LAI can avoid the potential errors arising from land surface heterogeneity. In addition, Chen and Cihlar (1996) have declared that more accurate overstory LAI estimation in forest can be obtained in late spring rather than in summer. A similar spring-summer difference was observed by Badhwar et al. (1986).

Aforementioned studies have demonstrated that LAI estimation could be improved by selecting the optimum spatial scale (or spatial resolution imagery) or the most appropriate estimation time. However, relatively few efforts have been made to improve LAI estimation by taking the comprehensive effects of land surface heterogeneity and

ecological parameters into account. Hence, this study aimed to estimate LAI via a LAI-VI relationship by taking both temporal and spatial variations into account. NDVI was chosen for LAI estimation, as it demonstrates a better and more stable performance than the other evaluated VIs, including the soil-line-related VIs in the study area (Li and Guo, 2010a). The procedures to achieve the objective are: 1) determining the optimum spatial scale for LAI estimation; 2) estimating LAI using ground NDVI by considering both temporal and spatial variations; and 3) validating the LAI estimation approach through satellite-level NDVI derived from satellite imagery.

3.2 Materials and Methods

3.2.1 Field Data

Field data used were LAI, soil moisture, and canopy reflectance collected over the sampling transect and plots through May to September in 2008.

3.2.2 Satellite Data and Preprocessing

Two SPOT 4 HRVIR 20m images were acquired on 4 June and 19 August, and two SPOT 5 HRV 10m images were collected on 30 August and 15 September 2008 for the study. Geometric correction was applied to all of the images based on the Saskatchewan road map and 18 ground control points around the study area taken by GPS with an accuracy of 2.0-5.0 m. The accuracy of geometric correction is higher than 0.5 pixel (RMSE <10m) for SPOT 4 and (<5m) for SPOT 5. Atmospheric correction was implemented by the Dark Object Subtraction (DOS) method, which is the most widely used image-based approach (Song et al., 2001). It is applicable due to the large water body in the area.

3.2.3 Methods to Identify the Optimum Spatial Scale for LAI Estimation

Logarithm10 transformation was made to make LAI and soil moisture collected over the sampling transect in or close to a normal distribution for the analyses. To determine the optimum spatial scale or suitable spatial resolution imagery for LAI estimation, the dominant co-variation scales of LAI and soil moisture were investigated through the wavelet approach. The spatial variation of soil moisture was considered, because He's et al. (2006a) research found that soil moisture and topography control two dominant spatial variation scales of LAI in semi-arid mixed grasslands. Besides, the spatial distribution of soil moisture is highly dependent on topography (Bindlish et al., 2008) in a natural landscape, thus the co-variation scale of soil moisture and LAI can partially represent the influence of topography on LAI spatial variation.

Although the observed spatial patterns of LAI would be similar (He et al., 2006a) to the result of a semivariogram analysis, the wavelet approach, including Morlet Wavelet Analysis (MWA), Cross-Wavelet Transform (XWT), and Wavelet Coherence Transform (WCT), was used due to the following advantages. First, the wavelet approach allows users to investigate the spatial co-variation scales of LAI and soil moisture. Second, wavelet analysis can identify the ranges of main variation scales of LAI and soil moisture and their co-variation scales, and define the exact location of transition. Due to the merits, the wavelet approach has been widely used since 1990s in many research areas, such as grassland remote sensing (He et al., 2006a), ecological landscape (Saunders et al., 2005), and vegetation biomass and topography (Si and Farrell, 2004). Details on algorithms of MWA, XWT, and WCT approaches refer to Torrence and Webster (1999), Grinsted et al. (2004), and Yates et al. (2007).

The wavelet analyses were conducted in the following procedure: 1) MWA was applied to the transformed data to investigate the spatial variation scales of LAI and soil moisture, respectively; 2) XWT was utilized to investigate spatial scales and locations where LAI and soil show high common power; and 3) WCT was performed to find the spatial scales and locations where LAI and soil moisture co-vary. The significance of wavelet spectra

was carried out against a Gaussian red noise (Pardo-Iguzquiza and Rodriguez-Tovar, 2000) due to the high spatial similarity of soil moisture (Si and Zeleke, 2005) and LAI at two adjacent locations in natural grasslands. The significant areas in their spectra are highlighted by black solid lines in the wavelet contour maps, which represent scales and locations at or above the 95% confidence interval.

Finity of LAI or soil moisture data results in edge effects on the results of the wavelet analyses. To minimize the edge effects, additional 128 zeros were padded to the 128 LAI data prior to the analysis according to the suggestion of Torrence and Compo (1998), and to the soil moisture data. The boundary represented by the effects of zero padding is called the Cone of Influence (COI) (Yates et al., 2007). Anomalous coefficients outside the COI may not be significant due to the fact that the decrease in variances outside the COI could be the results of zero padding. To avoid type I errors in which some locations may actually be significant by coincidence, only those significant locations that constitute an area greater than 5% of the area of the spectrum were accepted (Yates et al., 2007).

The spatial co-variation scales of LAI and soil moisture were determined based on the two criteria. First, the similar spatial variation scales of soil moisture and LAI at the same locations in the wavelet spectra of MWA are observable in their spatial distribution along the sampling transect (the profiles). Second, the spatial variation scales of LAI and soil moisture observed in MWA spectra can be supported by the XWT spectra, which can be further confirmed by the WCT spectra. Once the dominant spatial co-variation scale (s) between LAI and soil moisture is (are) observed, the suitable pixel size (s) of imagery and the optimum spatial scale (s) for LAI estimation can be determined to be one quarter of the spatial scale based on the sampling theorem (Yilmaz and Doherty, 1987). Spatial scales (or the pixel sizes of imagery), which are smaller than the optimum, cannot avoid the spatial autocorrelation issue on LAI estimation. Spatial scales, which are larger than the optimum, can eliminate the influence of spatial autocorrelation on LAI estimation. But they may introduce additional errors resulting from the effects of land surface heterogeneity (Chen, 1999; Jin et al., 2007).

3.2.4 Methods for LAI Estimation from Ground NDVI

LAI and canopy reflectance data over the sampling transect were utilized to investigate effects of spatial and temporal variations on LAI estimation at a ground-level. Canopy reflectance data were used to derive ground hyperspectral NDVI by calculating the ratio between the difference of Near Infrared (NIR, 800nm) and Red (670nm) reflectance to the sum of the two.

Three steps were taken to estimate LAI. First, a linear regression was applied to all ground LAI and NDVI data to establish their relationship. Second, relationships between LAI and NDVI were developed by considering the temporal variations in LAI (Li and Guo, 2010a). Third, LAI was estimated based on NDVI while considering both temporal and spatial variations. The spatial variation was considered by scaling up both LAI and NDVI data to the suitable scale determined by the wavelet analyses. Accuracy of LAI estimation was measured by the coefficient of determination (r^2), Average Relative Error (ARE), and Root Mean Squared Error (RMSE).

3.2.5 Methods for LAI Estimation from Satellite-Level NDVI

LAI data collected over the sampling transect and in each plot were arithmetically averaged, respectively, to estimate LAI from satellite-level NDVI data retrieved from NIR (band3) and Red (Band2) bands of SPOT 4/5 images. LAI zeros resulting from the senescence of vegetation in the late growing season were eliminated prior to the analyses. Relationships between LAI and NDVI were established via the linear regression approach with and without considering the temporal variation, respectively. The accuracy of LAI estimation was evaluated via the r^2 values.

3.3 Results and Discussion

3.3.1 The Optimum Spatial Scales for LAI Estimation

The spatial co-variation scales of LAI and soil moisture were investigated for each individual data collection. The dominant spatial scale on 17 June and 2 July was similar to that on 4 June (the early growing season), and data sets collected on 29 August (the early senescence season) demonstrated the same dominant spatial scale as those collected on 21 July and 15 August (the maximum growing season). Thus, to make the chapter readable, only results based on data collected on 4 June were illustrated.

The profiles of LAI and soil moisture along the sampling transect on 4 June 2008 are shown on **Figure 3.1**. LAI ranges from 0.02 to 1.83, with a mean of 0.64. The majority of values are under 0.60, and no certain spatial pattern is observed. Soil moisture has a mean of 0.20 and a range of 0.29. One cyclic pattern of soil moisture with three peaks is observed over the sampling transect, which is largely in consistent with the topography variation (**Figure 1.1c**). Higher LAI tends to be associated with higher soil moisture except for the two locations of 330-380m and 470-560m, where are temporal wetlands. Thus, vegetation species in there is different from other locations and greens later.

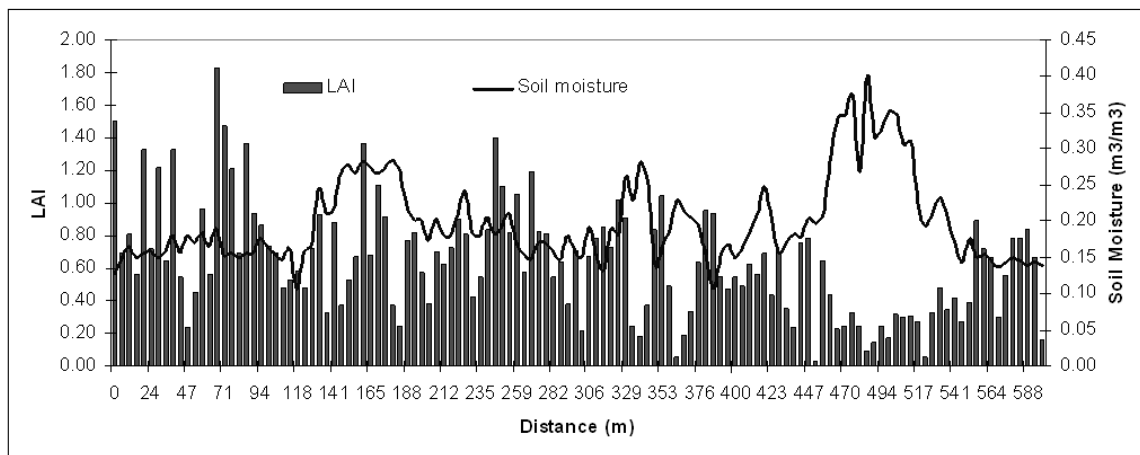


Figure 3.1 Profiles of LAI and soil moisture on 4 June 2008 in St. Denis, SK, Canada

The local wavelet power spectra for LAI and soil moisture are demonstrated in **Figure 3.2**. The spectra indicate that LAI has a significant spatial variation scale (approximate 80-

144m) at a distance between 330 and 400m (**Figure 3.2a**). At a similar distance, a significant scale of an approximate 120 to 160m is observed in the spectra of soil moisture (**Figure 3.2b**). The demonstrated scale is further confirmed by the large variation of LAI and soil moisture in the portion of the sampling transect (**Figure 3.1**). The other variation scales are either spurious or non-consistent scales between LAI and soil moisture.

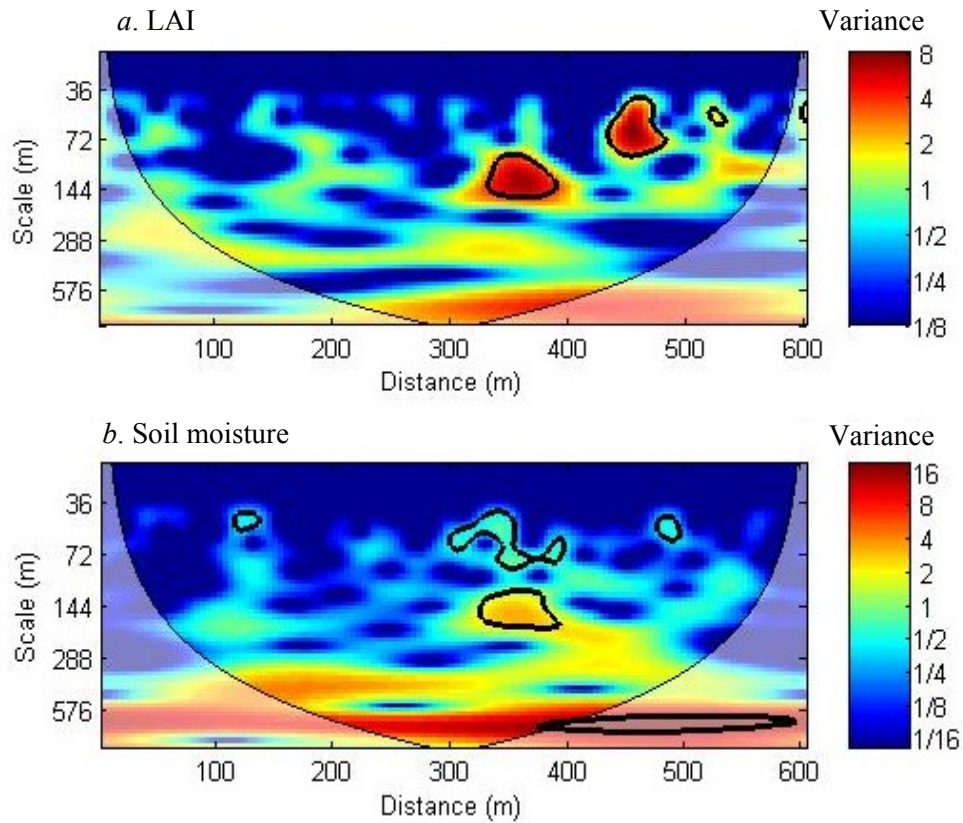


Figure 3.2 Spatial variations of (a) LAI and (b) soil moisture derived from Morlet wavelet analysis on 4 June 2008 in St. Denis, SK, Canada (Thin solid lines indicate the COI, and black solid lines indicate significant locations and scales at the 95% confidence interval)

The cross-wavelet spectra indicate a strong covariance between LAI and soil moisture at a 72-160m scale over a distance of 300-400m (**Figure 3.3a**). This is similar to the variation scale in the wavelet spectra for LAI and soil moisture (**Figure 3.2**). The arrows indicate that soil moisture and LAI covary in an opposite direction at this scale and distance. The other high covariance scales are either smaller than 5% of the spectral area or unobservable in the spectra of LAI or soil moisture, therefore are considered to be spurious.

As shown in **Figure 3.3b**, the wavelet coherency spectra confirm a significant relationship between LAI and soil moisture at a scale of 100-160m. The phase arrows point to the left, which indicates the relationship between LAI and soil moisture is negative due to the existing of temporal wetlands. All the other correlation scales observed in the spectra are considered to be spurious, because they are not observable in the spectra for LAI or soil moisture. Taking the spatial variation scales into account (**Figure 3.2&3.3**), the co-variation scale of LAI and soil moisture is 120-144m in the study area.

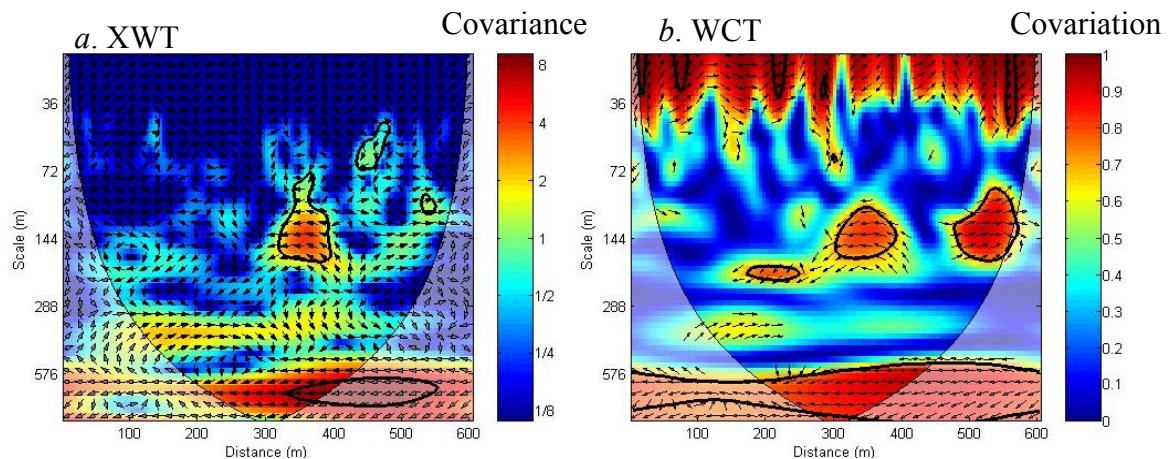


Figure 3.3 The spectra of (a) cross-wavelet and (b) wavelet coherency analysis between LAI and soil moisture on 4 June 2008 in St. Denis, SK, Canada. Thin solid lines indicate the COI, and black solid lines indicate significant locations and scales at the 95% confidence interval. Arrows in coherency wavelet spectra shows phase angles, pointing to left means negative effects and pointing to right indicates positive relationships.

Spatial variation scales of LAI controlled by soil moisture vary from a 120-144m scale in the early growing season to a 40-60m scale in the maximum growing season and early senescence season (not illustrated). However, no significant variation scale was observed in the late senescence season. According to the sampling theorem, the optimum spatial scale for LAI estimation is 30-38m in the early growing season and 10-15m in the maximum growing and early senescence seasons. Correspondingly, the current Earth Observing-1 (EO-1) 30m, the Satellite Disaster Monitoring Constellation (DMC)-1 32m, and Landsat TM/ETM+ 30m multispectral satellite images are the optimum spatial resolution imagery for LAI estimation in the early growing season in the study area. For LAI estimation in the maximum growing season and the early senescence seasons, however, the optimum satellite images are SPOT 5 10m, Advanced Spaceborne Thermal

Emission and Reflection Radiometer onboard on Terra (Terra-ASTER) 15m, and ALOS Advanced Visible and Near Infrared Radiometer type 2 (ALOS AVNIR-2) 10m multispectral images. Nonetheless, the suitable satellite images for LAI estimation in the late senescence season cannot be determined due to the lack of significant spatial variation scales. The nonsignificance is probably because LAI at that time is more controlled by vegetation phenology which is highly affected by local environment variables, such as temperature and precipitation.

The optimum spatial scales for LAI estimation in the early, maximum growing season, and early senescence season fall into the range of 10-50 m for estimating the coverage of C₄ species in GNP (Davidson and Csillag, 2001). He et al. (2006a) concluded that 35m is the suitable spatial scale for the grassland heterogeneity study in the summer in GNP. However, research carried out in southern California grassland indicates that roughly 6m would be optimum for grassland greenness estimation (Rahman et al., 2003). The difference in St. Denis and GNP from the southern California grassland could be possibly attributed to various grassland ecosystems controlled by dissimilar climate, topography, and soil.

3.3.2 LAI Estimation Based on Ground NDVI

The r^2 values of LAI-NDVI relationships from different approaches, and RMSE and ARE of LAI estimation while spatial variation is considered are listed in **Table 3.1**. Without considering temporal and spatial variation of LAI, the r^2 of LAI estimation is only 0.13. While the temporal variation was taken into account, r^2 increases to 0.20 and 0.22 in the maximum and the late growing season, respectively, while a slight decrease in r^2 (0.11) is observed in the early growing season.

An r^2 of 0.27 is obtained when the spatial variation was considered, while temporal variation was not. With both temporal and spatial variation considered, the r^2 increases to 0.32, 0.59, and 0.50 in the early, maximum, and the late growing season. At the same time, RMSE is 0.25 in both the early and maximum growing seasons and 0.12 in the late growing

season, and ARE is 0.30, 0.25, and 1.20 in the early, maximum, and late growing season, respectively.

Bivariate regression equations between NDVI and LAI at different growing stages are all formed by positive slopes (**Table 3.1**), which indicate an increase in LAI can be demonstrated by a rise in NDVI. However, the slopes are different in magnitude. The slope is the largest in the maximum growing season (3.47), followed by 1.84 in the late growing season, and 1.61 in the early growing season. Thus, a certain variation in LAI could cause a large variation in NDVI in the maximum growing season, moderate variation in the late growing season, and small variation in the early growing season.

Table 3.1 The r^2 , root mean squared error (RMSE), averaged relative error (ARE), and bivariate regression equations between NDVI and LAI (r_1^2 is from LAI estimation equations considering no spatial variations, while r^2 , RMSE, ARE considered)

Time Periods	r_1^2	r^2	RMSE	ARE	LAI-NDVI Equations
entire growing season	0.13 [†]	0.27 [†]	0.36	1.87	LAI=2.07NDVI-0.40 (n=154)
early Jun-early Jul	0.11 [†]	0.32 [†]	0.25	0.30	LAI=1.61NDVI+0.07 (n=66)
mid Jul-mid Aug	0.20 [†]	0.59 [†]	0.25	0.25	LAI=3.47NDVI-1.17 (n=44)
late Aug-mid Sep	0.22 [†]	0.50 [†]	0.12	1.20	LAI=1.84NDVI-0.71 (n=44)

[†]. The coefficient of determination is significant at the 0.05 level (2-tailed), and n is the sample size.

The LAI-NDVI relationship can provide the vegetative characteristics of a grassland community. When each vegetation growing season is considered individually, the relationship between LAI and NDVI is stronger due to LAI and chlorophyll content related spectral similarity. When the spatial variation in LAI is considered, the LAI-NDVI relationship is also stronger because of the species related spectral similarity among communities. Therefore, simultaneous consideration of the entire growing season and all communities results in a small model coefficient of determination. However, by taking both temporal and spatial variation into account, the r^2 values of LAI-NDVI models increase and prediction errors of models decrease.

The best LAI estimation is observed in the maximum growing season, indicated by the r^2 value (0.59), due to the fact that an increase in vegetation vigor enhances the capability of

NDVI which is quite sensitive to greenness (Rouse et al., 1974). The r^2 value is much higher than that (0.42) in GNP (He et al., 2006b), which might be attributed to the smaller percentage of exposed bare soil (3.5%) in St. Denis than that (19.3%) in GNP. It can also be accounted for by different vegetation species. The dominant vegetation along the sampling transect in St. Denis as stated in chapter 1 is different from the dominant vegetation in GNP discussed in Chapter 2. Besides, moss and lichen are also observed in GNP, but not in St. Denis. Additionally, the more complex terrain characteristic in GNP than St. Denis could also be responsible for the weaker LAI-NDVI relationship (Friedl et al., 1994).

The r^2 value of 0.32 in the early growing season in St. Denis is much smaller than that of 0.70 obtained in early June in a tallgrass prairie site in USA (Wylie et al., 2002). The difference could be mainly attributed to different vegetation species and management practices. The dominant grass cover in St. Denis is represented by C_3 species, while the tallgrass prairie is dominated by C_4 species. Management practices can exert an influence on the NDVI-LAI relationships through the effects on the accumulation of dead vegetation in the early growing season (Price et al., 1993). In St. Denis, no burning or grazing management have been applied for a few decades, which results in a large amount of dead vegetation (67.6%) in the early growing season, and further lead to the smaller r^2 value. Nonetheless, in the tallgrass prairie, spring burning and subsequent cattle-grazing dramatically reduce the influence of dead vegetation on LAI estimation.

By taking temporal and spatial variations of LAI into account, the ARE between LAI estimates and ground measurements is 0.25 in the maximum growing season. LAI quadrat measurements range from 0.02 to 3.7, thus the possible bias of LAI estimation could be 0.0 to ± 0.9 . The accuracy of LAI estimation can meet the requirement (± 0.2 to ± 1.0) for terrestrial climate modeling of the Global Climate Observation System (GCOS) and the Global Terrestrial Observation System (GTOS) (GCOS/GTOS, 1998). In the early growing season, ARE is 0.30 and the quadrat LAI varies from 0.02 to 2.6. The difference of LAI estimation from measurements could be 0 to ± 0.8 , which can meet the requirement for terrestrial climate modeling as well. However, in the late growing season, ARE is as

large as 1.20, and the quadrat LAI ranges from 0.0 to 1.68. The large discrepancy (0 to ± 2.0) of LAI estimation from measurements makes it less qualified for the climate modeling.

3.3.3 LAI Estimation from Satellite-Level NDVI

LAI estimation based on satellite-level NDVI derived from SPOT 4/5 imagery with and without taking the temporal variation into account are illustrated in **Figure 3.4** and **Figure 3.5**, respectively. The r^2 is only 0.22, when the temporal variation was not considered (**Figure 3.4**). Taking the temporal variation of LAI into account, r^2 values are improved by 0.13 in early June, 0.15 in mid August, and 0.08 in late August to mid September (**Figure 3.5**), although the relationships are nonsignificant at the 95% confidence interval except that in mid August. The slopes in LAI-NDVI equations decrease in the sequence, which indicates a reduced sensitivity of NDVI to LAI, of the maximum, early, and late growing season (**Figure 3.5**).

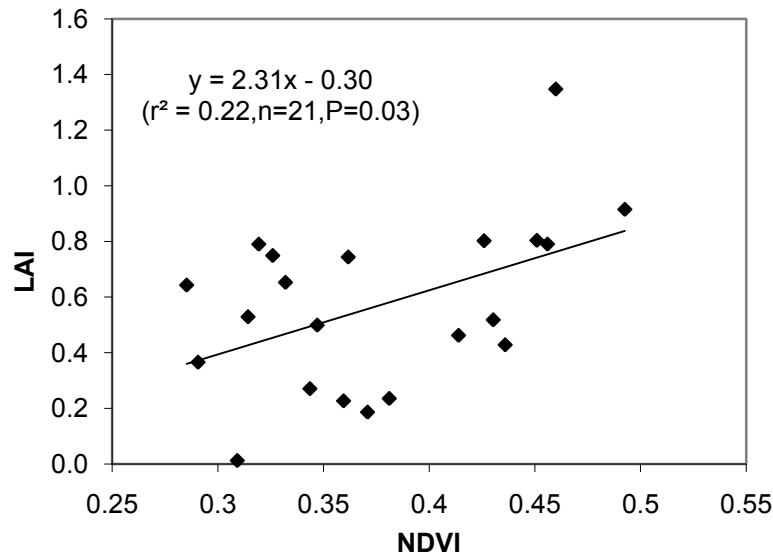


Figure 3.4 The relationship between LAI and satellite-level NDVI derived from SPOT 4/5 images at the 95% significance interval during the entire growing season (n is the sample number and P is the significant value)

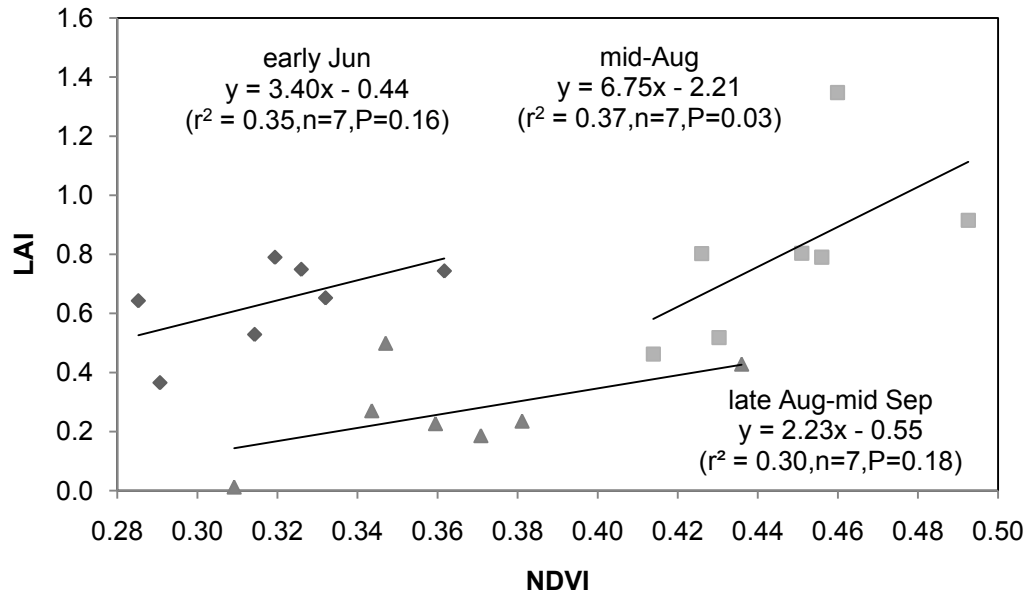


Figure 3.5 Relationships between LAI (y) and NDVI (x) derived from SPOT 4/5 images at the 95% significance interval in different vegetation growing seasons (n is the sample number and P is the significant value)

LAI estimation based on satellite-level NDVI confirmed the applicability of the proposed approach for LAI estimation. LAI estimation from the selected satellite imagery can be much improved by considering the temporal variations, although the r^2 values are not beyond 0.66 which currently is the largest number between LAI and satellite-level VIs (Haboudane et al., 2002). The relatively lower r^2 values may be resulting from the enlarged influence of dead vegetation and bare soil on NDVI derived from SPOT 4/5 images (Li and Guo, 2010b). Besides, the lower r^2 value in early June may also be attributed to the smaller pixel size of SPOT 4 than the suitable scale (30-38m), which is more likely to exhibit the spatial autocorrelation between pixels. However, the lower r^2 value in mid August is possibly influenced by the larger pixel size of SPOT 4 than the optimum (10-15m), which results in the mixture of ground covers within each pixel.

3.4 Conclusions

The optimum spatial scale for LAI estimation varied from 30-38m in the early growing season to 10-15m in the maximum growing and early senescence season. However, no specific spatial scale or spatial resolution imagery can be determined in the late senescence season.

LAI estimation can be greatly improved by taking the temporal and spatial variations of LAI into account to minimize spectral differences resulting from temporal variation of LAI and chlorophyll and the mixture of spatial species. The best LAI estimation can be obtained in the maximum growing season. Using ground data, the r^2 is significantly increased by 0.05 in the early growing season, 0.31 in the maximum growing season, and 0.23 in the late growing season. RMSE is dramatically decreased by 0.11, 0.11, and 0.24, while ARE is reduced by 1.57, 1.62, and 0.67 in the early, maximum, and late growing season, respectively. Based on the satellite data, the r^2 is improved by 0.13, 0.15, and 0.08 in early June, mid August, and late August-mid September, respectively. The improved LAI estimation is able to provide more accurate biophysical information for land surface-atmosphere interaction modeling.

3.5 References

- Badhwar, G.D., Macdonald, R.B., and Metha, N.C. 1986. Satellite derived leaf-area-index and vegetation maps as input to global carbon cycle models-a hierarchical approach. *International Journal of Remote Sensing*, Vol.7, pp. 265- 281.
- Bindlish, R., Jackson, T.J., Gasiewski, A., Stankov, B., Klein, M., Cosh, M.H., Mladenova, I., Watts, C., Vivoni, E., Lakshmi, V., Bolten, J., and Keefer, T. 2008. Aircraft based soil moisture retrievals under mixed vegetation and topographic conditions. *Remote Sensing of Environment*, Vol. 112, No. 2, pp. 375-390.
- Chen, J. M., and Cihlar, J. 1996. Retrieving leaf area index of boreal conifer forests using Landsat TM images. *Remote Sensing of Environment*, Vol. 55, pp. 153-162.
- Chen J.M. 1999. Spatial scaling of a remotely sensed surface parameter by contexture. *Remote Sensing of Environment*, Vol. 69, pp. 30-42.

- Davidson, A., and Csillag, F. 2001. The influence of vegetation index and spatial resolution on a two-date remote sensing derived relation to C4 species coverage. *Remote Sensing of Environment*, Vol. 75, No. 1, pp. 138-151.
- Friedl, M.A., Michaelson, J., Davis, F.W., Walker, H., and Schimel, D.S. 1994. Estimating grassland biomass and leaf area index using ground and satellite data. *International Journal of Remote Sensing*, Vol.15, pp. 1401-1420.
- Global Terrestrial Observing System and Global Climate Observing System (GCOS/GTOS).1998. Report of the GCOS/GTOS terrestrial observation panel for climate. Available online at: <http://www.fao.org/gtos/doc/pub15.pdf> (accessed 10 September 2009).
- Grinsted, A., Jevrejeva, S., and Moore, J. 2004. Application of the cross wavelet transform and wavelet coherence to geophysical time series. *Nonlinear Processes in Geophysics*, Vol. 11, No.(5, 6), pp. 561-577.
- Haboudane, D., Miller, J., Pattey, E., Zarco-Tejada, P.J., and Strachan, I. 2002. Effects of chlorophyll concentration on green LAI prediction in crop canopies: modeling and assessment. In *Proceedings of the First International Symposium on Recent Advances in Quantitative Remote Sensing*. pp. 891-899 (Valencia: Publicacions de la Universitat de València).
- He, Y., Guo, X., Wilmschurst, J., and Si, B. 2006a. Studying mixed grassland ecosystems II: optimum pixel size. *Canadian Journal of Remote Sensing*, Vol. 32, No. 2, pp. 108-115.
- He, Y., Guo, X., and Wilmschurst, J. 2006b. Studying mixed grassland ecosystems I: suitable hyperspectral vegetation indices. *Canadian Journal of Remote Sensing*, Vol. 32, No. 2, pp. 98-107.
- Jin, Z., Tian, Q., Chen, J.M., and Chen, M. 2007. Spatial scaling between leaf area index maps of different resolutions. *Journal of Environmental Management*, Vol. 85, pp. 628-637.
- Li, Z., and Guo, X. 2010 (a). A Suitable Vegetation Index for Monitoring Temporal Variations of LAI in Semi-arid Mixed Grassland. Submitted.
- Li, Z., and Guo, X. 2010 (b). Evaluation of NDVI Products for Monitoring Spatiotemporal Variations of LAI in Semi-arid Mixed Grassland. Submitted.
- Pardo-Igu'Zquiza, E. and Rodri'Guez-Tovar, F.J. 2000. The permutation test as a non-parametric method for testing the statistical significance of power spectrum estimation in cyclostratigraphic research. *Earth and Planetary Science Letters*, Vol. 181, pp. 175-189.

- Price, K.P., Varner, V.C., Rundquist, D.C., and Peake, J.S. 1993. Influences of land management and weather on plant biophysical and hyper-spectral response patterns of tallgrass prairies in northeastern Kansas. In PECORA12, 24-26 August 1993, Sioux Falls, South Dakota, pp. 441- 450.
- Rahman, A.F., Gamon, J.A., Sims, D.A., and Schmidts, M. 2003. Optimum pixel size for hyperspectral studies of ecosystem function in southern California chaparral and grassland. *Remote Sensing of Environment*, Vol. 84, pp. 192-207.
- Rouse, J.W., Haas, R.H., Schell, J.A., Deering, D.W., and Harlan, J.C. 1974. Monitoring the vernal advancement of retrogradation of natural vegetation. National Aeronautics and Space Administration, Goddard Space Flight Center (NASA/GSFC), Type III, Final Report, Greenbelt, Md. 371 pp.
- Running, S.W., Baldocchi, D.D., Turner, D.P., Gower, S.T., Bakwin, P.S., and Hibbard, K.A. 1999. A global terrestrial monitoring network integrating tower fluxes, flask sampling, ecosystem modeling and EOS satellite data. *Remote Sensing of the Environment*, Vol. 70, pp. 108-127.
- Saunders, S.C., Chen, J., Drummer, D., Gustafson, E.J., and Brosofske, K.D. 2005. Identifying scales of pattern in ecological data: a comparison of lacunarity, spectral and wavelet analyses. *Ecological Complexity*, Vol. 2, pp. 87-105.
- Si, B.C., and Farrell, R.E. 2004. Scale-dependent relationships between wheat yield and topographic indices: A wavelet approach. *Soil Science Society of America Journal*, Vol. 68, pp. 577-588.
- Si, B.C., and Zeleke, T.B. 2005. Wavelet coherency analysis to relate saturated hydraulic properties to soil physical properties. *Water Resources Research*, Vol. 41, W11424.
- Song, C., Woodcock, C.E., Seto, K.C., Lenney, M.P., and Macomber, S.A. 2001. Classification and Change Detection Using Landsat TM Data: When and How to Correct Atmospheric Effects? *Remote Sensing of Environment*, Vol. 75, No. 2, 230-244.
- Torrence, C., and Compo, G.P. 1998. A practical guide to wavelet analysis. *Bulletin of the American Meteorological Society*, Vol. 79, pp. 61-78.
- Torrence, C., and Webster, P.J. 1999. Interdecadal changes in the ENSO monsoon system. *Journal of Climate*, Vol. 12, pp. 2679-2690.
- Wulder, M.A., Drew Le, E.F., Franklin, S.E., and Lavigne, M.B. 1998. Aerial image texture information in the estimation of the northern deciduous and mixed wood forest leaf area index (LAI). *Remote Sensing of Environment*, Vol. 64, pp. 64-76.

- Wylie, B.K., Meyer, D.J., Tieszen, L.L., and Mannel, S. 2002. Satellite mapping of surface biophysical parameters at the biome scale over the North American grasslands: A case study. *Remote Sensing of Environment*, Vol. 79, pp. 266-278.
- Yates, T.T., Si, B.C., Farrell, R. E., and Pennock, D.J. 2007. Time, location, and scale dependence of soil nitrous oxide emissions, soil water, and temperature using wavelets, cross-wavelets, and wavelet coherency analysis. *Journal of Geophysical Research*, Vol. 112, No. D09, pp. 104-119.
- Yilmaz, O., and Doherty, S.M. (Eds.). 1987. *Seismic data processing. Investigations in Geophysics*, pp536 (Society of Exploration Geophysicists, Tulsa, Okla).

CHAPTER 4 - EVALUATION OF NDVI PRODUCTS FOR MONITORING SPATIOTEMPORAL VARIATIONS OF LAI IN SEMI-ARID MIXED GRASSLAND

4.1 Introduction

The NDVI product is an important intermediary of biophysical parameters in modeling. The wide application of NDVI products have stimulated considerable research on the inter-annual consistency of NDVI products related to spectral differences and spatial consistency. However, the performance of NDVI products on monitoring intra-annual spatial variability in LAI was rarely discussed. In addition, inconsistency between MODIS and SPOT-VGT NDVI products is land cover-dependent and is higher in semi-arid regions than in some other moist areas (Brown et al., 2006). The inconsistency is possibly even higher in semi-arid mixed grassland, which is characterized by complex canopy covers, substantive dead materials, and exposed bare soil (Asner et al., 1998; Guo, 2002). Besides, NDVI demonstrates a quite good and stable performance on quantifying intra-annual variation of LAI in semi-arid mixed grassland (Li and Guo, 2010a). Therefore, it is necessary and feasible to determine a suitable NDVI product on monitoring spatial and temporal variations of LAI in semi-arid mixed grasslands for the purpose of improving grassland modeling.

This study aims to evaluate the performances of version 5 (V5)16-day MODIS 250m, 1km, and 10-day SPOT-VGT NDVI products on monitoring spatiotemporal variations of LAI in semi-arid mixed grassland. More specifically, 1) the consistency between ground hyperspectral NDVI and satellite-level SPOT 4/5 NDVI, MODIS 250m, 1km, as well as SPOT-VGT 1km NDVI products was evaluated; 2) the capability of NDVI data in differentiating spatiotemporal variations of LAI was investigated based on the ground hyperspectral and SPOT 4/5 NDVI; 3) performances of MODIS 250m NDVI products on monitoring spatiotemporal variations of LAI were assessed; 4) performances of MODIS 1km and SPOT-VGT 1km NDVI products on describing temporal variations of LAI in the

grassland were evaluated; and 5) a semivariogram analysis of the SPOT 4/5 NDVI data was conducted to investigate a suitable spatial resolution for differentiating spatial variation of NDVI in the landscape.

4.2 Materials and Methods

4.2.1 Ground-level Data

Ground-level data used were LAI and canopy reflectance collected over the sampling transect and the plots. Canopy reflectance data were used to derive ground hyperspectral NDVI, which minimizes possible errors introduced by radiometric unreliability (Teillet et al., 2001) and other factors including topography, atmospheric conditions, and sun-sensor geometry (Steven et al., 2003). Therefore, it is a sound base for the comparison of NDVI datasets from different sensors at different time (Steven et al., 2003).

4.2.3 Satellite-level Data

Satellite-level data used are multispectral imagery and NDVI products (**Table 4.1**). Multispectral imagery includes SPOT 4 20m images and SPOT 5 10m images. Details on the data information and pre-processing were given in Chapter 3. NDVI was then derived over the sampling transect and plots from the calibrated images (**Figure 4.1a**), and was averaged for tamed and native grassland, respectively. The averaged NDVI data were compared to the ground hyperspectral NDVI obtained in the adjacent date.

Table 4.1 Characteristics for ground hyperspectral and satellite-level NDVI datasets

Sensor	Spectro-radiometer	MODIS	SPOT-VGT	SPOT 4	SPOT 5
Data Source	field measure	LP DAAC	VITO	purchased level-2 scenes	purchased level-2 scenes
Nominal pixel size	~1m	250m, 1000m	1000m	20m	10m
Compositing period	\	16-day	10-day	\	\
Compositing method	\	CV-MVC; MVC	MVC	\	\
Spectral wavelength	Red: 670 nm NIR:800 nm	Red: 620-670 nm NIR:840-880 nm	Red: 610-680 nm NIR:780-890 nm	Red: 610-680 nm NIR:780-890 nm	Red: 610-680 nm NIR:790-890 nm
Radiometric resolution	\	12 bit	10 bit	8 bit	8 bit
Off-nadir view angle	\	65°	50.5°	27°	27°
Date period	Biweekly, Jun-Sep, 2008	May 1-Oct 1,2007,2008	May 1-Oct 1,2007,2008	May 2, Jun 4, and Aug 19, 2008	Aug 30 and Sep 15, 2008

The selected NDVI products are 10-day SPOT-VGT 1km NDVI products and V5 16-day MODIS 250m, 1km NDVI products due to their advantages over AVHRR NDVI composites in spectral and radiometric properties. MODIS 500m NDVI products were not evaluated because they demonstrate similar spatial variability with MODIS 1km NDVI products in grasslands (Tarnavsky et al., 2008). The characteristics of sensors and NDVI products are listed in **Table 4.1**. Full discussion of differences in the spectral properties (eg. waveband width) can be found from Trishchenko et al. (2002) and Van Leeuwen et al. (2006).

The 10-day synthesis SPOT-VGT 1km NDVI products used covered May to October in both 2007 and 2008 and were downloaded from the website (<http://free.vgt.vito.be/>) hosted by VITO (Flemish Inst. Technological Research, Belgium). The products were produced in geographic coordination using the maximum value compositing (MVC) technique (Holben, 1986) to minimize effects of spectral properties, radiometric resolution, atmosphere, and most importantly, to minimize the effects of clouds (Brown et al., 2006).

The regional subsetting was implemented before the data retrieval based on the geographic coordination.

The V5 16-day MODIS NDVI products from May to October in both 2007 and 2008 were downloaded from <https://wist.echo.nasa.gov/api/>, owned by the NASA Land Processes Distributed Active Center (LP DAAC). They were produced in a sinusoidal projection (SIN). A constrained-view MVC (CV-MVC) approach was used to minimize the off-nadir tendencies of the MVC when the input data were cloud free. However, MVC was used instead of the CV-MVC when the input data were affected by varied lighting attributed to different cloud conditions (Didan and Huete, 2006). Post-processing includes reprojection from SIN to Universal Transverse Mercator (UTM), regional sub-setting, and data retrieval. Both SPOT-VGT and MODIS NDVI products were compared to ground hyperspectral NDVI data in their corresponding compositing period.

4.2.4 Methods

4.2.4.1 Consistency between Satellite-Level and Ground Hyperspectral NDVI

To measure the data consistency, the averaged SPOT 4/5 NDVI, MODIS 250m, 1km, and SPOT-VGT 1km NDVI in tamed and native grassland were plotted against the averaged ground hyperspectral NDVI. Pearson's r between them was also computed. If satellite-level NDVI products are highly consistent with ground-level NDVI, then they have a similar capability with ground NDVI to describe spatiotemporal variations of LAI.

4.2.4.2 Ground Hyperspectral NDVI and SPOT 4/5 NDVI to Differentiate Spatiotemporal Variations of LAI

Intra-annual spatial variations of ground hyperspectral NDVI and SPOT 4/5 NDVI were compared to the spatiotemporal variation of LAI in 2008 in tamed and native grassland. The capability of NDVI data was measured based on two criteria: 1) intra-annual NDVI variation is consistent with LAI temporal variation in both tamed and native grassland, and 2) discrepancy of LAI in tamed and native grassland can be identified by the difference in NDVI.

4.2.4.3 MODIS 250m NDVI Products to Differentiate Spatiotemporal Variations of LAI
 Spatiotemporal variations of MODIS 250m NDVI products and LAI in 2008 were compared to evaluate performances of NDVI products based on the same criteria used for ground hyperspectral NDVI and SPOT 4/5 NDVI data. To evaluate the stability of the performance, spatiotemporal variations of MODIS 250m NDVI products in 2007 were also described.

4.2.4.4 MODIS and SPOT-VGT 1km NDVI Products to Differentiate Temporal Variations of LAI

Considering the size of tamed and native grassland is smaller than $1\text{km} \times 1\text{km}$, performances of MODIS and SPOT-VGT 1km NDVI products were evaluated only based on their temporal profiles in the entire grassland in 2007 and 2008. Also, their performances were compared to MODIS 250m NDVI products based on the calculated change rates (slopes) between two adjacent observation dates.

4.2.4.5 A Suitable Spatial Resolution to Differentiate LAI Spatial Variations in the Landscape

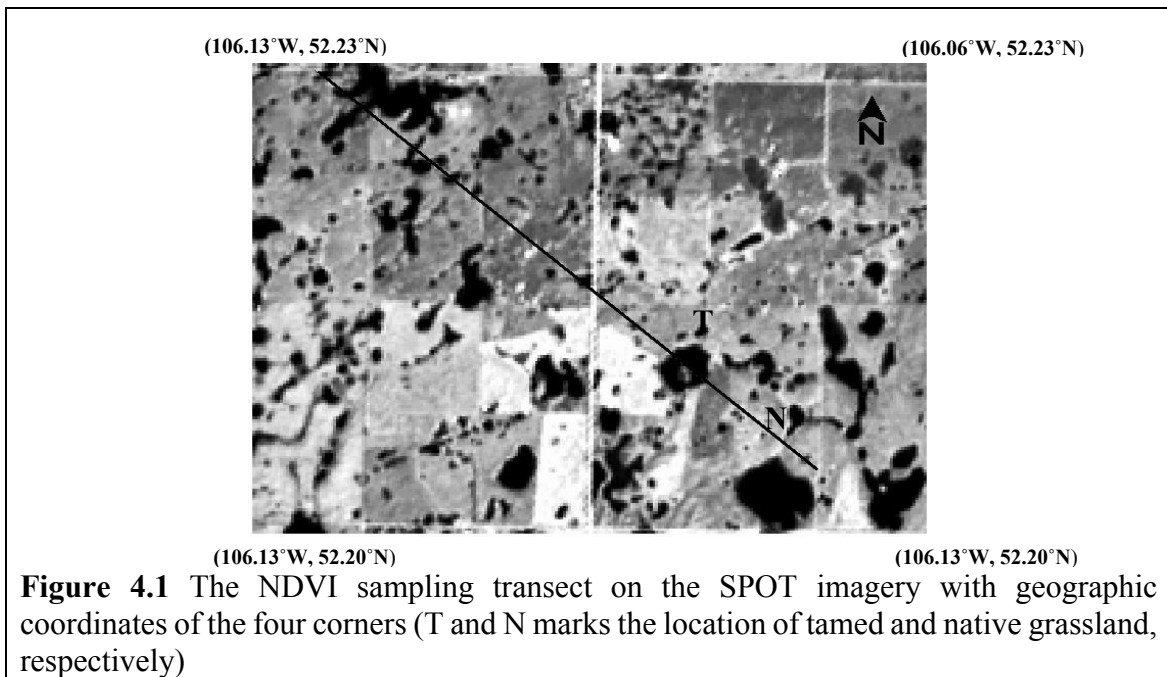
A semivariogram analysis of SPOT 4/5 NDVI data was conducted to determine a suitable spatial resolution for differentiating LAI spatial variations controlled by different land covers, such as tamed grassland, native grassland, wetlands, and croplands in the landscape. The finding was used to support the suitable NDVI product on describing spatiotemporal variations in LAI in tamed and native grassland.

The semivariance between any two samples of $n(h)$ pairs with an interval lag h is expressed by:

$$\lambda(h) = \frac{1}{2n} \sum_{i=1}^n (z(x_i) - z(x_i + h))^2 \quad (4.1)$$

where $z(x_i)$ is the NDVI derived at a geolocation x over the sampling transect from the SPOT 4/5 images. The 4500m-long transect was randomly set up across native and tamed

grassland, wetland, and cropland in the St. Denis area (**Figure 4.1**). $\lambda(h)$ is an unbiased estimation of the population variance, which is a measure of similarity between spatially regionalized variables. The smaller the value of $\lambda(h)$, the greater is the similarity of the samples. A semivariogram for the population is demonstrated by the relationship between semivariance (λ) and lag vectors of h . Details on a semivariogram analysis were given by Rahman et al. (2003) and He et al. (2006).



4.3 Results and Discussion

4.3.1 Comparisons between Satellite-Level and Ground Hyperspectral NDVI

The comparisons between SPOT 4/5, MODIS 250m, 1km, and SPOT-VGT 1km NDVI data and ground hyperspectral NDVI in the growing season of 2008 are shown in **Figure 4.2**. The closer the satellite-level NDVI data sets are to the 1:1 line, the more similar they are to the ground NDVI. The satellite-level NDVI is moderately to highly consistent with the ground NDVI. The MODIS 250m NDVI shows the highest consistency with the

ground NDVI, especially when the ground NDVI is greater than 0.55. The MODIS 1km NDVI also demonstrates high consistency, while both the SPOT 4/5 and SPOT-VGT NDVI are in moderate agreement with ground NDVI. Despite the moderate to high consistency, the majority of satellite-level NDVI are smaller than the ground hyperspectral NDVI.

All the satellite-level NDVI data are linearly correlated with the ground NDVI data, showing moderate to high relationships, although the statistical significances cannot be tested due to the autocorrelation of NDVI determined by the overlapping of bandwidths (Steven et al., 2003). The MODIS 250m NDVI products have the strongest relationship with ground NDVI data with an r of 0.90, followed by the MODIS 1km NDVI, SPOT4/5 NDVI, and SPOT-VGT 1km NDVI data in the decrease sequence of r values. The moderate to high linear relationships indicate that: 1) satellite-level NDVI data can be calibrated through ground hyperspectral NDVI to improve their performances; and 2) if ground NDVI data are able to differentiate spatiotemporal variations of LAI in the mixed grassland, then satellite-level NDVI data, especially MODIS 250m NDVI products, can also at least capture the variations to a certain degree.

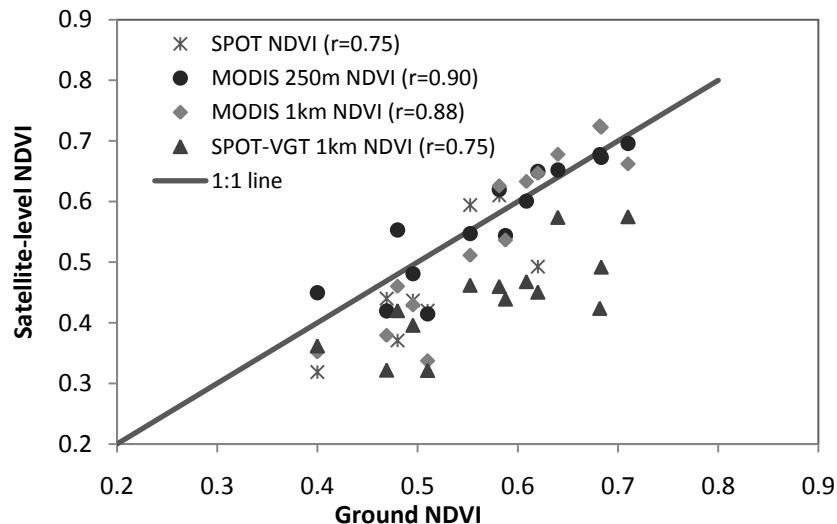


Figure 4.2 The scatter plot of satellite-level NDVI against ground NDVI, with Pearson's r values

Deviation of satellite-level NDVI from ground hyperspectral NDVI could be due to: 1) large differences in spatial resolution; 2) large differences in the position and width of the NIR and red spectral bands which are used to calculate NDVI; 3) data acquisition date; and 4) atmospheric effects related to viewing angle and acquisition time. The consistency between V5 16-day MODIS 250m, 1km NDVI products and ground hyperspectral NDVI data is high, especially when ground NDVI is greater than 0.55. This finding is supported from another perspective by the conclusion of Goetz (1997) that the maximum NDVI compositing of low spatial resolution AVHRR 1km data are highly consistent with medium spatial resolution Landsat Thematic Mapper (Landsat TM) 5 NDVI. The possible reason for the high consistency is that the improved CV-MVC compositing method in V5 data constrains the effects of a large viewing angle (65°) of MODIS and minimizes the issues related to the consequent bidirectional reflectance distribution function (BRDF) (Didan and Huete, 2006). In addition, the improved Aerosol filtering (Didan and Huete, 2006) and the 16-day compositing period (Fensholt et al., 2007) minimize the atmospheric effects related to the viewing angle and data acquisition time. The consistency between MODIS NDVI products and ground NDVI is reduced when the latter is smaller than 0.55. This could be due to the effects of large amounts of dead vegetation on ground during the early and late growing season in the study area (Li and Guo, 2010). Dead vegetation has a great contribution to the variation of NIR and red reflectance (Galvao et al., 2000; Steven et al., 2003), thus enlarges the spectral differences resulting from the different spectral and spatial resolution in MODIS NDVI products and ground hyperspectral NDVI.

Comparatively, larger differences between SPOT 4/5 NDVI, SPOT-VGT NDVI, and ground NDVI were observed. The larger difference between SPOT 4/5 and ground NDVI is possibly attributed to the much broader bandwidth of red and NIR (lower spectral resolution) of SPOT sensors (Teillet et al., 1997; Galvao et al., 2000; Steven et al., 2003). Moreover, a large amount of dead vegetation could enlarge the NDVI difference resulted from the broader wavelength ranges of SPOT 4/5 images. The other possible reason is related to image acquisition dates. For example, variation in vegetation condition between the image acquisition and the ground measure collection day could partly account for the difference. Similarly, the larger difference of SPOT-VGT NDVI from ground NDVI could

be due to the much broader bandwidth (same as SPOT 4). The lower geolocation accuracy of about 300m at nadir (Carmona-Moreno, 2000) of SPOT-VGT could also contribute to the larger difference. In addition, the deficiency of cloud-screening algorithm (Saint, 1995; Brown et al., 2006; Fensholt et al., 2006) due to the lack of a thermal band of SPOT possibly results in the larger difference as well.

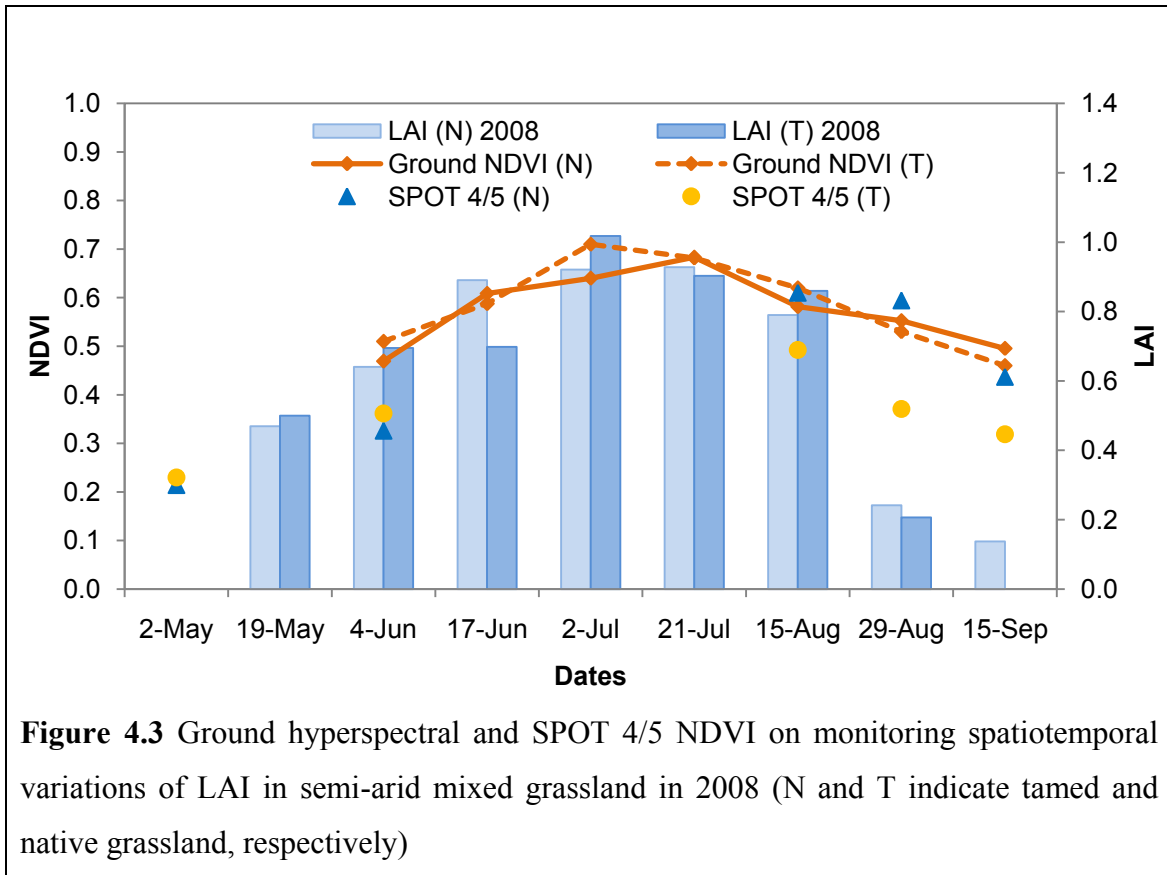
The linear relationships between satellite-level NDVI and ground NDVI were consistent with the finding of Steven et al. (2003) that NDVI from different sensors are strongly linearly correlated based on the simulated NDVI from ground hyperspectral reflectance in cropland. Thus, satellite-level NDVI can be calibrated based on ground NDVI by a linear regression approach.

4.3.2 Differentiating Spatiotemporal Variations of LAI

4.3.2.1 Ground Hyperspectral and SPOT 4/5 NDVI Data

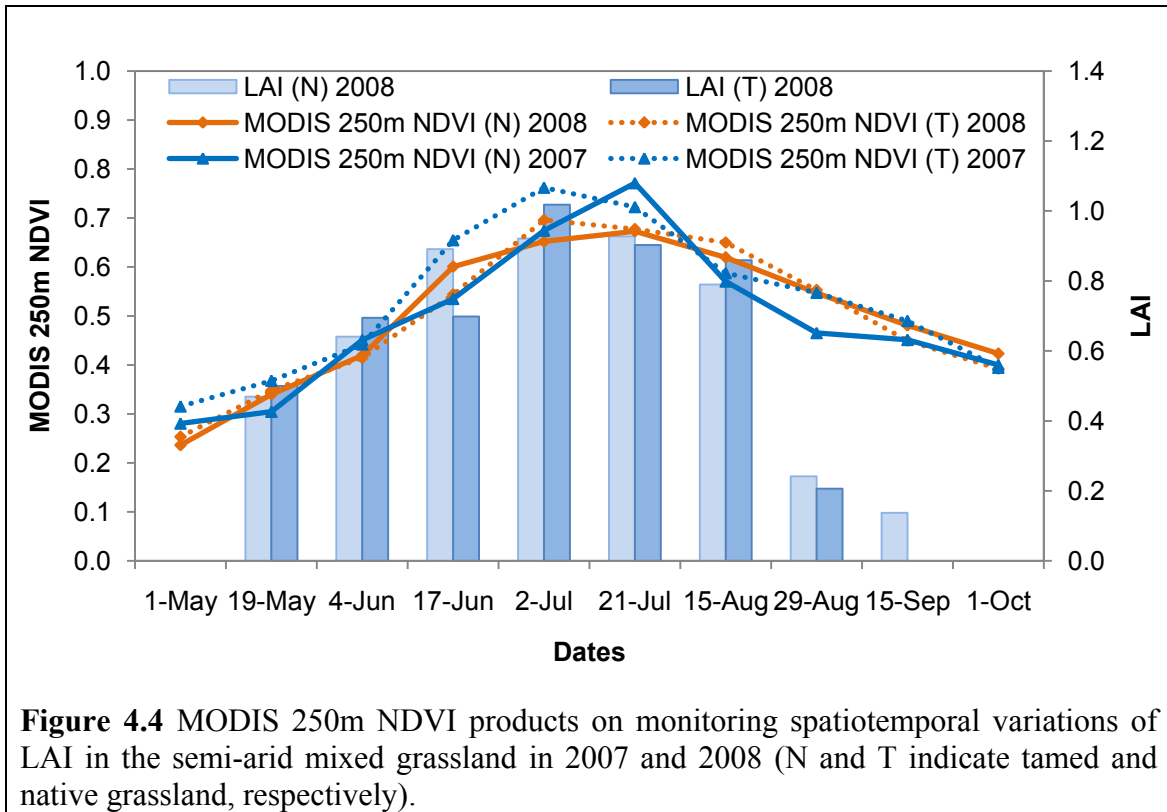
Performances of ground hyperspectral and SPOT 4/5 NDVI in 2008 on monitoring spatiotemporal variations of LAI are demonstrated in **Figure 4.3**. Ground hyperspectral NDVI data can successfully differentiate the spatiotemporal variations of LAI caused by different vegetation communities in the study area. They can capture the earlier greenup, peak growing, and senescence of dominant vegetation in tamed grassland. Both LAI and NDVI in tamed grassland are larger than native grassland in early June due to the earlier vegetation greenup. They are smaller than native grassland in mid June due to the quick growth of forbs in native grassland. In early July, both LAI and NDVI in tamed grassland have reached their peaks, while native grassland did not reach the maximum until late July. From late August to mid September, both LAI and NDVI in tamed grassland are smaller than those in native grassland due to the earlier onset of senescence. The success of ground NDVI on monitoring spatiotemporal variations of LAI shows a promising capacity of satellite-level NDVI to describe LAI spatiotemporal variations based on the moderate to high consistencies between ground NDVI and satellite-level NDVI. Although differences in SPOT 4/5 and ground NDVI data are observable (**Figure 4.2&4.3**), SPOT 4/5 NDVI

data are able to basically capture spatiotemporal variations of LAI. This is supported by the moderate linear relationship between the two datasets. But one exception was observed in mid August when a lower LAI in native grassland was falsely indicated by a higher NDVI.



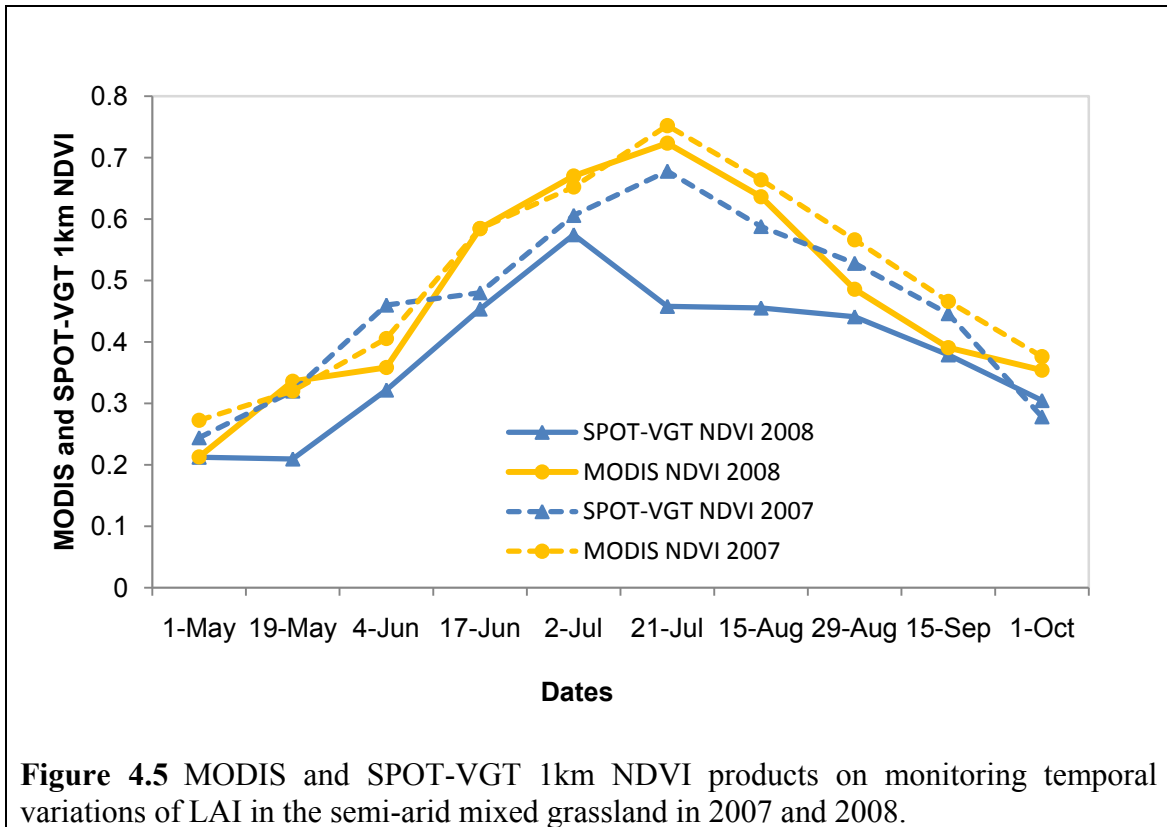
4.3.2.2 Satellite-level MODIS 250m NDVI products

The earlier greenup, peak growing and the corresponding higher LAI values, as well as the earlier senescence and the corresponding lower LAI values in tamed grassland can be basically represented by MODIS 250m NDVI data (**Figure 4.4**). The only exception occurred in early June when there was a larger LAI but a slightly smaller NDVI in tamed grassland. MODIS 250m NDVI products in 2007 are also able to capture the earlier vegetation phenology in tamed grassland than native grassland, which confirmed their capability to monitor spatiotemporal variations of LAI. Nonetheless, dissimilarities in the NDVI temporal profiles in tamed and native grassland was observed in 2007 and 2008 attributed to different inter-annual vegetation condition determined by varied macro- and micro-environments.



4.3.2.3 MODIS and SPOT-VGT 1km NDVI Products

Figure 4.5 illustrates the temporal variations of MODIS and SPOT-VGT 1km NDVI products in 2007 and 2008. MODIS 1km NDVI products demonstrate a similar temporal variation pattern with the peak values observed in late July in 2007 and 2008, although differences in NDVI values are noticeable. SPOT-VGT 1km NDVI products exhibit an analogous temporal variation profile with MODIS 1km NDVI products in 2007, although an obvious dissimilarity is observed in early June. Nonetheless, the temporal variation of SPOT-VGT 1km NDVI products in 2008 shows a distinct pattern from MODIS 1km NDVI products, with a peak value in early July and an abrupt decrease in mid-July. The temporal variation patterns of SPOT-VGT NDVI products in 2007 and 2008 are obviously different. The similarity of MODIS 1km NDVI products and dissimilarity of SPOT-VGT NDVI products in 2007 and 2008 indicate that MODIS 1km NDVI products have more stable performances in the semi-arid mixed grassland.



Besides, the performances of MODIS and SPOT-VGT 1km NDVI products were also compared against the MODIS 250m NDVI products through comparisons on NDVI change rates (slopes) at an approximately biweekly interval (**Table 4.2**). Slopes in 2008 indicate that MODIS 250m NDVI products have the greatest ability to capture the temporal variations in LAI, although differences in their slopes are large from mid-August to mid-September. The large slopes of LAI during that time period are accounted for by a dramatic decrease possibly resulted from the validation procedure of PAI to obtain LAI. The procedure was developed based on vegetation clipped in the maximum growing season and could underestimate LAI in the late growing season (**Appendix 1**).

Thus, the closer change rate of the 1km spatial resolution NDVI products to MODIS 250m NDVI products at each two adjacent observation dates, the better performances they would have on monitoring intra-annual variations in LAI. From **Table 4.2**, differences in slopes of MODIS 1km from MODIS 250m NDVI products are commonly much smaller than deviations in change rates of SPOT-VGT 1km from MODIS 250m NDVI products. The

similarity of MODIS 1km with MODIS 250m NDVI products can probably be attributed to the data processing procedure. MODIS 1km NDVI products are produced by aggregating red and NIR reflectance from MODIS 250m NDVI products through MODIS Gridding and Aggregation Process (Wolfe et al., 1998; Tarnavsky et al., 2008).

Table 4.2 Change rates (Slopes) at each two adjacent observation dates of MODIS 250m, 1km, and SPOT-VGT 1km NDVI products in 2007 and 2008 (with slopes of LAI included in 2008)

Date Periods	NDVI Composites in 2007			NDVI Composites and LAI in 2008			
	SPOT-VGT	MODIS 1km	MODIS 250m	SPOT-VGT	MODIS 1km	MODIS 250m	LAI
May 1- May 19	0.13	0.08	0.06	-0.01	0.22	0.17	\
May 19 - Jun 4	0.18	0.12	0.14	0.21	0.03	0.10	0.16
Jun 4 - Jun 17	0.02	0.18	0.14	0.17	0.24	0.16	0.09
Jun 17- Jul 2	0.12	0.05	0.09	0.12	0.07	0.08	0.10
Jul 2-Jul 21	0.06	0.07	0.02	-0.11	0.04	0.00	0.03
Jul 21 - Aug 15	-0.07	-0.06	-0.13	0.00	-0.06	-0.03	-0.08
Aug 15 - Aug 29	-0.05	-0.08	-0.07	-0.02	-0.13	-0.07	-0.57
Aug 29 - Sep 15	-0.08	-0.10	-0.04	-0.08	-0.11	-0.08	-0.53
Sep 15 - Oct 1	-0.23	-0.11	-0.08	-0.11	-0.05	-0.07	\

Note: “\” means no LAI data obtained during those time periods.

Sixteen-day MODIS 1km NDVI products are superior to 10-day SPOT-VGT 1km NDVI composites to monitor temporal variations in LAI. This observation contradicts the claim of Brown et al. (2006) that MODIS and SPOT-VGT NDVI time series products are capable of capturing the annual vegetation phenology to a similar degree. However, it is in agreement with Fensholt et al (2007)’s conclusion that 16-day MVC MODIS NDVI composites outperform 10-day MVC NDVI composites in the semi-arid area of West Africa. The different performances of MODIS and SPOT-VGT 1km NDVI products could be due to differences in their compositing methods and periods, intrinsic properties including viewing angle, bandwidth (spectral resolution), radiometric resolution, spectral band response function (SRF), and the point spread function (PSF), as well as other factors, such as atmospheric correction and co-registration.

In terms of compositing methods and periods, the 16-day compositing period of MODIS 1km NDVI products can reduce more noise induced by atmospheric effects (Fensholt et al., 2007) than the 10-day period of SPOT-VGT NDVI products. The CV-MVC compositing approach is used for cloud-free pixels of MODIS NDVI products to address the inherent angular variations of most space-based imaging instruments. This is considered to be an advantage over the MVC method used for SPOT-VGT NDVI products and is able to increase the temporal continuities in the multi-day composites (Huete et al., 2002).

As for the intrinsic properties, the narrower bandwidth (higher spectral resolution) of NIR and red of MODIS makes it less sensitive to atmospheric water vapor, compared to SPOT-VGT sensor. Besides, a large amount of dead vegetation in semi-arid mixed grasslands would possibly enlarge the effects of the lower spectral resolution of SPOT-VGT NDVI products. The higher radiometric resolution of MODIS means the higher capability to record the subtle differences of reflectivity than SPOT-VGT, which could account for the more accurate MODIS NDVI. The PSF characterizes the multi-directional blurring (Tarnavsky et al., 2008). MODIS uses the triangular and approximately rectangular PSF in along-scan and along-track direction, respectively (Wolfe et al., 1998; Tan et al., 2006), which makes the nominal pixel size approximate 1km. However, the SPOT-VGT PSF is non-rectangular, which makes the actual spatial support larger than 1km (Tarnavsky et al., 2008). The larger spatial support of SPOT-VGT increases the mixture of land surface covers and the multi-directional blurring. Besides, different SRFs of MODIS and SPOT-VGT sensors could also result in the differences in numeric values of NDVI (Trishchenko et al., 2002).

In addition to the possible reasons discussed above, the atmospheric correction methods on Rayleigh scattering, ozone absorption, aerosol optical thickness, and water vapor content (Tanré et al., 1992; van Leeuwen et al., 2006) have some effects on NDVI comparisons from multiple sensors as well. Considering different spectral signatures of surface types (snow, vegetation cover, and soil), the uncertainties of atmospheric correction and SRFs can reduce or increase NDVI values by 20% (van Leeuwen et al., 2006). The improved aerosol filtering approach of MODIS NDVI products (Didan and Huete, 2006) make them

superior to SPOT- VGT NDVI products which have a deficiency in cloud-screening algorithm due to the lack of a thermal band (Saint, 1995; Brown et al., 2006; Fensholt et al., 2006). The deficiency in cloud-screening of SPOT- VGT sensor could also be responsible for the abrupt decrease of NDVI observed in mid-July, 2008. Different view angles and sun geometry also possibly change NDVI values of MODIS and SPOT-VGT (Cihlar et al., 2004). Besides, accuracy of co-registration is of importance for multiple sensor NDVI comparisons. Geolocation accuracy of MODIS is about 50m at nadir (Wolfe et al., 2002), which is more accurate than SPOT-VGT whose geolocation accuracy at nadir is about 300m (Carmona-Moreno, 2004). All the discussed factors could possibly account for the superiority of MODIS 1km to SPOT-VGT 1km NDVI products.

4.3.2.4 A suitable Spatial Resolution for Describing Spatial Variation of NDVI in the Landscape

The results of the semivariogram analysis of SPOT 4/5 NDVI data are demonstrated in **Figure 4.6**. The experimental and modeled semivariance of SPOT 4 NDVI data on May 2 is shown in **Figure 4.6a**. The range of the semivariogram is about 690m, which indicates that NDVI similarity exist within a 690m distance. According to the sampling theorems, the suitable spatial resolution of images for studying spatially distributed characteristics equals a half of the semivariogram range (Yilmaz and Doherty, 1987). Consequently, images with a spatial resolution higher than 345m are able to capture the spatial variations in LAI resulted from different land covers in early May.

The semivariogram with NDVI derived from the SPOT 5 10m multispectral image on August 30, 2008, is also illustrated (**Figure 4.6b**). The largest semivariance indicates that spatial autocorrelation of NDVI is present within a range of around 500m. Besides, semivariogram analyses of NDVI derived from SPOT 4 images on June 4, August 19 and from SPOT 5 on September 15 all indicate a spatial autocorrelation range of an approximate 500m. Their results therefore are omitted from this chapter. Based on the sampling theorem, images having a spatial resolution higher than 250m are able to differentiate LAI spatial variations of varied land covers from June to September. In summary, images with a spatial resolution of 250m or higher can support NDVI

differentiation of LAI allowing the identification of land cover types during the entire growing season in the study area.

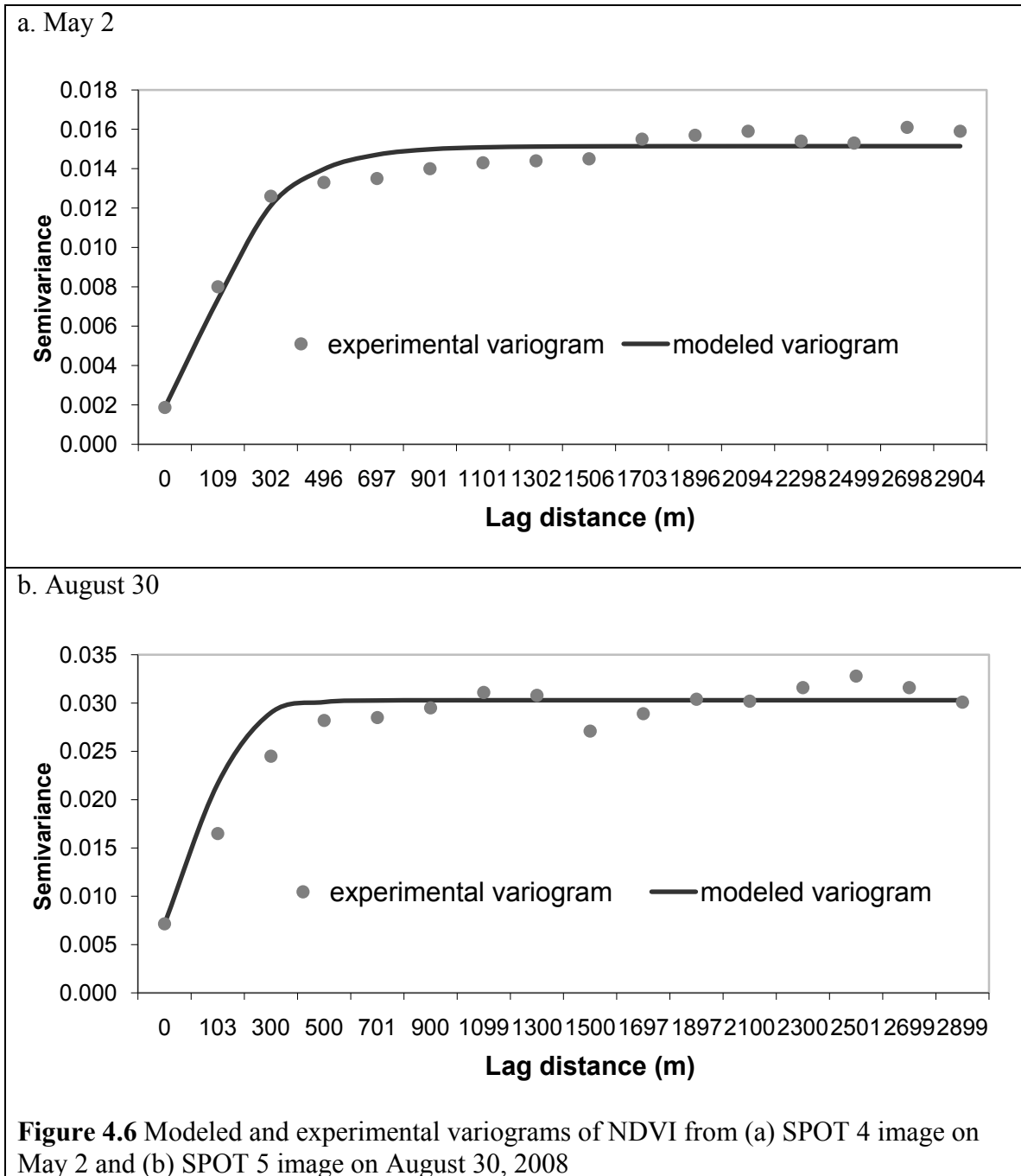


Figure 4.6 Modeled and experimental variograms of NDVI from (a) SPOT 4 image on May 2 and (b) SPOT 5 image on August 30, 2008

MODIS 250m NDVI composites can successfully monitor spatiotemporal variations of LAI in tamed and native grassland, although vegetation phenology and condition may be subjected to inter-annual change due to the high dependence on climatic variations. The

good performance of MODIS 250m NDVI products can be attributed to a higher spatial resolution which reduces effects of a mixture of land covers on NDVI than MODIS and SPOT-VGT 1km NDVI products (Stefanov et al., 2005). The performance is also supported by the finding that MODIS 250m NDVI products with a small nominal pixel size can capture higher spatial variations in the surface than lower spatial resolution products, such as MODIS and SPOT-VGT 1km NDVI products (Tarnavsky et al., 2008). It is also consistent with the conclusion of Kustas et al. (2004) that a 250m spatial resolution is adequate to discriminate evapotranspiration from individual crop fields of 100m×100m in size. However, MODIS 250m NDVI products are still inferior to ground NDVI data indicated by the bad performance in early June, 2008. Calibration of MODIS 250m NDVI products based on ground NDVI data, or data fusion with higher spatial and spectral resolution satellite-level NDVI data, would be considered in the future to further improve their capability.

4.4 Conclusions

There are moderate to high linear relationships between the satellite-level NDVI and ground hyperspectral NDVI. In a decrease sequence of the relationship, the satellite-level NDVI data are MODIS 250m, 1km, SPOT 4/5, and SPOT-VGT NDVI. The linear relationships indicate that satellite-level NDVI data can be calibrated using ground NDVI. The high correlation and the similarity to the numeric values of ground NDVI data demonstrate that MODIS 250m NDVI products have a similar capability to capture spatiotemporal variations of LAI as ground NDVI does. The success of ground NDVI to differentiating spatiotemporal variations of LAI in tamed and native grassland shows a promise of the application of MODIS 250m NDVI products.

MODIS 250m NDVI products are the most qualified to describe spatiotemporal variations of LAI among the three evaluated NDVI Products, which is further confirmed by the semivariogram analysis of SPOT 4/5 NDVI data. MODIS 1km NDVI products slightly outperform SPOT-VGT 1km NDVI composites, although neither can successfully

distinguish the spatiotemporal differences in tamed and native grassland due to the low spatial resolution. The determined suitable NDVI product will contribute to more accurate LAI temporal and spatial variation quantification, which will further be beneficial for modeling in semi-arid mixed grassland.

Further research is required to investigate the influence of effect factors on the difference of satellite-level NDVI from ground hyperspectral NDVI. It is also interesting to further investigate effects of viewing angle, PSF, SRF, length of compositing period, gridding method, and atmosphere on satellite-level NDVI products in dead vegetation dominated semi-arid mixed grassland. It would be useful to evaluate the possibility to combine long-term AVHRR NDVI datasets with MODIS and SPOT-VGT datasets to support climate change study in semi-arid mixed grassland. There may be a similar opportunity to combine the Sea-viewing Wide Field-of-view Sensor (SeaWiFS) products with the MODIS and SPOT-VGT NDVI products.

4.5 References

- Asner, G.P., Wessman, C.A., Schimel, D.S., and Archer, S. 1998. Variability in leaf and litter optical properties: implications for canopy BRDF model inversions using AVHRR, MODIS, and MISR. *Remote Sensing of Environment*, Vol. 63, pp. 200-215.
- Brown, M.E., Pinzón, J.E., Didan, K., Morisette, J.T., and Tucker, C.J. 2006. Evaluation of the consistency of Long-Term NDVI Time Series Derived from AVHRR, SPOT-Vegetation, SeaWiFS, MODIS, and Landsat ETM+ Sensors. *IEEE Transactions on Geoscience and Remote Sensing*, Vol. 44, No. 7, pp. 1787-1793.
- Carmona-Moreno, C. 2004. VEGETATION L-band image processing system. Geometric performances and spatio-temporal stability. *International Journal of Remote Sensing*, Vol. 25, No. 9, pp. 1769-1777.
- Cihlar, J., Latifovica, R., Chena, J., Trishchenko, A., Duc, Y., Fedosejevs, G., and Guindona, B. 2004. Systematic corrections of AVHRR image composites for temporal studies. *Remote Sensing of Environment*, Vol. 89, No. 2, pp. 217-233.
- Didan, K., and Huete, A. 2006. MODIS Vegetation Index Product Series Collection 5 Change Summary. Available in <http://landweb.nascom.nasa.gov/QA_WWW/

- forPage/MOD13_VI_C5_Changes_Document_06_28_06.pdf>. Accessed on 15 Jan 2009.
- Fensholt, R., Nielsen, T.T., and Stisen, S. 2006. Evaluation of AVHRR PAL and GIMMS 10-day composite NDVI time series products using SPOT-4 vegetation data for the African continent. *International Journal of Remote Sensing*, Vol. 27, No. 13, pp. 2719-2733.
- Fensholt, R., Anyamba, A., Stisen, S., Sandholt, I., Pak, E., and Small, J. 2007. Comparison of compositing period length for vegetation index data from polar-orbiting and geostationary satellites for the cloud-prone region of West Africa. *Photogrammetric Engineering and Remote Sensing*, Vol. 73, No. 3, pp. 297-309.
- Galvao, L. S., Vitorello, I., and Pizarro, M.A. 2000. An adequate band positioning to enhance NDVI contrasts among green vegetation, senescent biomass, and tropical soils. *International Journal of Remote Sensing*, Vol. 21, pp. 1953-1960.
- Goetz, S.J. 1997. Multi-sensor analysis of NDVI, surface temperature, and biophysical variables at a mixed grassland site. *International Journal of Remote Sensing*, Vol. 18, No. 1, pp. 71-94.
- Guo, X. 2002. Discrimination of Saskatchewan prairie ecoregions using multitemporal 10-day composite NDVI data. *Prairie Perspectives*, Vol. 5, pp. 174-186.
- He, Y., Guo, X., Wilmschurst, J., and Si, B. 2006. Studying mixed grassland ecosystems II: optimum pixel size. *Canadian Journal of Remote Sensing*, Vol. 32, No. 2, pp. 108-115.
- Holben, B.N. 1986. Characteristics of maximum-value composite images from temporal AVHRR data. *International Journal of Remote Sensing*, Vol. 7, No. 11, pp. 1417-1434.
- Huete, A., Didan, K., Miura, T., and Rodriguez, E. 2002. Overview of the radiometric and biophysical performance of the MODIS vegetation indices. *Remote Sensing of Environment*, Vol. 83, No. 1 & 2, 195-213.
- Kustas, W.P., Li, F., Jackson, T.J., Prueger, J.H., MacPherson, J.I., and Wolde, M. 2004. Effects of remote sensing pixel resolution on modeled energy flux variability of croplands in Iowa. *Remote sensing of environment*, Vol. 92, pp. 535-547.
- Li, Z., and Guo, X. 2010. A Suitable Vegetation Index for Monitoring Temporal Variations of LAI in Semi-arid Mixed Grassland. Submitted.

- Rahman, A.F., Gamon, J.A., Sims, D.A., and Schmidts, M. 2003. Optimum pixel size for hyperspectral studies of ecosystem function in southern California chaparral and grassland. *Remote Sensing of Environment*, Vol. 84, No.2, pp. 192-207.
- Saint, G. 1995. SPOT-4 vegetation system-association with high-resolution data for multiscale studies. *Advance in Space Research*, Vol. 17, pp. 107-110.
- Stefanov, W.L., and Netzband, M. 2005. Assessment of ASTER land cover and MODIS NDVI data at multiple scales for ecological characterization of an arid urban center. *Remote Sensing of Environment*, Vol.99, No. 1-2, pp. 31-43.
- Steven, M.D., Malthus, T.J., Baret, F., Xu, H., and Chopping, M.J. 2003. Intercalibration of vegetation indices from different sensor systems. *Remote Sensing of Environment*, Vol. 88, No. 4, pp. 412-422.
- Tan, B., Woodcock, C.E., Hu, J., Zhang, P., Ozdogan, M., Huang, D., Yang, W., Knyazikhin, Y., and Myneni, R.B. 2006. The impact of geolocation offsets on the local spatial properties of MODIS data: Implications for validation, compositing, and band-to-band registration. *Remote Sensing of Environment*, Vol. 105, pp. 98-114.
- Tanré, D., Holben, B.N., and Kaufman, Y.J. 1992. Atmospheric correction algorithm for NOAA-AVHRR products: Theory and applications. *IEEE Transactions on Geoscience and Remote Sensing*, Vol.30, No. 2, pp.231- 248.
- Tarnavsky, E., Garrigues, S., and Brown, M.E. 2008. Multiscale geostatistical analysis of AVHRR, SPOT-VGT, and MODIS global NDVI products. *Remote Sensing of Environment*, Vol. 112, pp. 535-549.
- Teillet, P.M., Staenz, K., and Williams, D.J. 1997. Effects of spectral, spatial, and radiometric characteristics on remote sensing vegetation indices of forested regions. *Remote Sensing of Environment*, Vol. 61, pp. 139-149.
- Teillet, P. M., Fedosejevs, G., Gauthier, R. P., O'Neill, N. T., Thome, K. J., Biggar, S. F., Ripley, H., and Meygret, A. 2001. A generalized approach to the vicarious calibration of multiple earth observation sensors using hyperspectral data. *Remote Sensing of Environment*, Vol. 77, No.3, pp. 307-327.
- Trishchenko, A.P., Cihlar, J., and Li, Z. 2002. Effects of spectral response function on surface reflectance and NDVI measured with moderate resolution satellite sensors. *Remote Sensing of Environment*, Vol. 81, pp. 1-18.
- van Leeuwen, W.J.D., Orr, B.J., Marsh, S.E., and Herrmann, S.M. 2006. Multi-sensor NDVI data continuity: Uncertainties and implications for vegetation monitoring applications. *Remote Sensing of Environment*, Vol. 100, pp. 67-81.

- Wolfe, R.E., Roy, D.P., and Vermote, E.F. 1998. MODIS land data storage, gridding, and compositing methodology: Level 2 grid. *IEEE Transactions Geosciences and Remote Sensing*, Vol. 36, No. 4, pp. 1324-1338.
- Wolfe, R.E., Masahiro, N., Fleig, A.J., Kuyper, J.A., Roy, D.P., Storey, J.C., and Patt, F.S. 2002. Achieving sub-pixel geolocation accuracy in support of MODIS land science. *Remote Sensing of Environment*, Vol. 83, pp. 31-49.
- Yilmaz, O., and Doherty, S.M. (Editors). 1987. *Seismic data processing. Investigations in Geophysics*, Vol. 2. Society of Exploration Geophysicists, Tulsa, Okla. 536 pp.

CHAPTER 5 – SUMMARY

LAI is the most important biophysical parameter to represent vegetation vertical structures. Therefore, it is a common input in climate, hydrology, biochemistry, and ecosystem models. Currently, VI-LAI relationships are the most widely used method for obtaining LAI data for modeling. However, the accuracy of LAI estimation greatly varied due to different performances of the selected VIs, the effects of soil moisture and topography, and the temporal and spatial variations in LAI. Thus, the first objective of this research was to determine a suitable VI for LAI estimation, and the second objective was to improve LAI estimation by taking both temporal and spatial variations in LAI into account. As NDVI has been routinely produced from NOAA/AVHRR images since 1981 (Cracknell, 2001; Tucker, 1979, 1980; Tarnavsky et al., 2008), the resulting products have been widely used in various models as an intermediary of biophysical parameters, including LAI. However, differences are observed in various NDVI products. Thus, the third objective was to evaluate 16-day MODIS 250m, 1km and 10-day SPOT-VGT 1km NDVI products on monitoring intra-annual and spatiotemporal variations in LAI in semi-arid mixed grassland. The findings, potential applications, and limitations of this research were summarized.

5.1 Conclusions

5.1.1 A Suitable Vegetation Index for Quantifying Temporal Variations of LAI in Semi-Arid Mixed Grassland

LAI demonstrated a distinct temporal variation. The 91.2% of the variations in LAI can be accounted for by variations in grasses, forbs, standing dead, and litter. Standing dead has the most significant effect on LAI temporal variations although, the effect is negative. It, together with litter, can explain 47.4% variations in LAI, while grasses and forbs can only account for 43.8% temporal variations in LAI. The important roles of dead materials, including standing dead and litter, on LAI variations will cause a serious problem to an interpretation of a VI. Thus, an optimum VI is required for accurate LAI estimation.

Performances of VIs on LAI estimation vary as the vegetation growing stage changes. VIs demonstrate the most capability to be a representative of LAI during the time period of Jul 21-Aug 15, followed by Aug 29-Sep 15 and Jun 4-Jul 2. Also, VIs perform differently at each growing stage, although the discrepancy is small or even subtle among some VIs. NDVI, SLAIDI, and TSAVI demonstrate the best performances, whereas SARVI and TVI have the worst performances on LAI estimation in the early, maximum, and late growing season, respectively. NDVI is competent for quantifying temporal variation of LAI in the study area, which is consistent with the research of Broge and Leblanc (2000) that NDVI is the best index at low and medium LAIs.

5.1.2 Improved LAI Estimation While Considering Temporal and Spatial Variations

This study revealed that spatial variations in LAI are highly associated with soil moisture. It also concluded that spatial relationships between LAI and soil moisture regularly varied throughout the growing season. Negative spatial relationships between soil moisture and LAI were observed in the early and maximum growing seasons, while positive relationships existed in the early senescence season and no obvious correlation in the late senescence season. Correspondingly, the most suitable spatial resolution for LAI estimation changed from 25-40m in the early growing season to the 10-15m in the maximum growing and early senescence season, and it is uncertain in the late senescence season. This is falling into the 10-50m range for C_4 species coverage estimation and 35m for the grassland heterogeneity study in summer in GNP (Davidson and Csillag, 2001; He et al., 2006). However, this differs with Rahman's et al. (2003) finding that an approximate 6m pixel size would capture variations in greenness in southern California grassland.

LAI estimation can be much improved by taking both the temporal and spatial variations of LAI into account and the maximum growing season is the most appropriate time for LAI estimation in the semi-arid mixed grassland. Based on ground hyperspectral reflectance data, LAI estimation in the maximum growing season has an r^2 of 0.59 and ARE of 0.25.

LAI estimation based on the satellite-level data also confirmed that more accurate LAI estimation can be obtained by taking both temporal and spatial variations into account. The r^2 can be increased by 0.08, 0.10, and 0.02 in the early, maximum, and late growing season. This is supported by the conclusions that LAI estimation can be much improved based on an appropriate scale (Rahman et al., 2003; He et al., 2006) and time (Chen and Cihlar, 1996).

5.1.3 The Most Suitable NDVI Products on Monitoring Variations in LAI

Moderate to high linear relationships are observed between the ground hyperspectral and satellite-level NDVI data, and a decrease sequence MODIS 250m, 1km, SPOT 4/5, and SPOT-VGT NDVI in. The similarity indicates that satellite-level NDVI data have a similar capability as ground NDVI data to identify spatiotemporal variations of LAI in semi-arid mixed grassland. However, MODIS 250m NDVI composites have advantages over MODIS and SPOT-VGT 1km NDVI data. This coincides with the conclusion of Tarnavsky et al. (2008) that MODIS 250m NDVI products can capture higher spatial variations than MODIS and SPOT-VGT 1km NDVI composites. This is also supported by the finding that a 250m spatial resolution can discriminate evapotranspiration from individual crop fields 100m×100m in size (Kustas et al., 2004).

MODIS 1km NDVI composites are superior to SPOT-VGT NDVI products on the applications on LAI. This is in consistent with the research which has shown that spatial variations of MODIS and SPOT-VGT 1km NDVI products considerably differ (Tarnavsky et al., 2008). This is also in an agreement with the conclusion that 16-day MVC NDVI composites of MODIS outperform 10-day MVC NDVI composites in the semi-arid area of West Africa (Fensholt et al., 2007). However, this is contradictory with the assertion of Brown et al. (2006) that both MODIS and SPOT-VGT NDVI data can similarly capture the annual phenology.

5.2 Potential Applications

Potentially, this research can be scientifically and ecologically applied. Scientifically, this research evaluated the influence of dead vegetation, green vegetation, and bare soil on the performances of selected VIs. This will contribute to the estimation of biophysical parameters in grasslands. In addition, this study discussed the constrained factors on LAI estimation from VIs, and then improved LAI estimation by taking the factors into account. The LAI estimation method and the approaches to identifying the effects of ecology factors on LAI spatial variations can be used in other studies, such as hydrological and biochemical modeling in grasslands, where annual vegetation is dominant.

As for the ecological applications, the improved LAI estimation and the most suitable NDVI products will contribute to the modeling of interactions between land surface and atmosphere, such as climate, hydrology, and biochemistry. It also contributes to CO₂ estimation and prediction, which further benefits climate change study. In addition, the optimum spatial resolutions for LAI estimation at different growing stages are also useful for grassland productivity modeling and other ecological studies, such as hydrological modeling in grasslands.

5.3 Limitations

This research determined the optimum VI for estimating LAI, proposed and validated an approach to improving LAI estimation based on LAI-VI relationships and evaluated the current NDVI products for monitoring temporal and spatiotemporal variations in LAI. The results will be beneficial for modeling communities. However, some limitations still need to be addressed in future studies.

5.3.1 Remote Sensing Products

As explored in spatial relationships between LAI and soil moisture, the optimum spatial resolution of satellite imagery is 25-40m in early growing season. Higher spatial resolution

imagery, such as SPOT 4 20m is definitely able to capture the spatial variations of LAI controlled by soil moisture. However, higher spatial resolution images demonstrate a higher degree spatial autocorrelation of pixels (Stuckens et al., 2000), which introduces more errors on LAI estimation. Hence, it would be useful to try EO-1 30m, DMC-1 32m, and Landsat TM, ETM+ 30m multispectral images for LAI estimation in the early growing season in future study.

Although MODIS and SPOT-VGT NDVI products have been perceived to have advantages over NOAA/AVHRR NDVI products, AVHRR NDVI products have their own unique advantage of being long-time data records. It is worth evaluating AVHRR and other NDVI products including SeaWiFS to combine a long-term data set for studies in future.

5.3.2 Validation of LAI

PAI measured from the LAI-2000 instrument was validated by the destructive clipping method to obtain LAI data. The clipping was done on July 21, 2008. The relationship between PAI and LAI was then used to validate PAI in the other growing stages. This validation will more or less affect the quantified LAI values. Corresponding destructive clippings for each field data collection in the future can resolve this problem.

5.3.3 Accuracy of LAI Estimation in the Late Growing Season

LAI estimation in the late growing season cannot meet the requirements of models using an ARE as a measure. The causation is worthy to be further investigated. Introduction of new technique to LAI estimation, such as Geographically Weighted Regression (GWR) (Propastin, 2009), possibly can increase the accuracy of LAI estimation.

5.4 References

- Broge, N.H., and Leblanc, E. 2001. Comparing prediction power and stability of broadband and hyperspectral vegetation indices for estimation of green leaf area index and canopy chlorophyll density. *Remote Sensing of Environment*, Vol.76, pp. 156-172.

- Brown, M.E., Pinzón, J.E., Didan, K., Morisette, J.T., and Tucker, C.J. 2006. Evaluation of the Consistency of Long-Term NDVI Time Series Derived From AVHRR, SPOT-VGT, SeaWiFS, MODIS, and Landsat ETM+ Sensors. *IEEE Transactions on Geoscience and Remote Sensing*, Vol. 44, No. 7, pp.1787-1793.
- Chen, J. M., and Cihlar, J. 1996. Retrieving leaf area index of boreal conifer forests using Landsat TM images. *Remote Sensing of Environment*, Vol. 55, pp.153-162.
- Cracknell, A.P. 2001. The exciting and totally unanticipated success of the AVHRR in applications for which it was never intended. *Advances in Spatial Research*, Vol. 28, No.1, pp. 233-240.
- Davidson, A., and Csillag, F. 2001. The influence of vegetation index and spatial resolution on a two-date remote sensing derived relation to C4 species coverage. *Remote Sensing of Environment*, Vol. 75, No. 1, pp. 138-151.
- Fensholt, R., Anyamba, A., Stisen, S., Sandholt, I., Pak, E., and Small, J. 2007. Comparison of compositing period length for vegetation index data from polar-orbiting and geostationary satellites for the cloud-prone region of West Africa. *Photogrammetric Engineering and Remote Sensing*, Vol. 73, No. 3, pp. 297-309.
- He, Y., Guo, X., Wilmschurst, J., and Si, B. 2006. Studying mixed grassland ecosystems II: optimum pixel size. *Canadian Journal of Remote Sensing*, Vol. 32, No. 2, pp.108-115.
- Kustas, W.P., Li, F., Jackson, T.J., Prueger, J.H., MacPherson, J.I., and Wolde, M. 2004. Effects of remote sensing pixel resolution on modeled energy flux variability of croplands in Iowa. *Remote sensing of environment*, Vol. 92, pp. 535-547.
- Propastin, P.A. 2009. Spatial non-stationarity and scale-dependency of prediction accuracy in the remote estimation of LAI over a tropical rainforest in Sulawesi, Indonesia. *Remote Sensing of Environment*, Vol. 113, pp. 2234-2242.
- Rahman, A.F., Gamon, J.A., Sims, D.A., and Schmidts, M. 2003. Optimum pixel size for hyperspectral studies of ecosystem function in southern California chaparral and grassland. *Remote Sensing of Environment*, Vol. 84, pp.192-207.
- Stuckens, J., Coppin, P.R., and Bauer, M.E. 2000. Integrating Contextual Information with Per-pixel Classification for Improved Land Cover Classification. *Remote Sensing of Environment*, Vol. 71, pp.282-296.
- Tarnavsky, E., Garrigues, S., and Brown, M.E. 2008. Multiscale geostatistical analysis of AVHRR, SPOT-VGT, and MODIS global NDVI products. *Remote Sensing of Environment*, Vol. 112, pp. 535-549.

Tucker, C.J. 1979. Red and photographic infrared linear combinations in monitoring vegetation. *Remote Sensing of Environment*, Vol. 8, No. 2, pp. 127-150.

Tucker, C.J. 1980. Remote sensing of leaf water content in the near infrared. *Remote Sensing of Environment*, Vol. 10, No. 1, pp. 23-32.

APPENDIX A - THE VALIDATION OF PLANT AREA INDEX

Vegetation clippings were done on July 21st, 2008 to determine green leaf area index (LAI) by a destructive sampling method. The LAI values were used to build a relationship with plant area index (PAI) measured with a LAI-2000 instrument. The relationship was then used to validate the measured PAI data over the sampling transect and plots to obtain LAI.

A total of 30 samples were clipped from communities consisting of a mixture of grasses and forbs. Each clipping was done within one 25cm×50cm quadrat. Quadrats were placed on areas with different vegetation densities. PAI was measured before clipping within the quadrat.

The clipped samples were put into paper bags immediately after cutting, and stored in coolers in the field and a fridge after coming back to campus. In the second day, each clipping sample was sorted out into green grass, green forbs, and dead materials. The green leaves were taken off from both grass and forbs and scanned by Li-Cor 3001 (LICOR, Inc., Lincoln, NewYork) with an accuracy of $\pm 0.01 \text{ mm}^2$. The LAI of each sample was then obtained by dividing the area of all green leaves by the area of one quadrat. The relationship between LAI and PAI was established and shown in **Figure A1**. There is a strong linear relationship between LAI and PAI, and 77% of variations in LAI are associated with variations in PAI. PAI was then validated by the equation (B1) to obtain LAI.

$$y=0.68x-0.54 \quad (r^2=0.77, n=30) \quad (\text{A1})$$

Where y is green leaf area index and x is plant area index, and n is the sample size.

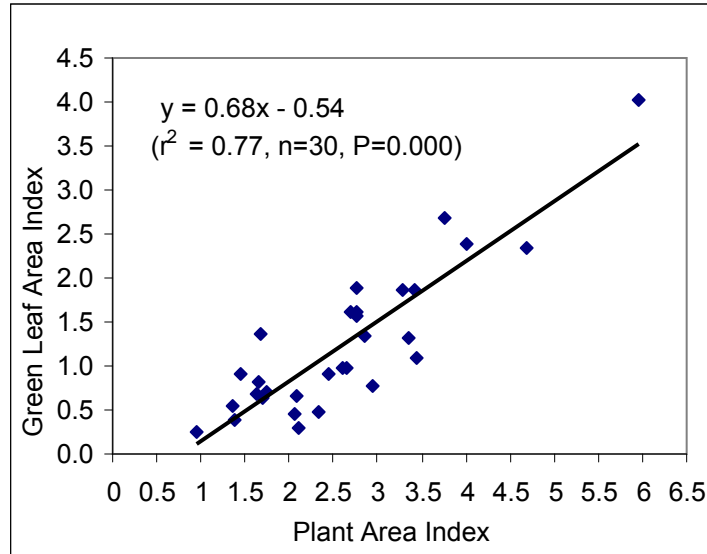


Figure A.1 The relationship between green leaf area index and plant area index

After validation, the differences between LAI and PAI were computed (**Table A1**). The results indicate that the PAI measured by LAI-2000 largely overestimates LAI. This is contrary with the conclusions that LAI-2000 instrument underestimates LAI in forest areas (e.g., Comeau et al., 1998; Küßner et al., 2000). The relative differences $((PAI-LAI)/LAI)$ varied from 0.4 to 4.02. These variations may result from large quantities of dead materials in semi-arid mixed grasslands. The big differences make PAI less useful as validation data for space-level LAI products. In addition, parameterization of these PAI data into models as a substitute for LAI will definitely introduce extra uncertainties. Therefore, it is necessary to validate PAI by destructive sampling methods to obtain LAI.

Table A.1 Differences between plant area index (PAI) and green leaf area index (LAI)

Samples	LAI	PAI	Differences	Relative Differences
1	0.98	2.64	1.66	1.70
2	1.86	3.42	1.56	0.84
3	1.89	2.76	0.87	0.46
4	0.63	1.70	1.07	1.69
5	0.92	2.45	1.53	1.66
6	0.47	2.34	1.87	4.02
7	0.65	2.09	1.44	2.19
8	1.09	3.44	2.35	2.15
9	0.31	2.11	1.80	5.90
10	0.98	2.61	1.63	1.66
11	0.45	2.05	1.60	3.58
12	0.25	0.96	0.71	2.84
13	0.38	1.38	1.00	2.67
14	1.37	1.68	0.31	0.22
15	0.54	1.36	0.82	1.51
16	0.92	1.45	0.53	0.58
17	0.69	1.62	0.93	1.35
18	1.34	2.85	1.51	1.13
19	1.62	2.77	1.15	0.72
20	1.57	2.77	1.20	0.76
21	0.70	1.75	1.05	1.51
22	0.81	1.65	0.84	1.04
23	0.76	2.94	2.18	2.84
24	1.31	3.36	2.05	1.57
25	2.35	4.69	2.34	1.00
26	2.38	4.01	1.63	0.68
27	1.86	3.29	1.43	0.77
28	1.61	2.69	1.08	0.67
29	2.68	3.76	1.08	0.40
30	4.02	5.95	1.93	0.48

References:

- Comeau, P.G., Gendron, F., and Letchford, T. 1998. A comparison of several methods for estimating light under a paper birch mixed wood stand. *Canadian Journal of Forest Research*, Vol. 28, pp. 1843 -1850.
- Küßner, R. and Mosandl, R. 2000. Comparison of direct and indirect estimation of leaf area index in mature Norway spruce stands of eastern Germany. *Canadian Journal of Forest Research*, Vol. 30, pp. 440 - 447.

APPENDIX B - VALIDATION OF SOIL MOISTURE METER

The Soil Moisture Meter used for measuring soil moisture content in this study is comprised of two major parts. One is the data logger which can show and save the collected data in the assigned format. The other is the ThetaProbe sensor (Dynamax Inc, Houston, USA) which is used to collect data. The type of ThetaProbe used in my measure is the ML2x.

The sensor is sensing the dielectric constant of the soil (ε), which can be related to soil water content. However, a relationship between ε and soil water content depends on the particular composition of soil. The ThetaProbe therefore requires a calibration for specific soils in order to minimize the errors in the process of converting Probe outputs (voltage) into soil water content. The accuracy of ML2x ThetaProbe for measuring volumetric soil moisture content is $\pm 0.01 \text{m}^3 / \text{m}^3$ for a specific soil after calibration.

According to the manual, a generalized calibration had been carried out with typical errors of $\pm 0.05 \text{m}^3 / \text{m}^3$. The relationship between the complex refractive index (which is equivalent to $\sqrt{\varepsilon}$) and volumetric water content (θ) is shown in the linear form (equation B1).

$$\sqrt{\varepsilon} = a_0 + a_1 \cdot \theta \quad (\text{B1})$$

while the relationship between ThetaProbe outputs (voltage) and $\sqrt{\varepsilon}$ is shown as below,

$$\sqrt{\varepsilon} = 1.07 + 6.4V - 6.4V^2 + 4.7V^3 \quad (R^3 = 0.998) \quad (\text{B2})$$

To obtain an accurate θ for a specific soil, a_0, a_1 in equation (B1) are the only two coefficients need to be determined when the soil meter is validated. The following steps had been done to calibrate the soil meter for application in my study area.

Steps 1 Five damp samples were randomly collected from the slope, elevation, and downfold close to wetlands. Before collecting each sample, the probe was inserted into soil to obtain the probe outputs (V_w). This operation had been implemented three times for each

sample. The three measures were averaged to obtain an accurate V_w . The V_w values were then introduced into the Equation (B2) to calculate $\sqrt{\varepsilon_w}$. After measuring, the sample was taken and immediately put into zipped bags, and then placed into the cooler. Each sample has an approximate 10cm width and length, and a 6cm height. This height is consistent with the depth that the soil moisture meter is able to measure.

Step 2 The damp samples were put in Tins, immediately weighed and put into the dry-oven. In the oven, they were dried for 24 hours at 105°C. After that, the dried soil samples ($\theta \approx 0$) were weighed. The Soil moisture (θ) was then calculated by the following equation.

$$\theta = (\text{Wet-Dry})/\text{Dry} \times \text{soil Bulk Density} \times 100 \quad (\text{B3})$$

In St. Denis, soil Bulk Density ranges from 1.27 to 1.37 (Credit to X. Fang).

Step 3 Voltages of the dry soil were measured using the same method as used for damp soil samples. Probe outputs from five samples were then obtained and averaged. The mean value was introduced into Equation (B2) and then $\sqrt{\varepsilon_0}$ was calculated. In fact, $\sqrt{\varepsilon_0}$ equals a_0 based on Equation (B1). The calculated a_0 is 1.35 which is within the recommended range from 1.0 to 2.0.

Step 4 By introducing a_0 , θ , and $\sqrt{\varepsilon_w}$ into Equation (B1), a_1 was calculated and it has a value of 8.6. This value is reasonable because it is within the recommended range from 7.6 to 8.6 given in the manual. After the two coefficients are determined, the volumetric soil water content can be calculated by the following equation.

$$\theta = \frac{[1.07 + 6.4V - 6.4V^2 + 4.7V^3] - 1.35}{8.6} \quad (\text{B4})$$

APPENDIX C - THE SOIL LINE IN St. DENIS

The soil line, defined as the linear relationship between NIR and red reflectance (R) of bare soil, is expressed as $NIR=aR+b$ (Richardson and Wiegand, 1977; Fox et al., 2004), where “a” is the slope and “b” is the intercept. The slope (a) and intercept (b) are used extensively in developing VIs (**Table 2.1**).

There are three ways to establish a soil line for a certain type of soil in a certain area. The first method is to develop a soil line from remotely sensed images (Fox et al., 2004). This is successful for a soil line development with 95% confidence intervals around the estimated actual soil line. However, this method really depends on the bandwidth parameters and the initial subset size which is arbitrarily defined (Fox et al., 2004). The second is modeling the soil line (Baret et al., 1993). It is too complex to be used in practice. The third method is what I used. I collected soil samples in the field, put them into zipped bags, and then put them into a cooler to keep the disturbance of samples minimized. Those samples were taken back to the laboratory, and their spectra were measured by an ASD SpectroRadiometer (the one used in the field for spectral measurements) using the indoor light source to minimize the atmospheric effects.

C1. Descriptions on Soil Samples Collected in St. Denis, SK, Canada

- 1) Quantity: 16
- 2) Size: 10cm×10cm×6cm
- 3) Soil type: dark brown Chernozem
- 4) Sampling area: random distribution in the native grassland
- 5) Sampling time: late October, 2008

C2. Spectral Measures

For each soil sample, three spectral measures were made from different view angles. The wavelength range of the SpectroRadiometer is 350-2500 nm with a spectral resolution of 3nm at 700nm, and 10nm at 1400 and 2100nm. The reflectance between 790 and 890nm

was aggregated for NIR reflectance, and the 610-680nm reflectance was aggregated for Red reflectance. This aggregation is consistent with the wavelength ranges of NIR and red bands of SPOT 4 and SPOT 5 sensor, because they will be used for LAI estimation in my study. Finally, the NIR and red reflectance from three different views were averaged and used for establishing the soil line.

C3. The Soil Line

As shown in Fig. 1, the established soil line can be expressed as:

$$\text{NIR} = 1.9534\text{Red} - 0.0124 \quad (r^2 = 0.96, n = 16) \quad (\text{C1})$$

Where the slope value is 1.9534, and the intercept is -0.0124. These two values were used in vegetation derivation in Chapter 2.

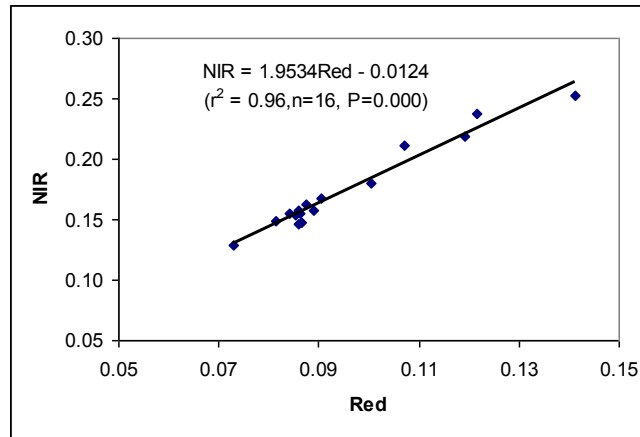


Figure C.1 The soil line developed in St. Denis, Saskatchewan, Canada

C4. References

- Baret, F., Jacquemoud, S., and Hanocq, J. F. 1993. About the soil line concept in remote sensing. *Advances in Space Research*, Vol.13, No. 5, pp. 221-284.
- Fox, G.A. Sabbagh, G.J., Searcy, S.W., and Yang, C. 2004. An automated soil line identification routine for remotely sensed images. *Soil Science Society of America Journal*, Vol. 68, pp. 1326-1331.
- Richardson, A.J. and Wiegand, C.L. 1977. Distinguishing vegetation from soil background information. *Photogrammetric Engineering & Remote Sensing*, Vol.43, pp.1541-1552.